

# **COMPARATIVE INVESTIGATION OF SOLID DESICCANTS AS WORKING MEDIUM IN HEATLESS AIR DRYERS**

A Thesis submitted to Gujarat Technological University  
for the Award of

**Doctor of Philosophy**  
in  
**Mechanical Engineering**  
by

**D'SOUZA ALICE JUDE**  
(Enrollment No. 159997119001)

Under supervision of  
**Dr. P. K. Brahmbhatt**



**GUJARAT TECHNOLOGICAL UNIVERSITY**  
**AHMEDABAD**

**June -2023**

© D'souza Alice Jude

# DECLARATION

I declare that the thesis entitled **“Comparative Investigation of Solid Desiccants as Working Medium in Heatless Air Dryers.”** submitted by me for the degree of Doctor of Philosophy is the record of research work carried out by me during the period from 2015 to 2023 under the supervision of Dr. P.K. Brahmhatt and this has not formed the basis for the award of any degree, diploma, associate ship, fellowship, titles in this or any other University or other institution of higher learning.

I further declare that the material obtained from other sources has been duly acknowledged in the thesis. I shall be solely responsible for any plagiarism or other irregularities, if noticed in the thesis.

Signature of the Research Scholar:



Date: 30/06/2023

Name of Research Scholar: **D'souza Alice Jude**

Place: Chandkheda (Gujarat, India)

# CERTIFICATE

I certify that the work incorporated in the thesis “**Comparative Investigation of Solid Desiccants as Working Medium in Heatless Air Dryers.**” submitted by **D’souza Alice Jude** was carried out by the candidate under my supervision/guidance. To the best of my knowledge: (i) the candidate has not submitted the same research work to any other institution for any degree/diploma, Associate ship, Fellowship or other similar titles (ii) the thesis submitted is a record of original research work done by the Research Scholar during the period of study under my supervision, and (iii) the thesis represents independent research work on the part of the Research Scholar.

Signature of Supervisor:



Date: **30/6/2023**

Name of Supervisor: **Dr. P. K. Brahmbhatt**

Place: Chandkheda (Gujarat, India)



## Course-work Completion Certificate

This is to certify that **D'souza Alice Jude** enrollment no. **159997119001** is a PhD scholar enrolled for PhD program in the branch **Mechanical Engineering** of Gujarat Technological University, Ahmedabad.

(Please tick the relevant options(s))

- ☐ He/She has been exempted from the course-work (successfully completed during M.Phil Course)
- ☐ He/She has been exempted from Research Methodology Course only (successfully completed during M.Phil Course)
- ☒ He/She has successfully completed the PhD course work for the partial requirement for the award of PhD Degree. ~~His~~/ Her performance in the course work is as follows

Grade Obtained in Research Methodology (PH001)	Grade Obtained in Self Study Course (Core Subject) (PH002)
<b>BB</b>	<b>AA</b>

Supervisor's Sign

**Dr. P. K. Brahmhatt**

*P. K. Brahmhatt*

# Originality Report Certificate

It is certified that PhD Thesis titled “**Comparative investigation of solid desiccants as working medium in heatless air dryers.**” by **D’souza Alice Jude** has been examined by us. We undertake the following:

- a. Thesis has significant new work / knowledge as compared already published or are under consideration to be published elsewhere. No sentence, equation, diagram, table, paragraph or section has been copied verbatim from previous work unless it is placed under quotation marks and duly referenced.
- b. The work presented is original and own work of the author (i.e. there is no plagiarism). No ideas, processes, results or words of others have been presented as Author own work.
- c. There is no fabrication of data or results which have been compiled / analysed.
- d. There is no falsification by manipulating research materials, equipment or processes, or changing or omitting data or results such that the research is not accurately represented in the research record.
- e. The thesis has been checked using Urkund’s anti-plagiarism system (copy of originality report attached) and found within limits as per GTU Plagiarism Policy and instructions issued from time to time (i.e. Permitted similarity index <10%).

Signature of the Research Scholar:



Date: 30/06/2023

Name of Research Scholar: **D’souza Alice Jude**

Place: Chandkheda (Gujarat, India)

Signature of Supervisor:



Date: 30/6/2023

Name of Supervisor: **Dr. P. K. Brahmhatt**

Place: Chandkheda (Gujarat, India)

## Document Information

Analyzed document	Plag check COMPARATIVE INVESTIGATION OF SOLID DESICCANTS USED IN HEATLESS AIR DRYERS.pdf (D163625275)
Submitted	2023-04-11 13:41:00
Submitted by	
Submitter email	alicedsz08@gmail.com
Similarity	6%
Analysis address	alicedsz08.gtuni@analysis.arkund.com

## Sources included in the report

SA	<b>Gujarat Technological University / Template ajd.pdf</b> Document Template ajd.pdf (D151191077) Submitted by: alicedsz08@gmail.com Receiver: alicedsz08.gtuni@analysis.arkund.com	24
SA	<b>EXPERIMENTAL INVESTIGATION OF SOLAR POWERED AIR CONDITIONING SYSTEM WITH DESICCANT BASED HEAT EXCHANGER BY AMIT KUMAR, ROLL. NO. 6140032.pdf</b> Document EXPERIMENTAL INVESTIGATION OF SOLAR POWERED AIR CONDITIONING SYSTEM WITH DESICCANT BASED HEAT EXCHANGER BY AMIT KUMAR, ROLL. NO. 6140032.pdf (D21304175)	2
SA	<b>3331-6307-1-SM.docx</b> Document 3331-6307-1-SM.docx (D134771133)	20
SA	<b>Thesis(15m223,16,18).pdf</b> Document Thesis(15m223,16,18).pdf (D42876161)	2
SA	<b>190120721005.docx</b> Document 190120721005.docx (D104640152)	1
SA	<b>5.V.Suresh Kannan- 1314269258- Synopsis.pdf</b> Document 5.V.Suresh Kannan- 1314269258- Synopsis.pdf (D59230905)	2
SA	<b>190820721002 Ajay Padhiyar.docx</b> Document 190820721002 Ajay Padhiyar.docx (D104273493)	1
SA	<b>Gujarat Technological University / Result_12_23_2022__8_53_02_AM_1.docx</b> Document Result_12_23_2022__8_53_02_AM_1.docx (D154413681) Submitted by: kk_bhatt@gtu.edu.in Receiver: kk_bhatt.gtuni@analysis.arkund.com	1
SA	<b>Final Draft 29_oct.docx</b> Document Final Draft 29_oct.docx (D83169210)	4

*DD' saw*

*R. V. Bhatt*

# **PhD THESIS Non-Exclusive Licence to GUJARAT TECHNOLOGICAL UNIVERSITY**

In consideration of being a PhD Research Scholar at GTU and in the interests of the facilitation of research at GTU and elsewhere, I, **D'souza Alice Jude** having (Enrollment No.) **159997119001** hereby grant a non-exclusive, royalty free and perpetual license to GTU on the following terms:

- a. The University is permitted to archive, reproduce and distribute my thesis, in whole or in part, and/or my abstract, in whole or in part (referred to collectively as the "Work") anywhere in the world, for non-commercial purposes, in all forms of media;
- b. The University is permitted to authorize, sub-lease, sub-contract or procure any of the acts mentioned in paragraph (a);
- c. The University is authorized to submit the Work at any National / International Library, under the authority of their "Thesis Non-Exclusive License";
- d. The Universal Copyright Notice (©) shall appear on all copies made under the authority of this license;
- e. I undertake to submit my thesis, through my University, to any Library and Archives. Any abstract submitted with the thesis will be considered to form part of the thesis.
- f. I represent that my thesis is my original work, does not infringe any rights of others, including privacy rights, and that I have the right to make the grant conferred by this non-exclusive license.
- g. If third party copyrighted material was included in my thesis for which, under the terms of the Copyright Act, written permission from the copyright owners is required, I have obtained such permission from the copyright owners to do the acts mentioned in paragraph (a) above for the full term of copyright protection.
- h. I understand that the responsibility for the matter as mentioned in the paragraph (g) rests with the authors / me solely. In no case shall GTU have any liability for any acts/ omissions / errors / copyright infringement from the publication of the said thesis or otherwise.
- i. I retain copyright ownership and moral rights in my thesis, and may deal with the copyright in my thesis, in any way consistent with rights granted by me to my University in this non-exclusive license.

- j. GTU logo shall not be used /printed in the book (in any manner whatsoever) being published or any promotional or marketing materials or any such similar documents.
- k. The following statement shall be included appropriately and displayed prominently in the book or any material being published anywhere: “The content of the published work is part of the thesis submitted in partial fulfilment for the award of the degree of PhD. in **Mechanical Engineering** of the Gujarat Technological University”.
- l. I further promise to inform any person to whom I may hereafter assign or license my copyright in my thesis of the rights granted by me to my University in this nonexclusive license. I shall keep GTU indemnified from any and all claims from the Publisher(s) or any third parties at all times resulting or arising from the publishing or use or intended use of the book / such similar document or its contents.
- m. I am aware of and agree to accept the conditions and regulations of Ph.D. including all policy matters related to authorship and plagiarism.

Date: 30/6/2023

Place: Chandkheda (Gujarat, India)

Signature of the Research Scholar:

Recommendation of the Supervisor: Recommended,

Signature of the Supervisor:



## Thesis Approval Form

The viva-voce of the PhD Thesis submitted by Shri/Smt./Kum. **D'souza Alice Jude** having (Enrollment No. **159997119001**) entitled "**Comparative Investigation of Solid Desiccants as Working Medium in Heatless Air Dryers.**" was conducted on date **30<sup>th</sup> June 2023; Friday** at time **11.00 am** at Gujarat Technological University.

(Please tick any one of the following option)



The performance of the candidate was satisfactory. We recommend that he/she be awarded the PhD degree.



Any further modifications in research work recommended by the panel after 3 months from the date of first viva-voce upon request of the Supervisor or request of Independent Research Scholar after which viva-voce can be re-conducted by the same panel again.

(Briefly justify the modifications suggested by the panel)



The performance of the candidate was unsatisfactory. We recommend that he/she should not be awarded the PhD degree.

(The panel must give justification for rejecting the research work)

Dr. P.K. Brahmabhatt

Name and Signature – Supervisor

Dr. A.R. Sarathe

Name & Signature - External Examiner

Name & Signature - External Examiner

Name & Signature - External Examiner

# Abstract

In many industries presence of moisture in compressed air poses a potential threat and can cause damage to equipment. To remove moisture, desiccant based dehumidification can be considered a green alternative that is not dependent on the conventional dehumidification systems which are dependent on CFCs. One such desiccant based dehumidification system is the heatless desiccant air dryer; however, its efficiency and the performance is dependent on the type of desiccant used. In this work, the most commonly used solid desiccants such as silica gel, activated alumina, Molecular Sieve 4A and Molecular Sieve 13x and its heterogeneous mixtures' performance as a desiccant in the heatless air dryer is investigated. The investigation revealed that Molecular Sieve 13x when used individually in the heatless dryer gave the maximum moisture removal rate of 54.63 gm/hr and an effectiveness of 80% compared to the other desiccants investigated. While silica gel gave the least moisture removal rate at 22.51 gm/hr with an effectiveness of 47.18%. The research provides a road map for selection of the appropriate desiccant based on the need of moisture removal required by any industry. The experimental work is validated by the artificial neural network developed using neural designer with input parameters such as dry bulb temperature, wet bulb temperature and relative humidity. The output predicted the removal rate of moisture and effectiveness of the dryer which showed good agreement with the experimental results. The heat of adsorption released during the adsorption process is also investigated for each case. It is found that the towers do not over heat and a maximum temperature gradient recorded across the adsorption tower was 6°C, which suggests that external cooling to enhance the adsorption process is not essential in a heatless air dryer.

## Keywords

Solid desiccants, dehumidification, heatless air dryer, Molecular Sieve 13x, Activated Alumina, Silica Gel, Molecular Sieve 3A, Molecular Sieve 4A, adsorption, Artificial Neural Network.

# Acknowledgement

I thank almighty God for all his blessings. I am extremely grateful and indebted to acknowledge my respected guide **Prof. (Dr.) Pragnesh K. Brahmbhatt**, Head of Mechanical Engineering Department, Vishwakarma Government Engineering College, Chandkheda for his continuous motivation, guidance, critical review and support during this project work.

It is my honour and privilege to record my heartfelt and deep sense of gratitude to my Doctoral Progress Review Committee (DPC) members **Prof. (Dr.) Vijay D. Dhiman**, Professor, Mechanical Engineering Department, Government Engineering College, Valsad and **Prof. (Dr.) Ratnesh K. Shukla**, Head of Mechanical Engineering Department, Dr. S. and S. S. Gandhi Government Engineering College, Surat for enriching my work with their guidance, insightful comments and fruitful suggestions in doctoral progress review committee meetings.

I am thankful to **Unique Air Products** for providing technical assistance and facilities to help conduct my experimentation. I express my sincere gratitude to **Dr D. B. Jani** for providing me with his guidance and expertise in solid desiccants.

I extended my whole hearted gratitude to my parents **Jude** and **Bibiana D'souza**, my husband **Nelvin Johny** and my daughters **Leanna** and **Adlynn** without their indelible support, encouragement and love the completion of this work would not have been possible.

*Alice J. D'souza*



# Table of Contents

Abstract.....	ix
Acknowledgement .....	x
Table of Contents.....	xi
List of Figures .....	xv
List of Tables .....	xviii
List of Symbols.....	xix
Introduction.....	1
1.1 Principle of adsorption.....	1
1.2 Desiccant Materials.....	2
1.3 Liquid Desiccants .....	4
1.4 Solid Desiccants.....	7
1.4.1 Silica Gel.....	7
1.4.2 Activated Alumina .....	8
1.4.3 Molecular Sieve .....	8
1.4.3 Molecular Sieve - 3A .....	8
1.4.4 Molecular Sieve - 4A .....	9
1.4.5 Molecular Sieve - 5A .....	9
1.4.6 Molecular Sieve - 13X.....	9
1.5 Desirable properties of Desiccant .....	9
Literature Review .....	11
2.1 Introduction.....	11
2.2 Desiccant based Dehumidification technologies .....	11
2.2.1 Desiccant Wheel .....	11

2.2.2 Solar Energy Assisted Desiccant Based Dehumidification .....	18
2.2.3 Artificial Neural Network assisted Solid Desiccant-Based Technology .....	19
2.2.4 Solid Desiccant Composite Based Technology .....	20
2.2.5 Heat Pump Assisted Solid Desiccant Based Technology .....	20
2.2.6 Exergy Analysis For Solid Desiccant .....	21
2.2.7 Electro-Osmosis Regeneration for Solid Desiccant.....	21
2.2.8 Packed Bed Desiccant Based Dehumidification Systems .....	22
2.3 Literature review summary .....	29
2.4 Research Gap .....	30
2.5 Objective and scope of work .....	31
2.6 Research objectives.....	31
2.7 Scope of work .....	31
2.8 Organization of the thesis .....	31
2.9 Flowchart of Organization of the thesis.....	33
Experimentation.....	34
3.1 Design and development of the experimental set up .....	39
3.2 Experimental set up .....	40
3.2.1 Description of the experimental setup .....	41
3.2.2 Various components of the experimental set up.....	43
3.3 Performance parameters .....	50
3.4 Uncertainty Analysis.....	51
3.5 Summary.....	51
Results and Discussion .....	53
4.1 Experimental investigation results of solid desiccants used in heatless air dryer .....	54
4.2 Investigation results for heat of adsorption released across the tower for each case.	62
4.4 Validation of experimental work using Artificial Neural Network .....	74
4.5 Discussion.....	79

Conclusion .....	81
5.1 Suggestions for future work.....	82
List of References .....	84
A.1. Calibration certificate of dew point meter .....	90
A.2. Calibration Certificate for Pressure Gauge .....	91
A.3 Calibration Certificate for Hygrometer.....	92
Annexure-B: Test Certificates .....	93
B.1 Test Certificate for Activated Alumina.....	93
B.2 Test Certificate of Molecular Sieve 13X .....	94
B.3 Test Certificate for Molecular Sieve 4A .....	95
B.4 Test Certificate for Silica Gel .....	96
B.5 SEM analysis results .....	97
Annexure - C: Details of Purchase .....	98
C.1 Invoice of Desiccant Purchase .....	98
C.2 Invoice of Data Logger Purchase .....	99
Annexure-D: Experimental Data .....	100
Experimental Data .....	100
Experimental readings of Molecular Sieve 13x recorded by the dew point transmitter	101
Experimental readings of Activated Alumina recorded by the dew point transmitter ..	103
Experimental readings of Silica gel recorded by the dew point transmitter .....	106
Experimental readings of the heterogeneous mixture of Molecular Sieve 13x and activated alumina recorded by the dew point transmitter .....	108
Experimental readings of the heterogeneous mixture of silica gel and Molecular Sieve 13x recorded by the dew point transmitter .....	111
Experimental readings of the heterogeneous mixture of Molecular Sieve 4A and Molecular Sieve 13x recorded by the dew point transmitter .....	113
Experimental readings of the heterogeneous mixture of Molecular Sieve 4A and silica gel recorded by the dew point transmitter .....	115

Experimental readings of the heterogeneous mixture of activated alumina and Molecular Sieve 4A recorded by the dew point transmitter.....	117
Experimental readings of testing on Molecular Sieve 4A used to train ANN.....	119
Experimental readings of testing on silica gel used to train ANN.....	131
ANNEXURE-E Uncertainty Analysis.....	136
ANNEXURE-F List of Publications.....	139

# List of Figures

FIGURE 1. 1 Desiccant dehumidification and cooling principle (Rambhad et al., 2016) ....	2
FIGURE 1. 2 Relationship between vapor pressure and water content in dehumidification process. (Fu & Liu, 2017).....	3
FIGURE 1. 3 The basic functioning of an air-conditioning system that uses liquid desiccant (Fu & Liu, 2017).....	4
FIGURE 2. 1 The air conditioning system is based on desiccant wheels (Zouaoui et al., 2016). ....	12
FIGURE 2. 2 (a) Conventional packed beds and (b) intercooled packed beds make up the physical model of a silica gel bed operating in adsorption mode (A. Ramzy et al., 2015).....	24
FIGURE 2. 3 Schematic showing the flow of a two-desiccant vertical packed bed dehumidifier (A. K. Ramzy et al., 2013).....	25
FIGURE 2. 4 a) Typical silica gel particle. b) Suggested silica gel composite particle.....	26
FIGURE 2. 5 A dehumidification system that utilizes a fixed bed and a moisture damper (San et al., 2002). ....	27
FIGURE 2. 6 A test-based setup(Pesarant & Mills, 1987).....	27
FIGURE 2. 7 Schematic of a two-tower solid desiccant dehydrator(Gandhidasan et al., 2001). ....	28
FIGURE 2. 8 Plot depicting extent of research done in various domains of solid desiccant dehumidification. ....	29
FIGURE 3. 1 S.E.M image of Silica gel solid desiccant .....	34
FIGURE 3. 2 S.E.M image Molecular Sieve 13x of solid desiccant.....	35
FIGURE 3. 3 S.E.M image of Molecular Sieve 3A solid desiccant.....	35
FIGURE 3. 4 S.E.M image of Molecular Sieve 4A solid desiccant.....	35
FIGURE 3. 5 S.E.M image of Activated Alumina solid desiccant .....	36
FIGURE 3. 6 Actual image of Silica gel solid desiccant used for experimentation.....	36
FIGURE 3. 7 Actual image of Molecular Sieve 3A solid desiccant used for experimentation.....	37
FIGURE 3. 8 Actual image of Molecular Sieve 4A solid desiccant used for experimentation.....	37

FIGURE 3. 9 Actual image of Molecular Sieve 13x of solid desiccant used for experimentation. ....	38
FIGURE 3. 10 Actual image of Activated Alumina solid desiccant used for experimentation. ....	38
FIGURE 3. 11 Experimental test rig diagram .....	42
FIGURE 3. 13 Detailed view of the experimental set up with Laptop and Data Logger attached. ....	42
FIGURE 3. 15 External Image showing crown of the tower with wire mesh seal to prevent desiccant carryover in the process line .....	44
FIGURE 3. 14 Image of 4" diameter, 18 " height, 4mm thickness, SA1239 pipe used for tower fabrication. ....	43
FIGURE 3. 16 Internal Image showing crown of the tower with wire mesh seal to prevent desiccant carryover in the process line .....	44
FIGURE 3. 17 Image of the sub assembly fabrication .....	45
FIGURE 3. 18 Image depicting the fabricated test rig assembly of the desiccant towers with the pre filter , after filter and carbon filter. ....	45
FIGURE 3. 19 Image depicting the test rig assembly with the control panels, pressure gauges and solenoid valve. ....	46
FIGURE 3. 20 Dew point meter for testing outlet air dew point temperature .....	46
FIGURE 3. 21 Image of the final test rig with the thermowell testing facility across the length of the tower. ....	47
FIGURE 3. 22 Assembly and testing.....	47
FIGURE 3. 23 Dew point transmitter .....	48
FIGURE 3. 24 Dew point Transmitter with Digital Indicator .....	48
FIGURE 3. 25 Data logger with RS435 to USB converter. ....	49
FIGURE 3. 26 Temperature Indicator with sensing probe .....	49
FIGURE 3. 27 Hygrometer for measuring Humidity .....	50
FIGURE 4. 1 Plot depicting variation of dew point temperature with time recorded by data logger when Activated Alumina is is used in the heatless air dryer. ....	55
FIGURE 4. 2 Plot depicting variation of dew point temperature with time recorded by data logger when Molecular Sieve 13x is used in the heatless air dryer. ....	55
FIGURE 4. 3 Plot depicting variation of dew point temperature with time recorded by data logger when mixture of Molecular Sieve 13x and activated alumina is used in the air dryer. ....	56

FIGURE 4. 4 Plot depicting variation of dew point temperature with time recorded by data logger when silica gel is used in the heatless air dryer. ....	56
FIGURE 4. 5 Plot depicting variation of dew point temperature with time recorded by data logger when Molecular Sieve 4A is used in the heatless air dryer. ....	57
FIGURE 4. 6 Plot depicting variation of dew point temperature with time recorded by data logger when mixture of Silica gel and Molecular Sieve 4A is used in the heatless air dryer. ....	58
FIGURE 4. 7 Plot depicting variation of dew point temperature with time recorded by data logger when mixture of Molecular Sieve 13x and Molecular Sieve 4A is used in the heatless air dryer. ....	58
FIGURE 4. 8 Plot depicting variation of dew point temperature with time recorded by data logger when mixture of Activated Alumina and Molecular Sieve 4A is used in the heatless air dryer. ....	59
FIGURE 4. 9 Plot depicting variation of dew point temperature with time recorded by data logger when mixture of Silica Gel and Molecular Sieve 13x is used in the heatless air dryer. ....	60
FIGURE 4. 10 Plot depicting variation of dew point temperature with time recorded by data logger when mixture of Silica gel and Activated Alumina is used in the heatless air dryer. ....	60
FIGURE 4. 19 Temperature variation along the adsorption tower using Molecular Sieve 4A.....	68
FIGURE 4. 20 Temperature variation along the regeneration tower using Molecular Sieve 4A as the desiccant.....	68
FIGURE 4. 24 Temperature variation along the regeneration tower using mixture of Molecular Sieve 4A and Molecular Sieve 13x as desiccant. ....	70
FIGURE 4. 28 Temperature variation along the regeneration tower using mixture of Silica gel and Molecular Sieve 13x.....	72
FIGURE 4. 33 Comparisons between ANN predictions for outlet dew point temperature with experimental results .....	76
FIGURE 4. 35 Comparisons between the ANN predictions and experimental results for the rate of moisture removal of the dryer.....	78
FIGURE 4. 36 Comparisons between the ANN predictions and experimental results for the effectiveness of the dryer. ....	78

# List of Tables

Table 4. 1 Results table of experimental test for case 1 to 10. ....	61
Table 4. 2 Digressions of the absolute and percentage errors of the neural network for the testing data .....	76



# List of Symbols

$M$  = Total water absorbed, kg

$t$  = Temperature, °C

$P$  = Pressure, MPa

$p$  = Pressure, kPa

$c$  = Drying cycle, hours

$W$  = Water content of gas, kg/106 Std m<sup>3</sup>

$V$  = Volume, m<sup>3</sup>

$D$  = Bed Diameter, m

$Q$  = Gas flow rate, 106 Std m<sup>3</sup>/day

$Z$  = Compressibility factor, dimensionless

$v$  = Superficial gas velocity, m/min

$w$  = Wall thickness, m

Subscripts

$B$  = Bed

$V$  = Vessel

$D$  = Desiccant

$G$  = Gas

# CHAPTER – 1

## Introduction

The increase in ozone depletion and global warming potential is a cause of concern to all of mankind. It is extremely essential that efforts must be made to reduce the global warming effect. One of the contributors to ozone depletion are CFCs which are used in conventional refrigeration and air conditioning equipment. Researchers are constantly trying to find alternatives to these CFC dependent technologies. One such domain of refrigeration which has gained substantial attention in the past decade is that of dehumidification of air. Dehumidified air is essential in many industries such as pharmaceutical, printing press, textiles, painting and food preservation which are some of them. In pneumatics, the presence of vaporized water in compressed air systems will hasten the initiation of corrosion, which may then block the circulating tubing and lessen process effectiveness. Additionally, the life span of sensitive equipment will be shortened by suspended water vapour, requiring frequent and expensive replacements. Air can be dehumidified by use of desiccants which are a greener alternative to the conventional VCR systems which are dependent on CFCs. Desiccant based dehumidification can be achieved by use of solid or liquid desiccants. The commonly used solid desiccants are silica gel, activated alumina, molecular sieves while commonly used liquid desiccants are calcium chloride, lithium bromide, and lithium chloride. Solid desiccants are preferred over liquid desiccants as they do not pose the hazard of carryover in the process air stream and are not corrosive in nature. Dehumidification in an air stream using solid desiccants is achieved through the principle of adsorption.

### 1.1 Principle of adsorption

Adsorption is the process of retaining one substance inside another through physical bonding on the complex network of inner surface. A film of adsorbate is formed on the surface of the adsorbents even though the desiccants won't chemically interact. It is an exothermic process because when the water vapour is adsorbed, heat energy is released. As can be seen in Figure 1.1, it involves contacting a liquid or vapour with a packed column, allowing the contaminating or unwanted species to rest in the column, and allowing the continuous vapour

or liquid to pass through the column. The packed column could be stationary or moving in the opposite direction. Thermal or other methods can be used to replenish the adsorbed bed. Adsorption is mainly a transitory phenomenon.

Desiccant material can be regenerated by low grade heat sources like solar energy, waste heat, natural gas etc. Desiccants, broadly classified as solid and liquid desiccants, have the property of extracting and retaining moisture from air brought into contact with them. By using either type, moisture in the air is removed and the resulting dry air can be used for air-conditioning or drying purposes[1] When solid desiccant is employed, the desiccant dehumidification system consist of slowly rotating desiccant wheel of adsorbent bed. In liquid desiccant based dehumidification liquid desiccant is brought in contact with the moist air stream[2]

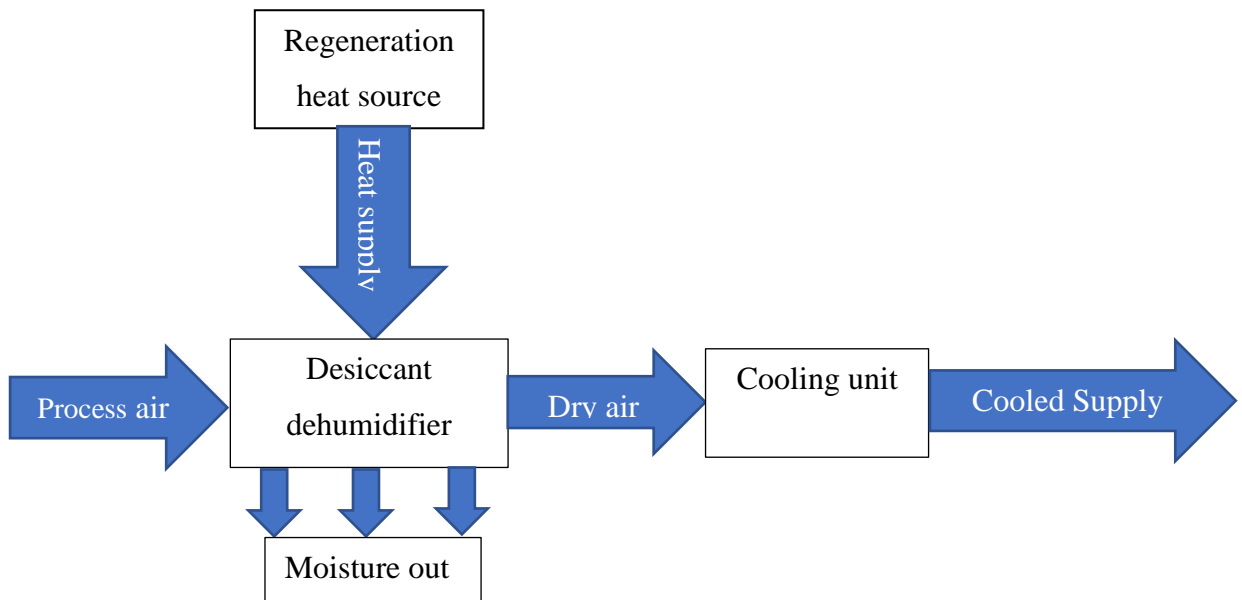


FIGURE 1. 1 Desiccant dehumidification and cooling principle [2]

## 1.2 Desiccant Materials

A desiccant is a material that has a strong attraction for water vapor. It may be classified into many ways e.g., solid or liquid desiccants, physisorption or chemisorption desiccants, natural or artificial desiccants, bio or rock-based desiccants, composite and polymer-based desiccants etc. The term physisorption or chemisorption reflects the strength of the bond between the adsorbate and adsorbent. The removal of water vapors from the air is normally considered as physisorption because of low bond strength between adsorbate and adsorbent

[3]Both solid and liquid desiccants are commonly used in industrial applications where low dew-point air is needed. Solid desiccants are also increasingly being used in HVAC systems to either increase an air conditioner's latent cooling or recover total energy from the building exhaust. The strength of a desiccant can be measured by its equilibrium vapor pressure (i.e., pressure of water vapor that is in equilibrium with the desiccant). This equilibrium vapor pressure increases roughly exponentially with the temperature of the desiccant/water system. It also increases as the desiccant absorbs water (a dilute liquid desiccant will have a higher equilibrium vapor pressure than a concentrated liquid desiccant)[4]

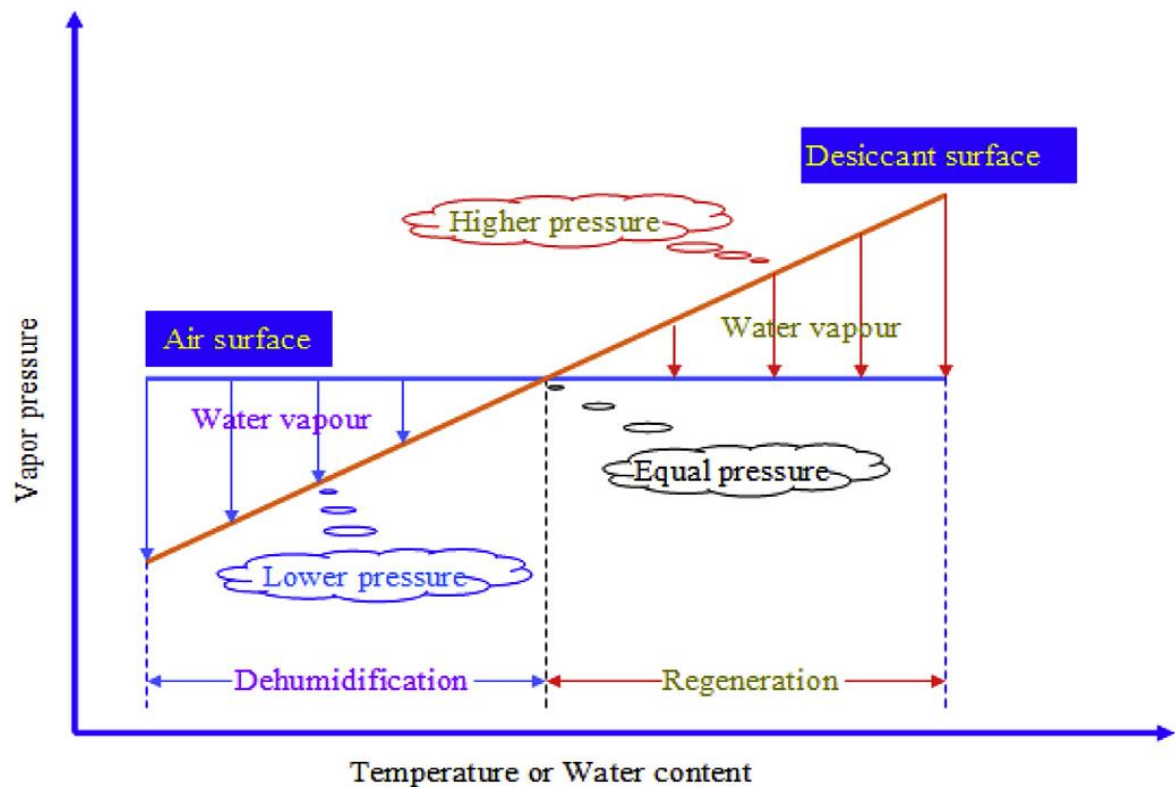


FIGURE 1. 2 Relationship between vapor pressure and water content in dehumidification process[5]

The driving force for mass transfer is the surface vapor pressure difference as depicted in Figure 1.2[5]. Desiccants have the property of extracting and retaining moisture from the air brought into contact with them. For dehumidification to occur, the vapor pressure of water above the desiccant solution must be lower than the partial pressure of water in the air. In other words, the driving force for dehumidification is the difference of the partial pressure of water in the air and the vapor pressure of water above the desiccant solution. Hence, the performance of a desiccant can be measured by its vapor pressure. The lower the vapor pressure, the better a desiccant performs [1].

### 1.3 Liquid Desiccants

In order to be suitable for use in HVAC systems, a liquid desiccant must be non-corrosive and non-volatile. LiCl, LiBr, CaCl<sub>2</sub>, and triethylene glycol (TEG) are the types of liquid desiccants that are utilised in industrial settings the most frequently. Although it has the lowest vapour pressure and is the most stable liquid desiccant, the cost of LiCl is quite high [6]. Using LiCl in conjunction with CaCl<sub>2</sub>, which is not only easily accessible but also the most cost-effective desiccant, is a solution to the problem of LiCl's high cost. Because of the qualities it possesses. Lithium chloride is the most stable liquid desiccant and has a considerable dehydration concentration, which ranges from 30% to 45%, however the cost of lithium chloride is very high. It is anticipated that lithium chloride will have a drying effect on the air, lowering the relative humidity to as low as 15%.

The downside of using calcium chloride as a desiccant is that it can be unstable depending on the air inlet conditions and the concentration of the desiccant in the solution. Nonetheless, calcium chloride is the most readily accessible and reasonably inexpensive desiccant. The two substances can be blended in a variety of proportions to achieve the desired effects of stabilizing calcium chloride and reducing the high cost of lithium chloride [1]. To improve the characteristics of a single desiccant material such as to improve its absorption capability and to lower its regeneration temperature, a number of composite desiccant materials have been developed [6].

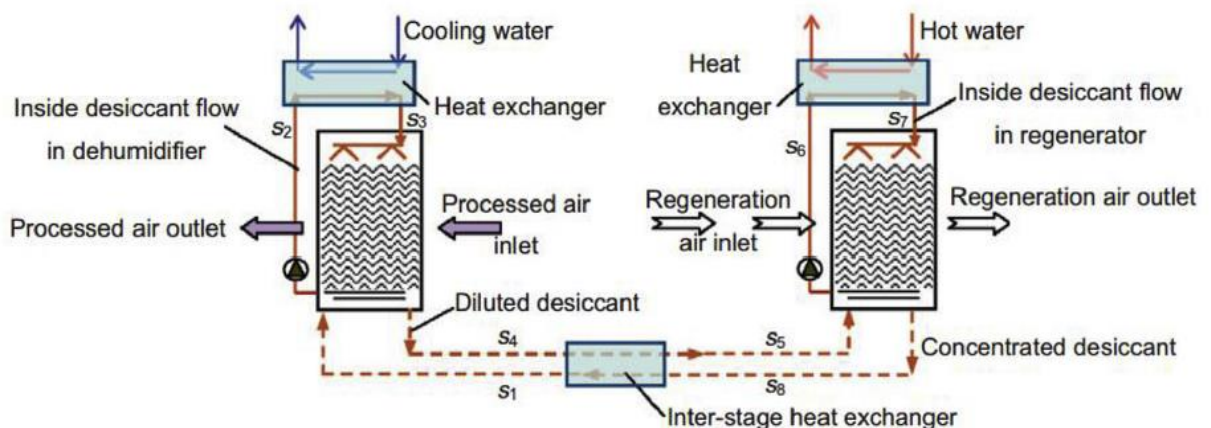


FIGURE 1. 3 The basic functioning of an air-conditioning system that uses liquid desiccant [5]

In a liquid desiccant air-conditioning system as seen in Figure 1.3 concentrated liquid desiccant from the regenerator comes to the dehumidifier, after being cooled by the diluted desiccant from dehumidifier in the inter-stage heat exchanger; The concentrated desiccant is

mixed with the desiccant in the tank of dehumidifier, then pumped into the cooling water heat exchanger, and finally sprayed into the packing and contacts the processed air; The diluted desiccant from dehumidifier then comes to the regenerator to be re-concentrated. The liquid desiccant includes organic desiccant, such as TEG solution, and inorganic salt solutions, such as LiBr solution, LiCl solution, and  $\text{CaCl}_2$  solution. TEG solution is the earliest solution utilised in LDAS. However, TEG solution is gradually replaced by some salt aqueous solutions, such as LiBr solution and LiCl solution, as the organic ingredient may evaporate into the processed air. Compared with organic liquid desiccants, salt solutions (LiBr, LiCl or  $\text{CaCl}_2$  solution) won't vaporize into air under ambient conditions[5]

The desiccant dehumidifier is considered the most important component of a liquid desiccant cooling system, which is almost often an adiabatic type or an inner cooled system. A high flow rate is necessary for the adiabatic kind of dehumidifier in order to ensure that the surface is thoroughly wetted, which prevents desiccant carry over. Using a dehumidifier that has its own internal cooling system is one way to get around the issue of required high flow rates and carry over. A rotary type of liquid desiccant dehumidifier was proposed so that there would be a lower pressure drop and no desiccant carry over. This dehumidifier would use a porous medium, such as thick cloth, to transport the desiccant solution inside of a rotor disc. This would allow for a lower pressure drop. Possibility to mitigate the corrosive effects of a desiccant by operating the dehumidifier and the regenerator at a very low flow rate for the desiccant were investigated. Continuous cooling of the desiccant in the dehumidifier is found to be essential for the system to operate at these low flow rates. This has been accomplished by a large number of researchers who have proposed various configurations of inner cooled dehumidifiers in order to meet this requirement. In order to solve the issue of droplet carryover, an innovative type of liquid–air membrane heat and mass exchanger in a counter flow arrangement was suggested for use as a dehumidifier because of the superior performance it offers. In addition, the development of a multistage membrane-based liquid desiccant dehumidifier would be the next step in the evolution of systems for liquid desiccant dehumidification. The performance of the desiccant dehumidifier is heavily dependent on the choice of packing material, as well as the arrangement of that material and the flow pattern that it creates. Further research needs to be done in the field in order to build and define liquid desiccant cooling systems that are capable of replacing traditional air conditioners in a comfortable manner [6].

A simplified model of a packed bed regeneration process in which the desiccant solution is heated in any of the two ways. With method A, the desiccant solution is heated in a heat exchanger with a fluid (water) heated by any low-grade thermal energy such as solar energy or waste heat sources. While in method B, the desiccant solution is heated by a conventional energy source such as a line heater. The adapted simplified model shows very good agreement with the experimental results available in the literature. With method B, the desiccant is heated by a conventional energy source and it is found that the water evaporation rate increases with the heat input and as the scavenging air flow rate increases the regeneration rate decreases [7].

Fu and Liu, [5] discussed the safety of liquid desiccant dehumidification due to the carryover of liquid desiccant. A review of the impact of liquid desiccant dehumidification on IAQ was conducted. It summarizes the research achievements related to the VOCs removal capability of liquid desiccant solution from indoor air. The deactivation effect of liquid desiccant solution on bacteria and virus was studied.

Misha et al., [8] observed that desiccant system in drying application has several advantages including continuous drying even during off-sunshine hours, increased drying rate due to hot and dry air, more uniform drying, and increased product quality especially for heat-sensitive products. The use of heat to regenerate desiccant material in a drying system was noted to have limitations in energy saving. Therefore, the desiccant material with low regeneration temperature is preferred.

Giampieri et al., [9] presented an overview which was intended to be a starting point in the determination of viable alternatives to halide salts solutions as working fluid, being able to overcome their main drawbacks, such as corrosion and crystallization issues. Towards this direction, ionic liquids seem to be a promising solution. Their employment in absorption technologies has been largely described in the past and seems feasible in liquid desiccant air-conditioning systems. The characteristics of low-vapour pressure, low density and viscosity, high solubility and non-corrosion to metals make this fluid an important and promising candidate for employment in the system that needs to be further investigated to get the best out of LDAC technology.

In general, using liquid desiccant in the construction of a dryer is more complicated than using solid desiccant because handling solid desiccant material is easier. Solid desiccant

systems are normally in the form of stationary or rotary wheel beds for packing the desiccant materials [8].

## **1.4 Solid Desiccants**

The adsorption of water vapour from the surrounding air is the fundamental operating mechanism of solid desiccant cooling systems. When the air that is being processed moves through the desiccant material, solid desiccant materials induce a pressure drop in the air. A revolving desiccant wheel is used in a solid desiccant cooling system. This wheel is responsible for removing moisture from the ventilated or recirculated process air. After that, the temperature of this process air that has been dried is decreased even more to the conditions that are wanted for the space by using sensible heat exchangers and cooling coils. In order to keep the system operating normally, the amount of water vapour that was absorbed by the rotating desiccant wheel must be driven out of the desiccant material. This allows the material to become sufficiently dry, which is what is meant by the term "regenerated," so that it can once again adsorb water vapour during the subsequent cycle. This is accomplished by heating the desiccant material to the temperature of regeneration, which varies with the type of desiccant that is being utilized. The rotary desiccant wheel receives the energy it needs to regenerate from a regeneration heat source, which could be an electrical heater, solar heat, or waste heat [10] Various solid desiccants are commercially available and are being used for different applications of solid desiccant systems. They are as discussed below:

### **1.4.1 Silica Gel**

Silica gel is a naturally occurring material that is non-toxic, odorless, and commonly produced into beads. It has a porosity of more than 70% of its surface area and can reach  $650 \text{ m}^2/\text{g}$ , with pore sizes ranging from 2 -3 nm (type A) to 0.7 nm (type B) with a heat absorption capability of roughly 2800 kJ/ kg. [3]Silica gel adsorbs water quickly and its retention capacity is high, whereas micro porous silica gel absorbs water slowly. To eliminate moisture from silica gel, a temperature of  $90^\circ$  to  $150^\circ\text{C}$  is usually required for regeneration. Singh et al., [11] Sultan et al., [3]Because of its thermal stability and better water vapour adsorption capacity than other desiccants, silica gel is the most commonly utilised desiccant material in commercial units [12].



### **1.4.2 Activated Alumina**

Dehydroxylating aluminum hydroxide produces activated alumina, which has a larger surface area. It has a surface area of 150–500m<sup>2</sup>/g, pore diameters ranging from 1.5 to 6 nm, and an adsorption heat of almost 3000kJ/kg . It's been used for desiccant dehumidification several times and produces interesting result [3]The temperature and duration of the thermal process, as well as the gases utilised to produce alumina, can influence its structural features [11]

### **1.4.3 Molecular Sieve**

Molecular Sieves, also known as synthetic zeolite, have a high moisture adsorption capacity and are thus used for various moisture removal and air conditioning applications. It is a crystalline material of aluminum silicate which is capable of separating molecules of different sizes by sorption. Molecular Sieve materials are used exclusively for the dehumidification of air to a very low level of humidity and extremely low dew points of about -40 °C to -60 °C. For the same reason, the Molecular Sieve has a better sorption capacity at higher temperatures than other sorbents[3] .The use of zeolite made from fly ash for solar cooling applications has demonstrated to be very promising. Composite desiccants are made up of synthetic zeolite and silica gel, and they have good adsorption properties in both low and high relative humidity, allowing for thorough dehumidification. Clinoptilolite, a natural zeolite, was used to study water sorption, although the amount of dehumidification was found to be smaller than that of silica gel and alumina. It's also thought that zeolite might only be considered for water sorption applications if it's economical[2] Molecular Sieves are classified on the basis of the pore size. Some of the commonly used Molecular Sieves are follows:

#### **1.4.3 Molecular Sieve - 3A**

The pore size of a 3A sieve is 3 angstrom. It can't adsorb anything bigger than 3A molecules. The potassium version of the type A crystal structure, Molecular Sieve, is an alkali metal alumino-silicate. 3A Molecular Sieve is typically used to remove moisture from liquid or gaseous materials. It has established itself as one of the most dependable desiccants for a variety of applications.

#### **1.4.4 Molecular Sieve - 4A**

The pore size of a 4A Molecular Sieve is 4 Å or 4 angstrom. Any molecule greater than 4A, it does not adsorb. The sodium forms of the type A crystal structure are 4 angstroms. The main application of a Molecular Sieve is to remove moisture from liquid and gaseous materials.

#### **1.4.5 Molecular Sieve - 5A**

The pore size of a 5A Molecular Sieve is 5 Å. It can't adsorb anything less than 5 Å molecules. Alkali aluminosilicates in the calcium form of Type A crystal structure make up this Molecular Sieve. Separation of normal and isomeric alkanes, co-adsorption of carbon dioxide and moisture, and pressure swing adsorption (PSA) for gases are the most common applications.

#### **1.4.6 Molecular Sieve - 13X**

The pore size of 13x Molecular Sieves is about 10 Å. This is a much larger opening than any of the A type openings. Because it delivers synchronized absorption for bi-molecule and tri-molecule, this desiccant is widely utilised for gas and liquid refining. It has the ability to co-adsorb CO<sub>2</sub> and H<sub>2</sub>O, as well as H<sub>2</sub>O and H<sub>2</sub>S. 13x Molecular Sieves have also been used as a desiccant in medical applications, compressors, and as a catalyze carrier in air conditioners [2]

### **1.5 Desirable properties of Desiccant**

- The solid desiccants must have large surface area for high capacity and high mass transfer rate.
- They must possess a high bulk density and activity for the components to be removed.
- They must be easily and economically regenerated.
- The resistance to gas flow through the desiccant bed must be small to have low pressure

drop since the unit cost is sensitive to pressure drop.

- They should have high mechanical strength to resist crushing and dust formation.
- They must be fairly cheap, non-corrosive, non-toxic, and chemically inert.
- There should be no appreciable change in volume during adsorption and desorption, and should retain strength when wet.

It is possible to draw the conclusion that no single desiccant possesses all of the ideal features that are desired; however, it is necessary to choose the desiccant that is the most suitable for the application. The vast majority of researchers have worked on applications based on desiccant wheels, with silica gel being the desiccant of choice in most cases. despite the fact that only a small percentage of people have investigated the packed bed desiccant dehumidification device. On the heatless air dryer-based applications, which are employed for compressed air dehumidification, there is scant literature available. Hence a systematic study is conducted in the next chapter to understand the technological advancements in the field of solid desiccant-based dehumidification system. In order to investigate the many technological breakthroughs that have been made in the sector of solid desiccant dehumidification. Laying emphasis on the amount of work done utilizing desiccant wheel as well as the number of possibilities for study, in the field of packed bed.

# **CHAPTER -2**

## **Literature Review**

### **2.1 Introduction**

As a result of the aforementioned factors in the previous chapter, an exhaustive literature analysis is provided in this article to emphasize the technological developments that have been made in the sector of solid desiccant dehumidification. A literature review is presented for the utilization of solid desiccants in desiccant wheels, packed beds, heat pumps, as well as the utilization of solar energy and electro osmosis for regeneration, which carries good potential for development, and the application of artificial neural networks in solid desiccant based technologies. This evaluation acts as a detailed road map that identifies the research gap as well as the goals of the study that was carried out for this thesis.

### **2.2 Desiccant based Dehumidification technologies**

Dehumidification with the help of solid desiccants has gained much attention in the past decade. Researchers have used different techniques to utilize solid desiccants in order to dehumidify process air. Application of desiccant wheel, packed bed to dehumidify air were found to be the most popular choice. Innovations in utilizing solid desiccants coupled with heat pump and use of electroosmosis for regeneration have also caught the attention of many. Potential of regeneration of solid desiccants by using solar energy has been quite successful. Researchers have used artificial neural network to predict the effectiveness of dehumidification caused by solid desiccants. Many have carried out exergy analysis for solid desiccants. A detailed literature review conducted below reveals the advancements achieved in these above segments of desiccant based dehumidification.

#### **2.2.1 Desiccant Wheel**

In desiccant systems, the sensible load is accomplished by direct and/or indirect evaporative coolers, while the latent load is accomplished by the desiccant itself. There are two separate

airflows present in desiccant cooling systems. As can be seen in Figure 2.1, the first stream is the process air that is brought into the conditioned space, and the second stream is the activation air that is utilised to regenerate the desiccant material[13]

A desiccant wheel has been the subject of a number of researches that have been carried out by a variety of researchers in an effort to improve dehumidification [14]. A method for determining the system's feasible operating range under a predetermined set of comfort parameters was offered using a case study of a solar desiccant air conditioning system. Panaras et al., [15] emphasized the significance of the values of air flow rate and regeneration temperature in not only determining the size of the desiccant system but also the size of the thermal energy system and the degree of energy efficiency.

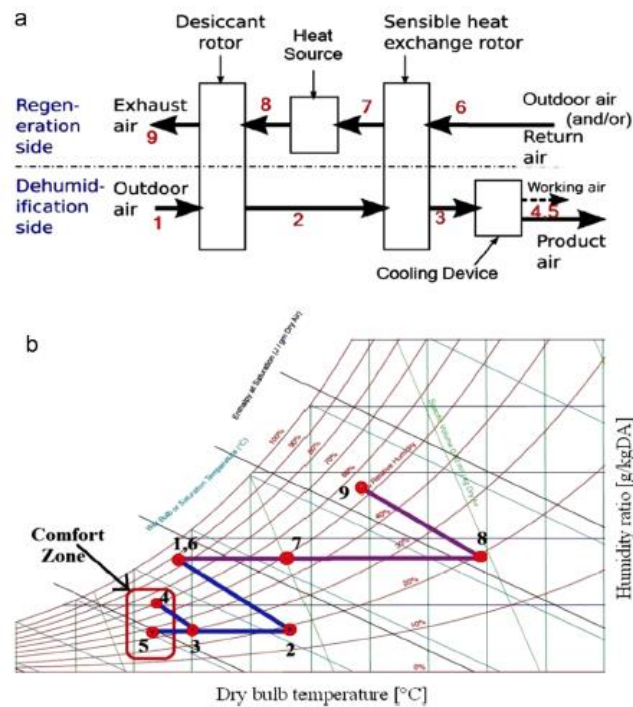


FIGURE 2. 1 The air conditioning system is based on desiccant wheels [13]

Eicker et al., [16] found that the rotation speed that is ideal for lithium chloride or compound rotors is lower than the rotation speed that is ideal for silica gel rotors. Greater regeneration air temperatures lead to increased dehumidification potentials at almost the same level of dehumidification efficiency. This is because rising regeneration specific heat input and process air enthalpy fluctuations cause regeneration air temperatures to rise. The dehumidification potential is increased by low relative humidities, and the degree to which regeneration air humidity played a role was substantial. The data also show that even though

there is not a significant impact on the dehumidification efficiency and that both the specific regeneration heat input and the latent heat change of the process air drop, the dehumidification capacity increases as the water content of the ambient air rises. This is the case even though the specific regeneration heat input and the latent heat change of the process air drop.

In vapor-compression cooling systems, passive desiccant wheels are often employed as an energy-saving method to relieve the cooling coil of the burden of controlling the humidity of the ventilation air stream from the outside. Active desiccant wheels, on the other hand, are designed to stimulate full dehumidification of external ventilation air. This, in turn, frequently makes it possible to employ an evaporative cooler, which not only provides a visible cooling effect but also uses only water as the refrigerant. It was discovered that during the process of passive dehumidification, heat transfer and mass transfer have opposing effects on the enthalpy recovery. As a result, the efficiency of the enthalpy recovery is not affected by the conditions of the atmosphere. When it comes to active dehumidification, it has been shown that heat transfer and mass transfer have interactions that are favourable to one another. Specifically, the dehumidification capacity increases with the regeneration temperature until the maximum dehumidification capacity is reached. The research demonstrates that silica gel is capable of effectively dehumidifying the air even at temperatures below its reactivation point. This paves the way for the system to be powered by solar energy or low-grade waste heat

Angrisani et al., [17] emphasized that it is widely known that the rotational speed of the desiccant wheel is an important factor: if the wheel turns too rapidly, the desiccant material won't have enough time to remove the moisture; on the other hand, if it rotates too slowly, saturation may occur. As a consequence of this, there ought to be a perfect spinning speed that, depending on the operational conditions, ensures the highest possible performance in terms of dehumidification. It is important to choose desiccant wheels that have a high dehumidification performance and a sufficiently low outlet temperature in order to reduce the cooling load that is placed on the cooling device. This is especially important if a conventional vapour compression chiller is used, which is typically the case in high humidity climates. The rate at which the desiccant wheel rotates is another factor that influences the temperature of the process air as it emerges from the wheel. The authors presented through experimental tests how the performance of a silica gel desiccant wheel is affected by the

spinning speed of the wheel. The adsorbent material was regenerated using thermal energy of up to 65°C.

Guidara et al., [18] created a design for a solar air conditioner in which a heat exchanger and humidifier are primarily used to assure cooling function. Also, a modelling analysis is described in depth for each part of the solar air conditioning unit. According to the simulation study, three modes of operation are represented by three different climate cases: relatively chilly and humid for Bizerte, hot and dry for Remada, and finally moderate for Djerba. The findings demonstrate that the solar air conditioning system can meet comparable needs satisfactorily, and the conditioned air produced in each mode of operation can ensure that office workers are in comfortable surroundings.

Narayan et al.,[19] found primary disadvantage of conventional desiccant wheels is the overheating of the desiccant material and supply air during dehumidification. As a result, less moisture can be drawn out of the air and the partial pressure of water on the desiccant material increases. A non-adiabatic desiccant wheel design has been looked upon to solve this issue. With alternative pathways for dehumidification and indirect cooling of the dehumidification process, this innovative wheel includes an internal heat transfer structure.

Guan et al., [20] suggested to use two-stage desiccant wheels in an unique desiccant wheel dehumidification and preheating system (DWDP) for blast furnaces. The trial results show that the DWDP's capacity to remove moisture may increase to 8.7 g/kg, which will increase steel production by 0.9% and save 2100 tonnes of coal annually. The DWDP would reduce energy usage by the cooling tower's slag flushing water by 7.3%.

Intini et al., [21] using the experimental data, created a one-dimensional, time-dependent numerical model and calibrated with root mean square deviations for the temperature and humidity ratio of the process exit of 0.99 °C and 0.66 g/kg, respectively. The maximum moisture removal capacity can only be reached with an equal area split, and higher process area ratios only increase latent cooling in the high regeneration temperature range. Additionally, moisture removal efficiency was found to be strongly correlated with inlet humidity ratio and only weakly correlated with process inlet temperature.

Misha et al., [22]with low sun radiation, kenaf core fiber was dried using a solid desiccant dryer with solar assistance. Through the employment of a heat exchanger and a solar collector, heat was transferred from the water to the air. After dehumidification, the hot air

was used to regenerate the desiccant wheel and raise the temperature of the process air. The drying chamber receives hot, dry air from the desiccant wheel system as a heat source. For comparison, drying outside in the sun was also done simultaneously. When compared to open sun drying, the drying time with this system was cut in half by 24%, from 20.75 hours to 15.75 hours, because the dryer system allows the drying to continue even when there is no sunlight. Dryer efficiency is around 12% at average solar radiation of  $394 \text{ W/m}^2$ .

Tu et al., [23] analyzed the effectiveness of desiccant cooling and dehumidification systems. Six different types of systems (systems A-F) were examined based on theoretical research as the system went from being reversible to being irreversible, drastically decreasing performance. System E, which includes a desiccant wheel, heat recovery exchanger, and single-stage heat pump, exemplifies the relatively high performance requirements that real-world systems can reach. System E has a COP and exergy efficiency of 5.0 and 18.3% under optimal circumstances of operation.

Jani et al., [24] found after passing through the rotating desiccant dehumidifier, the humidity ratio of the process air drops from  $18.5(\text{g/kg dry air})$  to  $7.10(\text{g/kg dry air})$ , allowing the system to function well even in hot and humid climates. Thus, the low dew point temperature of the evaporator cooling coil and subsequent warming are unnecessary when a desiccant dehumidifier is used as part of a hybrid cooling system to drastically reduce latent load.

Jani et al., [25] built an ANN (artificial neural network) model in order to foretell the cooling capacity, power input, and COP (coefficient of performance) of a solid desiccant vapour compression hybrid air-conditioning system. The majority of the data from the experiments were utilised to train the ANN model, while the remaining 20% were used to test the model. A strong connection ( $R > 0.988$ ) between the ANN model's anticipated outputs and actual system performance was found.

Misha et al., [26] used a solar-powered, solid desiccant dryer to dry crushed oil palm fronds. The solar collector heated the water, and then the water was used to heat the air via two heat exchangers. Drying air after dehumidification is heated using the hot air to facilitate desiccant wheel regeneration. Sun drying took around 30 hours and forty minutes to reduce the moisture content of crushed oil palm fronds from 69% to 29%. With a sensible and latent effectiveness of 74% and 67%, respectively, the desiccant wheel helped to improve drying air quality. Because solar energy was employed as the principal energy source, the



combination of desiccant and solar dryer resulted in better drying air condition, enhanced drying performance, and spent low electrical energy.

Tu et al.,[23] explored the efficiency of ventilation systems that employed desiccant wheel cooling. Suggestions were provided for effective system design based on the inherent influencing variables for exergy destructions of heat and mass transmission and heat sources. This is because the heat pump's exergy destruction was much lower than the exergy destruction of the heat source in the basic ventilation system and the first system, resulting to a significant increase in COP and exergy efficiency.

Zendehboudi.,[27] developed a novel hybrid model, which is based on least squares support vector machine (LSSVM) and genetic algorithm, and is able to accurately predict the dehumidification efficiency ( $g_{deh}$ ), moisture removal capacity (MRC), and sensible energy ratio (SER) for Silica Gel (WSG) and Molecular Sieve (LT3) materials under varying suction conditions. These three metrics are: dehumidification efficiency ( $g_{deh}$ ), moisture removal capacity (MRC), and sensible energy ratio (SER) (GA). With an MAE of less than 0.23, an  $R^2$  of better than 0.994, and an MSE of less than 0.072, the results showed that combining LSSVM with GA is an effective strategy for DW prediction. This was demonstrated by the fact that  $R^2$  was greater than 0.994.

Fong and Lee [28] stated that (Desiccant Cooling System) DCS could only be used with high-quality renewable energy or waste heat sources. As the DCS benefited from a solid desiccant wheel spinning at a high speed in conjunction with a sensible heat exchanger because it could not rely on regeneration heat. The desiccant wheel, sensible heat exchanger, and regenerative air evaporative cooler should all be operated at moderate speeds by the DCS when regeneration heat is present. Results showed that the performance coefficient dropped along with the regeneration temperature in this case. In addition, it was found that the regeneration temperature should be greater than 60 °C; otherwise, the DCS would perform much worse than it does without regeneration heat.

Fong and Lee [29] studied the various adsorbent characteristics and how they influence the performance of the desiccant wheel. Because different wheels have different physical properties, the results of the measurements will not be representative of the only influence that the adsorbents have on the situation. The relative effectiveness of desiccant wheels loaded with RD silica gel (SG), AQSOA-Z02, and CECA-3A was evaluated with the help

of computer simulations, and the results were compared with one another. The adsorption isotherms show that AQSOA-Z02 had a higher capacity for dehumidification. In general, the SG-based desiccant wheel will have better performances than other wheels due to its lower heat of adsorption. The CECA-3A ranked 29th among all dehumidifiers that were evaluated due to its limited capacity to absorb moisture.

Goodarzia et al.,[30] conducted analysis of the effects of air humidity ratio, regeneration process and air process temperatures, mass flow rates, and wheel revolution on the performance of a solid desiccant wheel.

Jani et al., [31] demonstrated that ANNs can be used to more accurately predict the efficiency of solid desiccant cooling systems. Air streamflow rates, temperature and humidity ratios, pressure drop, dehumidifier efficiency, cooling capacity, regeneration temperature, power input, coefficient of performance, and a number of other input and output parameters were used to test the trained ANN model's ability to predict the system's performance.

Narayan [32] investigated the rotor structure which was covered with the desiccant substance. The matrix has many channels that run parallel to the rotational axis of the wheel. Typically, a sinusoidal form is used for the desiccant wheel's flow path. There is a considerable improvement in dehumidification efficiency between channels with triangular, sinusoidal, and rectangular cross sections and those with hexagonal, circular, and square cross sections. The triangular channel is the most effective, followed by the 2:1 aspect ratio sinusoidal channel and the rectangular channel. Jani et al., [33] demonstrated and addressed the energy savings potential of solar-powered desiccant cooling methods when compared to traditional cooling systems that rely on vapour compression. When compared to traditional vapour compression cooling, solid desiccant integrated hybrid cooling systems were preferred due to their superiority as a cheap and environmentally friendly alternative.

Jani et al., [34] built the TRNSYS simulation studio project, in order to simulate the desiccant dehumidifier linked vapour compression hybrid system in its various configurations during the summer season. Moreover, experimental measurements were taken to see how different settings affect the system's efficiency. Based on the data collected, it was clear that the suggested system successfully reduced process air humidity at the dehumidifier exit without compromising the conditioned space's ambiance. The cooling system's efficiency was measured using an experimental test rig in the heat of summer. Dehumidifier performance

is discovered to be significantly impacted by the regeneration temperature of the heat source used to restart the device. Tu et al., [35] discovered dehumidifier performance is to be significantly impacted by the regeneration temperature of the heat source. Zendehboudi et al., [36] presented the results of an experimental investigation into the performance of six desiccant wheels made up of silica gel and Molecular Sieve desiccants and measuring 44 cm, 55 cm, and 77 cm in diameter. Regeneration temperature, volume flow rate, and, rotation speed were investigated as factors of process outlet temperature, dehumidification efficiency, moisture removal capacity, sensible energy ratio, and regeneration specific heat input for a variety of wheel diameters and materials.

It was discovered that the proposed Hybrid-ANFIS model had better predictability than the GA-LSSVM, validating the Hybrid-ANFIS technique as a straightforward method that could be readily included into dynamic simulation tools for the enhancement of desiccant cooling system management. Zhou et al., [37] created a new type of desiccant wheel—one with a tube-shell and an internal water-cooling system—and evaluated its effectiveness. With not more than two desiccant layers inside the heat-exchanger tubes, they were able to demonstrate isothermal dehumidification. There was less heat transmission from the air in the innermost layers to the cooling water as the number of layers increased. Air outlet humidity and temperature were reduced as a result of lower cooling water inlet temperatures.

### **2.2.2 Solar Energy Assisted Desiccant Based Dehumidification.**

Guidara et al., [18] designed a solar air conditioner that can reliably chill an indoor space with the help of a humidifier and a heat exchanger. Also, a comprehensive modelling analysis was provided for every facet of the solar air conditioner.

Misha et al.,[22] found that even with low solar radiation, the drying kinetics of kenaf core fiber utilising a solar-assisted solid desiccant dryer is superior to open sun drying. Because of the electric heater and constant air flow, drying can proceed even when the sun isn't out. The sample on the five random trays dried to a final moisture content below 18% in two days, indicating that the drying process was homogeneous throughout the drying chamber.

Misha et al., [26] found using a solar-assisted solid desiccant dryer has a faster drying kinetics for crushed oil palm fronds than drying them in the open sun. It takes about 30 hours and forty minutes of drying time in the open sun to bring the product's moisture level down

from 69% to 29%. There is an about 64 percent, 44 percent, and 33 percent reduction in drying time for items in the first, second, and third columns of the solar dryer, respectively, when compared to drying in the open sun.

Wang et al.,[38] found using a DCHE (desiccant coated heat exchanger) and a regenerative evaporative cooler, this paper seeks to verify the efficacy of a unique self-cooled solid desiccant cooling system. As part of the dehumidification process, the system pumps some of the air from the desiccant-coated heat exchanger's inlet into an evaporative cooler. In comparison to the solid desiccant coated heat exchanger system, the SDCHE (self-cooled solid desiccant coated heat exchanger) system is found to have a higher thermal coefficient of performance COP, and a higher moisture removal capacity.

### **2.2.3 Artificial Neural Network assisted Solid Desiccant-Based Technology**

Because of high accuracy and short computing time, an approach of ANN prediction can be very useful to simulate the performance of solid desiccant cooling systems at different operating conditions by conducting limited number of experimental tests instead of comprehensive testing study or developing a complicated mathematical model with enormous engineering efforts. The mathematical approach requires a large number of geometrical parameters defining the system, which may not be readily available and their predictions may not be sufficiently accurate in many cases. As an alternative, use of ANN requires less effort, time and cost to model the system. So, ANN allows modeling of physical phenomena in complex systems without requiring explicit mathematical representations or without requiring exhaustive and costlier experiments. The cited literature in this review confirmed that artificial neural network can be successfully used to predict performance of solid desiccant cooling systems with acceptable accuracy[31].

To estimate the performance of a rotary desiccant dehumidifier under varying conditions of the process air inlet, an artificial neural network (ANN) model was built. Tests are also carried out with the purpose of determining the effectiveness of the desiccant wheel, and the outcomes of the tests are utilised as target data in the training of the ANN model. The results of experimental testing and the performance predictions made by ANN were compared, and it was found that there was a close agreement between the two sets of data[25].

## **2.2.4 Solid Desiccant Composite Based Technology**

The potential ( $>2.0$  g/g) of the composite was found to be 5–7 times better than that of standard silica gel, demonstrating its outstanding ability to dehumidify air. Strong and possessing all the hallmarks of a perfect desiccant, the solid composite stands out for its increased adsorption capacity, low regeneration temperature, and eco-friendly composition[39].

A variety of silica gel-LiCl composite desiccant coated aluminum sheets were manufactured and examined for their impact on a number of critical parameters in this paper. The usage of composite desiccant in the DCHE system was found to increase its dehumidification capability[40]

## **2.2.5 Heat Pump Assisted Solid Desiccant Based Technology**

Jiang et al., [41] proposed a system, which integrates an innovative solid desiccant heat pump with a conventional variable refrigerant flow air conditioning system (VRF). Evaluation of how well workers did in a number of different types of office settings was analysed.

Nie et al.,[42] presented a theoretical model for estimating the VOC elimination and energy performance of a unique heat pump aided solid desiccant cooling system (HP-SDC). The heat pump supplied sensible cooling and regeneration heat for the desiccant rotor, which was utilised for dehumidification and cleansing the indoor air. The findings also indicated that the HP-SDC was an effective means of removing airborne pollutants and an attractive, energy-saving ventilation option.

Tu et al.,[43] presented a novel form of processor, which consisted of a heat pump and square desiccant plates for the purpose of dehumidifying outside air using solid desiccant. The cooling capability of the heat pump was utilised to chill the air that had been treated, and the heat from the heat pump's exhaust was reused to evaporate moisture from the desiccant.

Tu et al.,[44] studied a heat pump-powered, multi-stage fresh air handler that makes use of solid desiccant plates. There were four distinct modes that can be used to control this system, each of which is responsive to the relative humidity and temperature of the outside air. In this paper, we focus on the system's operation in solid desiccant dehumidification mode, which achieves the desired supply air humidity ratio with reduced power consumption by

varying the number of activated stages in response to changes in the temperature and humidity of the incoming process air.

### **2.2.6 Exergy Analysis For Solid Desiccant**

Lior & Al-Sharqawi [45] studied the water vapour adsorption in a desiccant-air stream system and analysed it in terms of exergy for laminar humid air flow over a desiccant flat bed with constant and variable characteristics, in a desiccant-lined channel, and for turbulent humid air flow in such a channel for varied turbulence intensities. The investigation revealed the amount of exergy that was wasted during the adsorption process as well as any associated heat and mass transfer procedures.

Tu et al., [23] investigated the efficiency of desiccant cooling and dehumidification systems to see how well they perform. As a result of theoretical research, an investigation into six distinct types of systems (systems A-F) was carried out as the system transitioned from being reversible to being irreversible, which caused the system's performance to significantly degrade. Under the same operational conditions, the COP and exergy efficiency of the proposed heat pump-driven system were equal to 5.01 and 18.0%, respectively. These values were determined using the same system E's schematic and performance parameters.

Tu et al., [46] studied the efficiency of ventilation systems that employ desiccant wheel cooling from the perspective of exergy destructions. Provide some recommendations for the efficient design of systems based on the intrinsic factors that influence exergy destructions, heat and mass transmission, and heat sources.

### **2.2.7 Electro-Osmosis Regeneration for Solid Desiccant**

Li et al., [47] presented an original method for solid desiccant regeneration that is predicated on electro-osmosis (EO), and investigated the possibility of using it in heating, ventilation, and air conditioning (HVAC), specifically in the dehumidification process that occurs in air conditioning systems. When compared to the conventional air conditioning system and taking into account the many different configurations of the air handling process, the data that was collected during the experiments indicate that the energy consumption of the EO integrated air conditioning system reduced by an average of 23.3% compared to the conventional air conditioning system.

Qi et al., [48] investigated the viability and performance of a one-of-a-kind electro-osmotic regeneration method for the solid desiccant system. This method can simultaneously absorb water from humid air and be regenerated by the electro-osmotic force. The purpose of this study was to use extensive experimental validation to look into the effectiveness and performance of this method. The results of the experiments show that the technology has the ability to achieve both low regeneration temperatures and significant energy savings. Hence, electro-osmotic regeneration should be considered a real possibility for the replenishment of solid desiccant systems.

It has been demonstrated that regeneration of the solid desiccant through the use of electro-osmotic methods offers a number of advantages, some of which include independence from a heat source, decreased energy consumption, and a basic design. Past studies have revealed that the significant Joule heating effect and electrode corrosion severely limit its performance. As a result, additional work needs to be done in order to bring it up to snuff so that it may be utilised in applications that are employed in the real world. They carried out a large number of tests and investigations, and the results showed that utilising platinum-plated titanium mesh as the anode extended the working lifetime from six hours to more than one hundred and twenty hours, while at the same time greatly reducing the Joule heating impact [49].

### **2.2.8 Packed Bed Desiccant Based Dehumidification Systems**

Owing to the difference in the vapour pressure between the humid air and the solid desiccant surface, the process of desiccant-based dehumidification and physical adsorption results in the transfer of water vapour from the humid air onto the solid desiccant surface. Packed beds, rotating horizontal beds, many vertical beds, rotating honeycomb, fluidized beds, inclined beds, and rotational desiccant wheels are all examples of the various types of solid desiccant systems that are used for dehumidification and air treatment [50]. Reactors, separators, dryers, filters, and heat exchangers are just few of the many applications that packed beds for gas-solid interaction find widespread use in across many industries. In most cases, they take the form of vertical tubes that are cylindrical in shape and contain adsorbent particles that are held in place and packed closely but randomly in order to facilitate fluid-solid contact. They offer a high ratio of solid surface area to volume, and on a macroscale, the packed adsorbent particle behaves as a porous medium. The packed bed system is relatively

free from mechanical concerns, which makes it an attractive choice for adsorption operations. Its straightforward design and accessibility of a wealth of accumulated design and operating knowledge contribute to this free-from-problems status.

Yeboah and Darkwa [50] conducted a comprehensive assessment of the literature on the subject of water vapour adsorption in packed beds and the elements that influence it. It was clear that the packing structure had a major impact on the physics of fluid motion and transport. It was also mentioned that the energy efficiency of any solid desiccant dehumidification system is negatively impacted by the heat of adsorption created during the adsorption of water vapour in a packed bed of adsorbent particles. This is because it does not make the adsorption process isothermal and alters the exit process airstream humidity ratio, both of which increase the cooling load on the sensible heat exchanger and, in turn, the amount of energy needed for regeneration and desorption. In order to make the adsorption process isothermal, several scientists experimented with different methods of cooling or dissipating the heat from packed beds.

The experimental performance of a solid packed bed desiccant system that was paired with an R407C vapour compression refrigeration air conditioning system was tested and evaluated. Desiccant systems were shown to operate in two different modes: dehumidification and regeneration. The variables that were taken into consideration were the desiccant load, the air mass flow rate, the shelf count, and the shelf span. By conducting an analysis of the data it was found that a desiccant-enhanced vapor-compression refrigeration system utilizes fewer electrical units and consumes 10.2 percent less electricity than conventional systems. It was observed that a hybrid system's coefficient of performance does not considerably change by the amount of desiccant that is used in the system. The amount of time that the system was able to operate with a low load and draw a low quantity of electricity increased by 54% when the mass of the desiccant was increased from 5 kg to 10 kg. It was noted that after only ten minutes of operation, there was a 37% increase in the adsorption rate. It was observed that increasing the air mass flow rate from 7.4 to 10.2 kg/min was one way to reduce the saturation time in the dehumidification mode by 39%, also lead to increase in the adsorption rate by 67% after 3 hours of operation, reduced the regeneration time by 87.5%, and increased the desorption rate by 16% after 10 minutes of operation. Other benefits of this change included shortening of the regeneration time by 87.5% and increasing the desorption rate by 16% after 10 minutes of operation [51].



Zouaoui et al.,[13] emphasized the capabilities of the desiccant cooling system to operate well and to function as a supplement to the vapour compression system, the evaporative cooling system, and the chilled-ceiling system. Consideration was given to the desiccant cooling system's viability as well as its potential financial benefits. It was found that desiccant system could be regarded as an environmentally benign method of air conditioning because the working fluid that is employed is a natural working fluid. Research and modelling were conducted on a number of different desiccant cooling systems, some of which also included direct and/or indirect humidification. The sensible load in these systems was handled by the direct and/or indirect humidification, while the latent load was handled by the desiccant system. The process of adsorption was completed using a vertical cylindrical bed that was packed with grains of silica gel. This bed operated without the use of a motor, which eliminated the potential for electrical and mechanical issues, as well as the noise that would be produced by a rotary desiccant wheel that was powered by a motor.

A. Ramzy et al., [52] presented an intercooled packed bed as a means of improving the utilisation of desiccant material within the bed's trailing layers as seen in Figure 2.2. Because of the heat that is generated during adsorption, the desiccant material that is in the trailing layers of packed beds is not utilised to its full potential.

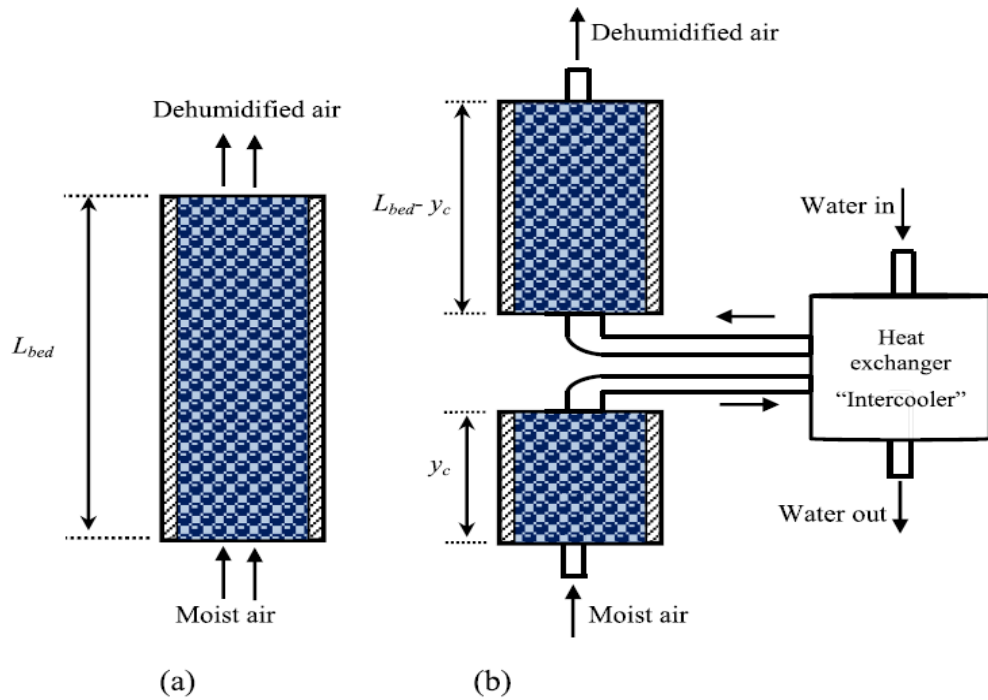


FIGURE 2. 2 (a) Conventional packed beds and (b) intercooled packed beds make up the physical model of a silica gel bed operating in adsorption mode [52].

The effect of the heat of adsorption can be eliminated by intercooling the desiccant bed, which also results in an increase in the consumption of the desiccant material. The optimal site for the intercooler,  $y_c/L_b$ , is located at 0.45  $y_c/L_b$  0.65 for bed lengths ranging from 0.05 to 1 m. This is the location at which the total adsorbed mass is at its greatest, indicating that it is the optimal location. It has been discovered that the operating conditions might determine the optimal bed length as well as the location of the intercooler. In the scenario that was investigated, 0.4 meters is the ideal bed length, and 0.5 meters is the ideal placement for the intercooler.

A.K. Ramzy et al., [53] carried out experimental testing for the thermal swing adsorption (TSA) cycle utilizing two packed beds of silica gel spherical particles as shown in Figure 2.3. These tests were successful. The mathematical model known as the pseudo gas side controlled (PGC) model was presented for the purpose of predicting the cycle performance.

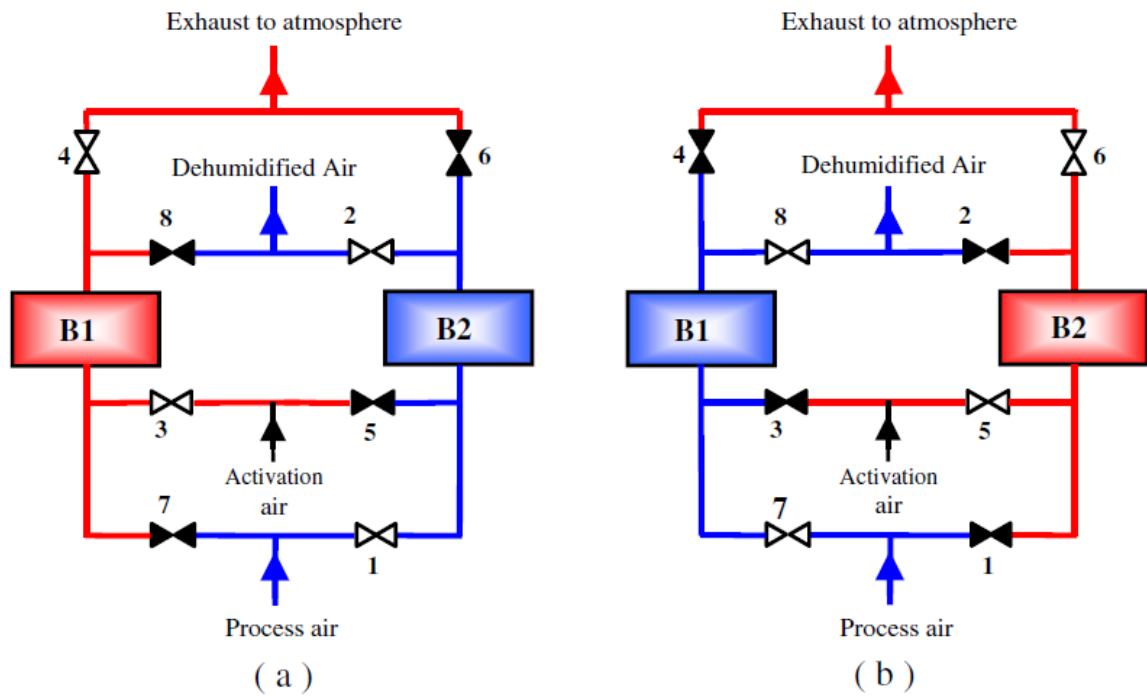


FIGURE 2. 3 Schematic showing the flow of a two-desiccant vertical packed bed dehumidifier [53].

The effect of various operational and design parameters of the TSA cycle that utilises two thermally isolated vertical packed beds of silica gel were explored numerically. The influencing parameters on cycle performance that were taken into consideration were the length of the desiccant bed ( $L$ ), the temperature of the regeneration air ( $T_{a,Reg}$ ), the temperature of the process air ( $T_{a,Deh}$ ), and the airflow velocity ( $v_{Deh}$  and  $v_{Reg}$ ).

Ramzy K. et al., [53] investigated a new desiccant composite particle, in which the unutilised portion of the spherical desiccant particle was replaced with an inert particle, is proposed. By replacing the conventional particles with composite particles for the same mass of desiccant material, the available area for heat and mass transfer increases and more amount of desiccant material is effectively utilised as can be seen in Figure 2.4.

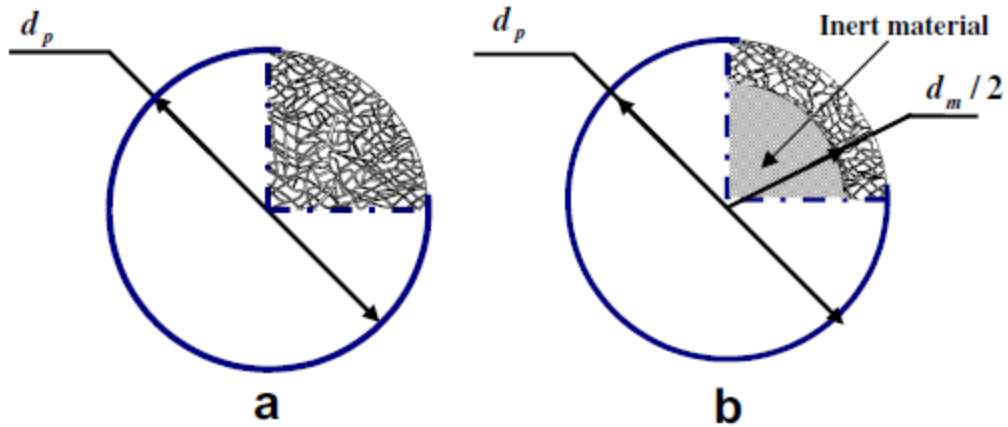


FIGURE 2. 4 a) Typical silica gel particle. b) Suggested silica gel composite particle [54].

After analysing the intra-particle water content profiles, the researchers discovered that composite silica gel particles provided greater utilisation of the desiccant material than their standard counterparts did when ordinary silica gel particles were used in place of them.

Shelpuk, [54] stated that it was reasonable to project that desiccant systems will make an increasing and significant penetration into the market for building air conditioning for the remainder of this decade, given the environmental concerns that call for reductions in CFC and greenhouse gases as well as the increasing cost of building the large central electrical generation plants required for an increasingly air conditioned society. Another factor that will hasten the development and commercialization of desiccant systems is the growing awareness of the importance of maintaining a high level of indoor air quality in buildings.

San et al., [55] The modelling of the heat and mass transmission in a silica gel packed bed uses three distinct sets of solid-side mass diffusivity in an individual capacity as depicted in Figure 2.5 In order to mitigate the cyclical changes in moisture content, the packed bed is positioned at the system's discharge point after the fixed-bed dehumidification unit.

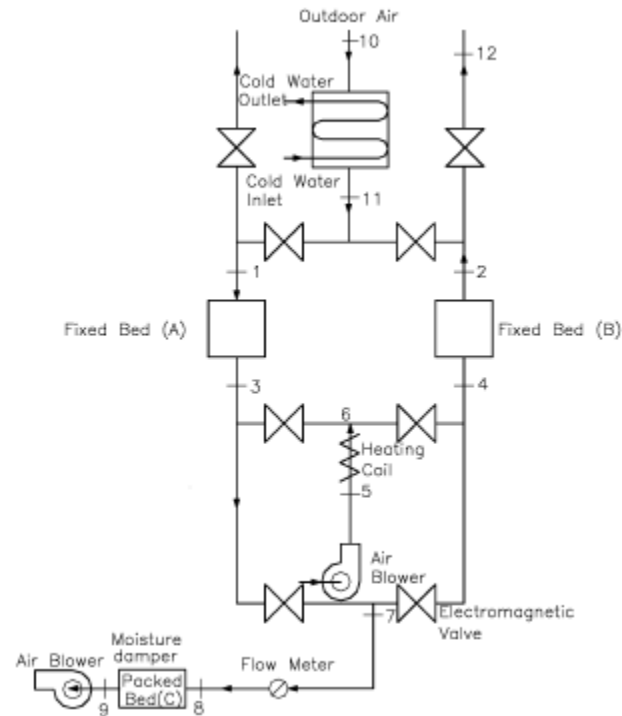


FIGURE 2. 5 A dehumidification system that utilizes a fixed bed and a moisture damper [56].

Pesarant and Mills, [56] carried out tests in order to obtain the transient reaction of a thin adiabatic packed bed of silica gel following a step change in the conditions of the air that enters the bed as shown in Figure 2.6. Comparisons were done with predictions utilising a solid-side resistance model and a pseudo-gas-side controlled model, and it was determined that the former model had a superior level of agreement.

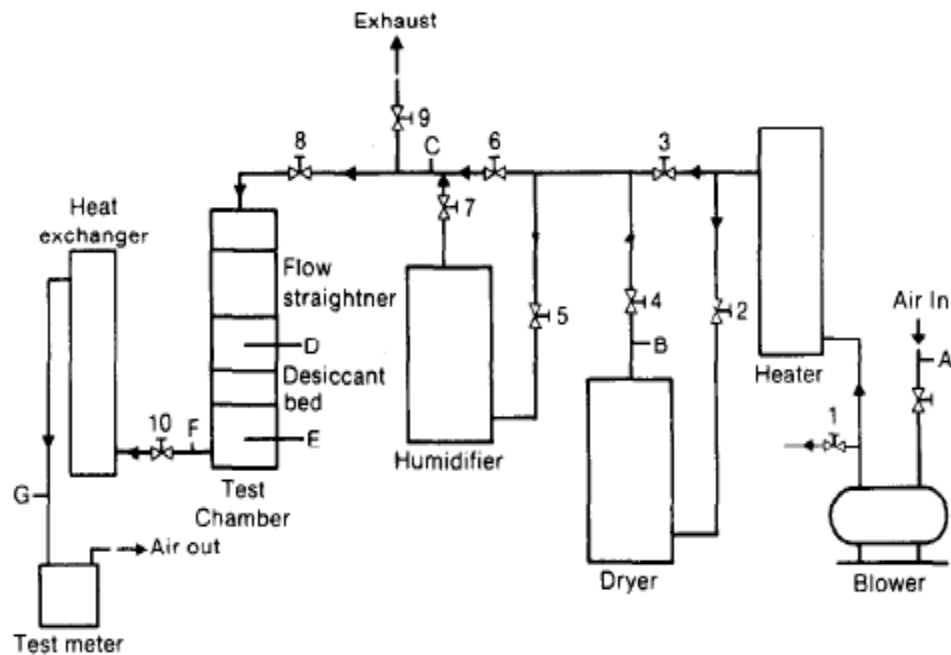


FIGURE 2. 6 A test-based setup[57]

Baghapour et al., [57] An experimental and modelling inquiry on the pressure drop inside the adsorption packed beds is carried out in this particular piece of research. In order to determine the pressure drop at varying bed sizes and airflow rates, a specialized apparatus for conducting experiments has been developed. The calculation of the pressure drop in a cylindrical packed bed with laminar, steady-state, axisymmetric, and fully-developed macroscopic fluid flow distributions was made possible with the use of a novel analytical model that was provided. The analytical model was modified to include both the Laplacian friction and the inertial effect. The influence of both factors on the pressure drop experienced within packed beds was examined. It was determined that when the pressure drop increased, the difference between the pressure drop of the dry particle and the pressure drop of the wet particle became insignificant.

Gandhidasan et al., [58] This study presented the design analysis of a two-tower silica gel dehydration unit as shown in Figure 2.7 that is intended to dry one million standard m<sup>3</sup> of natural gas each day. The implications of various operating parameters on the design of the unit are also explored in this research.

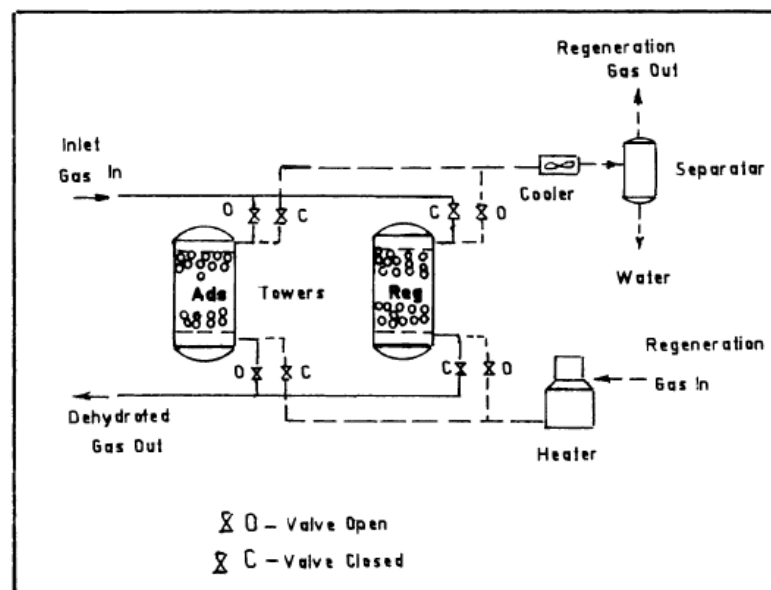


FIGURE 2. 7 Schematic of a two-tower solid desiccant dehydrator[58].

The packed bed desiccant based dehumidification system using external heat for regeneration was presented and investigated.

### 2.3 Literature review summary

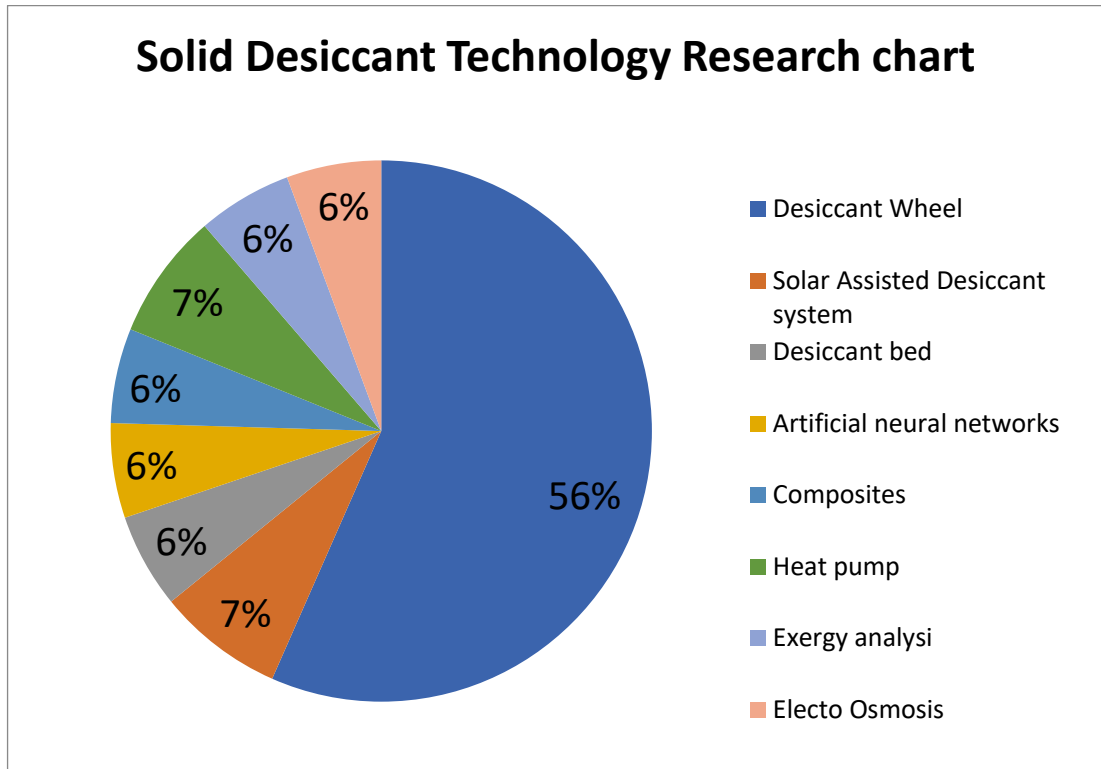


FIGURE 2. 8 Plot depicting extent of research done in various domains of solid desiccant dehumidification.

According to Figure 2.8, it is abundantly clear that solid desiccant-based dehumidification is becoming increasingly popular and attracting the attention of a large number of researchers to help in the process of dehumidification. Desiccant wheel was used by most researchers in their work while use of packed beds for dehumidification was relatively less explored. Use of solid desiccant in applications such as heat pump, electro osmosis is also observed. Utilization of solar energy in hybrid desiccant dehumidification also displays good potential. The foregoing literature analysis makes it quite evident, however, that the majority of the work that has been done has been done using a desiccant wheel. Nonetheless, packed bed desiccant dehumidification presents a substantial opportunity for further research and application of the technology. Which, in comparison to the desiccant wheel, consists mostly of unexplored areas. As a result, a comprehensive analysis of recent developments involving packed bed solid desiccant dehumidification is carried out. In order to have an understanding of its breadth and the possibilities for growth within it.

## 2.4 Research Gap

By conducting an in-depth literature review with the goal of understanding the scale of potential of applying and utilising solid desiccants in various technologies, particularly for dehumidification, the following research gap was discovered as a result of the study.

- Packed bed due to absence of moving part holds great potential for dehumidification, however was relatively less explored in comparison to desiccant wheel by researchers.
- Most researchers did not address the area of dehumidification of compressed air using solid desiccants
- Packed bed desiccant systems were mostly coupled with heater, giving room for investigation of heatless dryers
- Silica gel was the most used desiccant by most researchers in their experimental work, hence use of other desiccants in heatless air dryers was not addressed by any researcher.
- No desiccant can be termed ideal desiccant, a proper investigation for any particular application needs to be carried out separately.
- To the best of the author's knowledge, there is currently no literature on the selection of solid desiccants for the application of a heatless air dryer that has been located.
- The research that had previously been conducted on heatless dryers was scant and did not investigate the use of any desiccants other than silica gel.
- Because there is not a lot of published research on the different desiccants that are used in heatless air dryers, there is potentially a blind spot for additional research in both academia and industry.
- As there is a dearth of literature on investigation of solid desiccant used in heatless air dryer, availability of the relevant data will help researchers, designers and the industry to make the appropriate choice of desiccant as per the application.

The research gap identified serves as a clear road map for further investigation and objective of the experimental work which is stated as under.

## **2.5 Objective and scope of work**

After carrying out a detailed literature study and understanding the potential for research on solid desiccants used in heatless air dryer, the following research objectives and scope of work have been considered as the main focus of the present study.

## **2.6 Research objectives**

The objective of the current work is to investigate the utilization of various solid desiccants in heatless air dryer. Make a comparative analysis of the different solid desiccants used in the heatless dryer.

The above objective consists of the following sub-objectives:

1. Investigate the effect of performance parameters such as moisture removal rate and effectiveness of dehumidifier.
2. Compare the performance of different solid desiccants in the heatless air dryer.

## **2.7 Scope of work**

In order to achieve the above objectives, the following scope of work is broadly listed below:

- Development of an experimental setup of the heatless air dryer.
- Experimentation for evaluation of performance parameters.
- Interpretation of experimental data
- Validation of the experimental results using ANN.

## **2.8 Organization of the thesis**

The research works carried out as part of the thesis are presented in six chapters with reference section at the end. The present research work includes experimental investigation to draw a comparison between solid desiccants as a working medium in heatless air dryer. Artificial Neural Network was also developed with the help of a neural designer to predict the performance parameters of the solid desiccants.

Chapter 1 briefs about the need for developing desiccant based dehumidification systems and importance of dehumidified compressed air in industries, desiccant cooling, basic



principle of desiccant cooling system, classification of desiccants, desirable properties of the desiccant.

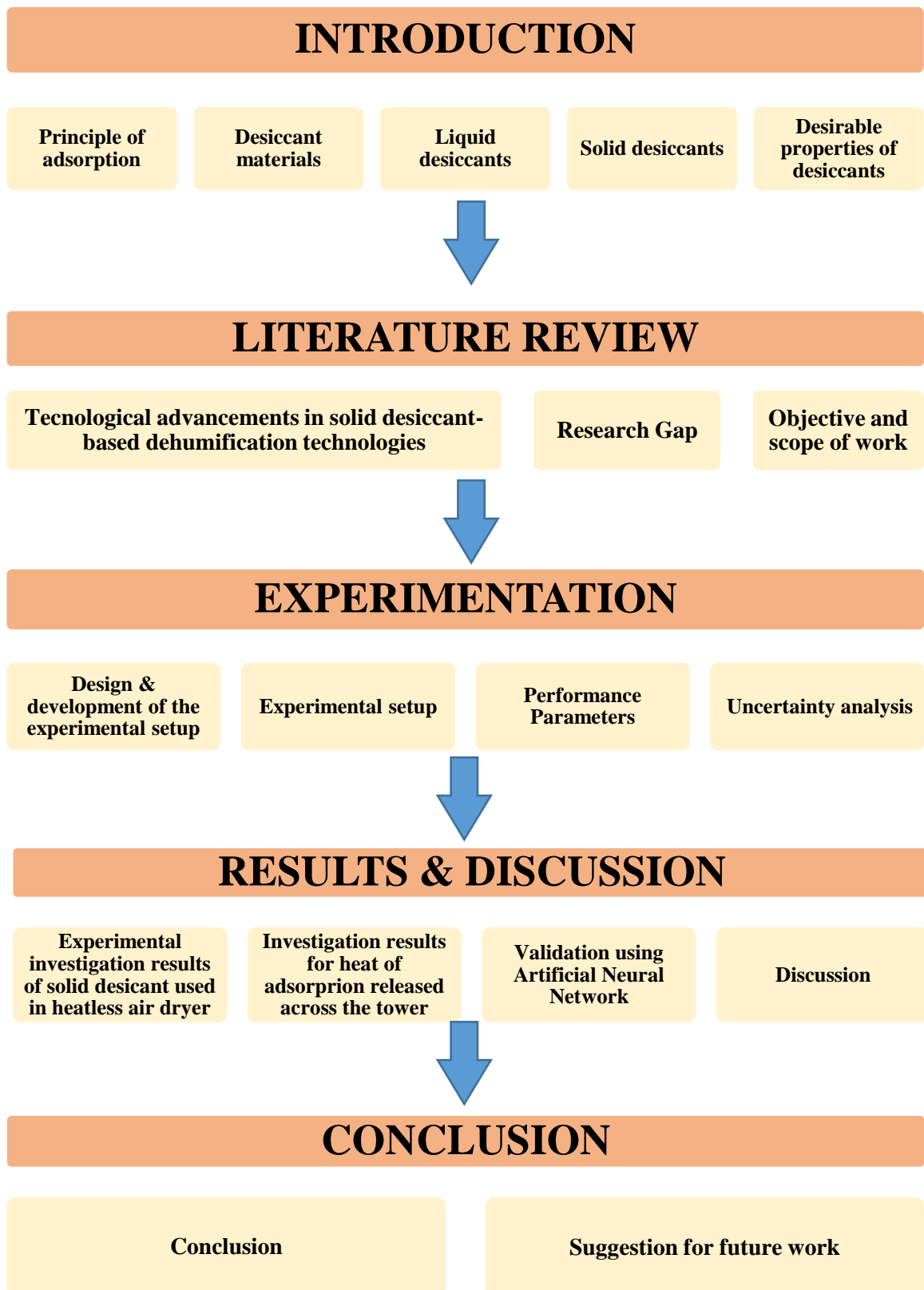
Chapter 2 outlines the detailed literature review on technological advancements in the field of dehumidification using solid desiccants and particularly packed bed desiccant systems which includes mathematical, simulation and experimental. At the end of the chapter, scope and objectives are described.

Chapter 3 presents the detailed experimental setup to investigate the solid desiccant such as silica gel, activated alumina, Molecular Sieve 4A and Molecular Sieve 13x as a working medium in heatless air dryer. At the end of the chapter, performance parameters and uncertainty analysis are described.

Chapter 4 presents the results and discussion for comparative investigation on solid desiccant as working medium in heatless air dryer in terms of moisture removal rate and dehumidifier effectiveness obtained experimentally. Also, the results of the thermal distribution across the adsorber tower and regeneration tower obtained through experimentation are presented and discussed. Results obtained through ANN are presented and discussed as a validation tool for the experimental results.

Chapter 5 elucidates the summary and important conclusions arrived from the study and scope for further research is also discussed.

## 2.9 Flowchart of Organization of the thesis



## CHAPTER - 3

### Experimentation

It was evident from the literature review that solid desiccants need to be investigated individually for any particular application. In this research work dehumidification of compressed air through a heatless air dryer is investigated. Experimental set up has been meticulously designed in order to acquire reliable data from experiments. The commonly used solid desiccants have been selected for the experimentation. The solid desiccants selected are

- 1) Silica gel
- 2) Activated Alumina
- 3) Molecular Sieve 3A
- 4) Molecular Sieve 4A
- 5) Molecular Sieve 13x

The above solid desiccants are selected as they have good crushing strength to withstand high pressures of compressed air, chemically stable, nontoxic and inflammable. In order to study and observe the surface of the solid desiccants, help of Scanning Electron Microscope (SEM) was used. Each solid desiccant was sent for testing to capture the magnified surface image of the solid desiccant. The 100  $\mu\text{m}$  S.E.M images obtained can be seen below:



FIGURE 3. 1 S.E.M image of Silica gel solid desiccant

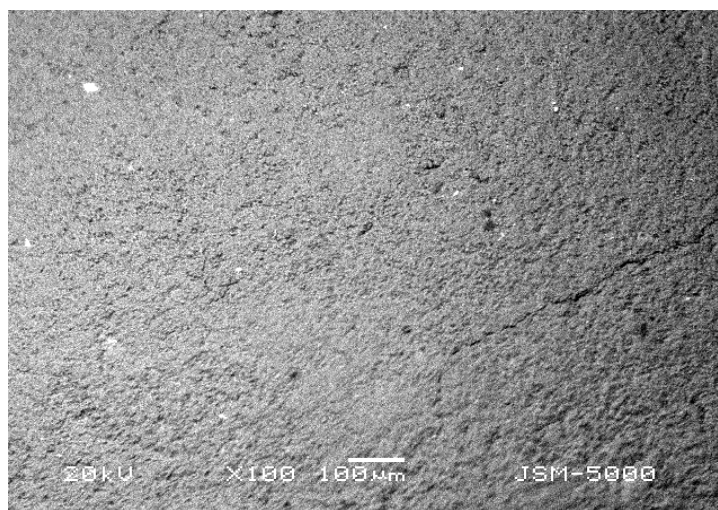


FIGURE 3. 2 S.E.M image Molecular Sieve 13x of solid desiccant

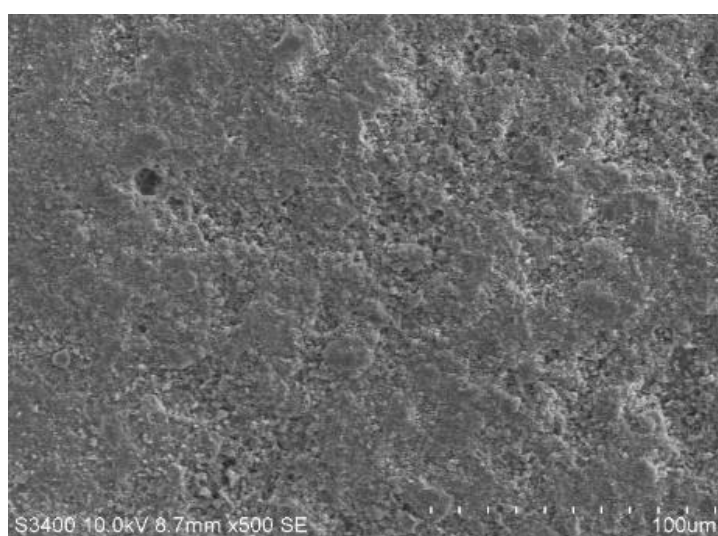


FIGURE 3. 3 S.E.M image of Molecular Sieve 3A solid desiccant

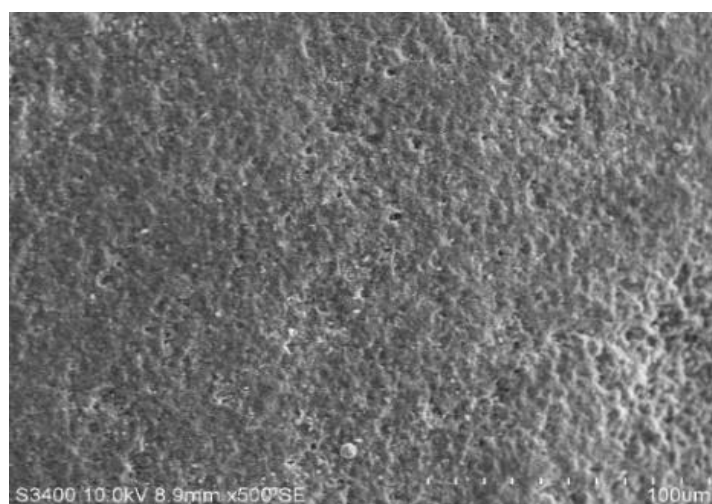


FIGURE 3. 4 S.E.M image of Molecular Sieve 4A solid desiccant

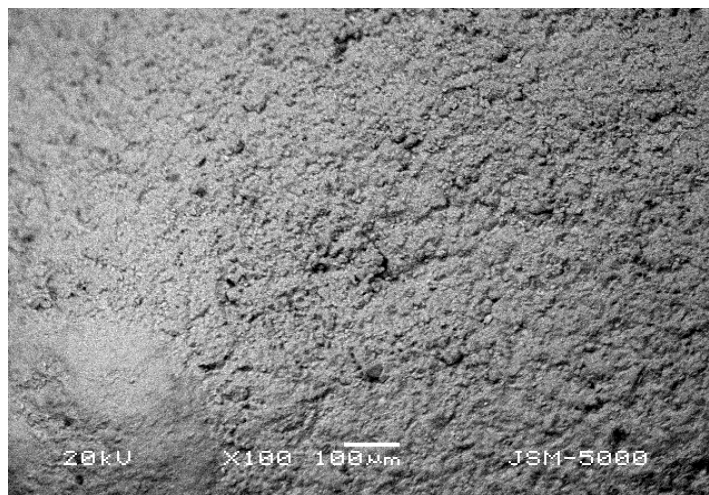


FIGURE 3. 5 S.E.M image of Activated Alumina solid desiccant

The SEM images as observed from Figure 3.1 to Figure 3.5 reveal even pore distribution to be maximum in Molecular Sieve 13x when compared to others while silica gel shows minimum pore distribution. This suggests better rate of adsorption must occur in Molecular Sieve13x when compared to silica gel.



FIGURE 3. 6 Actual image of Silica gel solid desiccant used for experimentation.

In Figure 3.6 Actual image of the Silica Gel White Beads having a size of 2-4 mm used for experimentation can be seen. The non-indicating type Silica Gel was used. Silica Gel white beads on saturation will not change color. Silica Gel White Beads widely used as desiccant



in packet form. It is used in Natural Gas Drying. Silica Gel White Beads used in Hydrocarbon Drying.

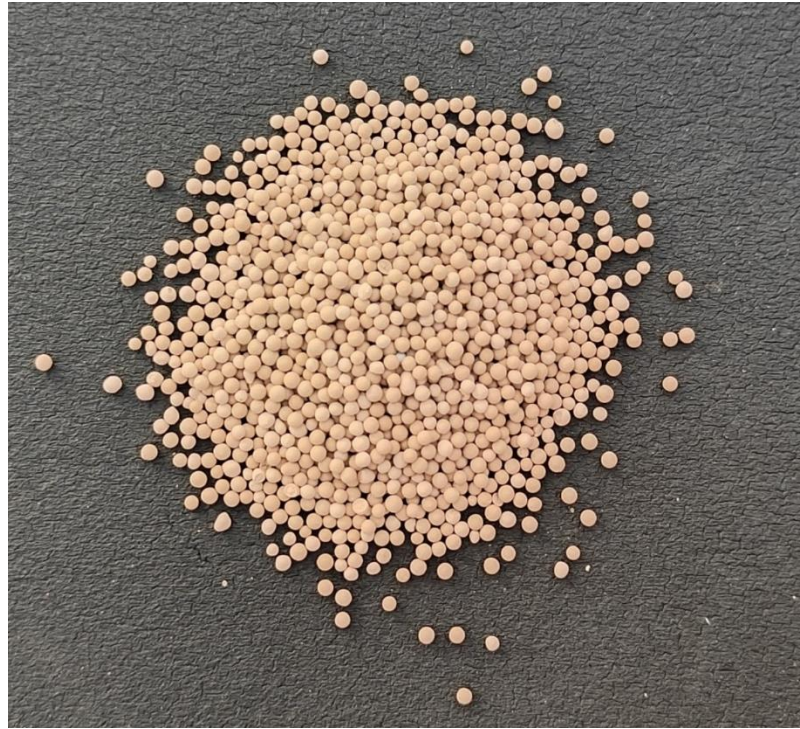


FIGURE 3. 7 Actual image of Molecular Sieve 3A solid desiccant used for experimentation.



FIGURE 3. 8 Actual image of Molecular Sieve 4A solid desiccant used for experimentation.



FIGURE 3. 9 Actual image of Molecular Sieve 13x of solid desiccant used for experimentation.



FIGURE 3. 10 Actual image of Activated Alumina solid desiccant used for experimentation.

Figure 3.6 to Figure 3.10 depict the actual images of the solid desiccants used for experimentation in this research work. The properties of these desiccants used in experimentation are available in Annexure-B

### 3.1 Design and development of the experimental set up.

Under normal production conditions, compressed air is saturated with water. Estimating the saturated water vapour content of the compressed air is fundamental to the design and operation of the heatless air dryer. Water content of the saturated gas entering the dryer at the given operating conditions is given by:

$$W = 593.335 \times \text{EXP}(0.05486 \times t_g) \times P^{(-0.81452)} \quad (1)$$

Take  $t_g = 45^\circ \text{C}$

$$P = 0.78$$

$$W = 593.335 \times \text{EXP}(0.05486 \times 45) \times 0.78^{(-0.81452)}$$

$$W = 72644.353 \text{ kg}/10^6 \text{ Std m}^3$$

It is reasonable to assume that virtually all of the water is adsorbed on the desiccant bed. In determining the drying cycle the designer is influenced by the desiccant capacity, water load to dryer, allowable system pressure drop, regeneration gas facilities and the investment economics [1]. Drying cycles generally range from 4 to 24 h. A common value of 8 h has been selected to avoid the tedious mechanism of determining optimum cycle length. The amount of water adsorbed per cycle is given by:

$$M = \frac{(Q_c W)}{24} \quad (2)$$

Now  $Q = 100 \text{ CFM}$

$$= \frac{0.0474}{60 \times 8}$$



$$= 9.81 \times 10^{-5} \text{ m}^3/\text{day}$$

$$M = \frac{Q \times C \times W}{24}$$

$$M = 2.32 \text{ kg}$$

The capacity of a desiccant for water is expressed normally in mass of water adsorbed per unit mass of desiccant

$$V_D = \frac{\text{Mass of water vapour adsorbed}}{\text{Mass of Desiccant}}$$

$$= \frac{2.32}{60}$$

$$V_D = 0.038 \text{ m}^3$$

The above volume is found to be in line with the company specification for 100 CFM dryer bed. Hence Diameter and length of the bed can be varied in accordance to pipe size availability in the market.

$$V_D = 0.0038 \text{ m}^3 \text{ for 10 CFM}$$

A 4" diameter pipe is used to construct the tower having a height of 18". Thus the actual volume of a single tower is 0.0037 m<sup>3</sup>.

### 3.2 Experimental set up

The heatless air dryer for 10 CFM capacity is designed and fabricated to experimentally test different solid desiccants such as Silica gel, Molecular Sieve 4A, Molecular Sieve 3A, Molecular Sieve 13x and Activated Alumina. The dryer utilizes compressed air which is provided by a reciprocating air compressor of 10 CFM capacity. The experimentation is conducted at the factory of M/s Unique Air Products.

### **3.2.1 Description of the experimental setup**

An experimental set up of a heatless air dryer for 10 CFM capacity is designed and manufactured to conduct the experiments. For every set of trial, compressed air from the compressor having a pressure of 7 bar was utilized. This compressed air is first supplied to the activated carbon filter in order to remove the oil content in the compressed air. As oil can be adsorbed by the solid desiccant, which can make the desiccant inactive. After passing through the activated carbon filter, the air is passed through the pre filter which has the filtration efficiency of 5 micron. After the pre filter the air enters the desiccant tower A or B as per the operating condition. The towers are completely packed with desiccant to ensure no desiccant particle is carried over in the compressed air stream, steel straps at the openings of the tower are installed. Desiccant material filled in the tower adsorbs the moisture of the compressed air and makes it dry. The dry air is now sent outside of the tower. Fraction of this dry air, referred as purge air, is bypassed via thin tube to the tower-B for the regeneration process. Remaining air, via non-return valve (also called check valve), is passed to the output line from where it goes to the after filter which removes dust particle if added by the desiccant (desiccant particles).

Rendering clean, compressed, dry air. The purge air is supplied to the tower-B from top. Bottom of the tower-B is kept open to the atmosphere, hence pressure in the tower-B is lower. The dry compressed purge air regenerates the desiccants. Now the cycle changes. Compressed air is passed through the tower-B while the tower-A gets regenerated. This cycle changes its direction after an interval of 5 minute. This cycle is controlled by a timer, which is attached with the solenoid valve, which controls the motion of the 5/2 direction control valve. This 5/2 control valve controls the direction of the compressed air (towards tower-A or tower-B) and opening of the tower-A or tower-B.

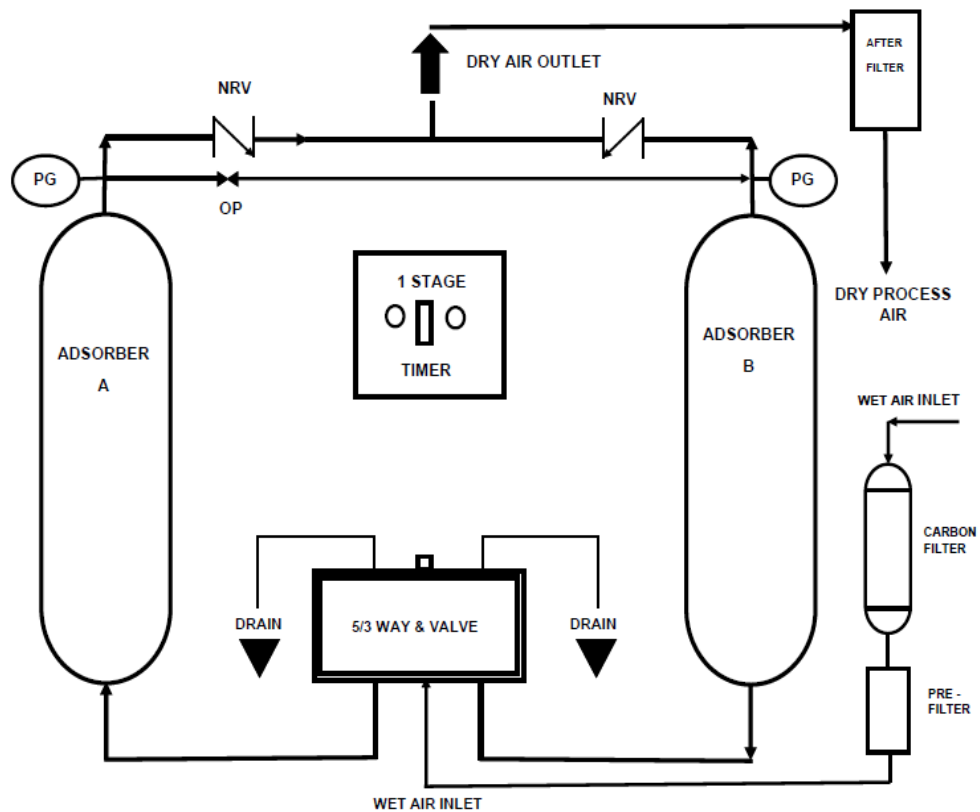
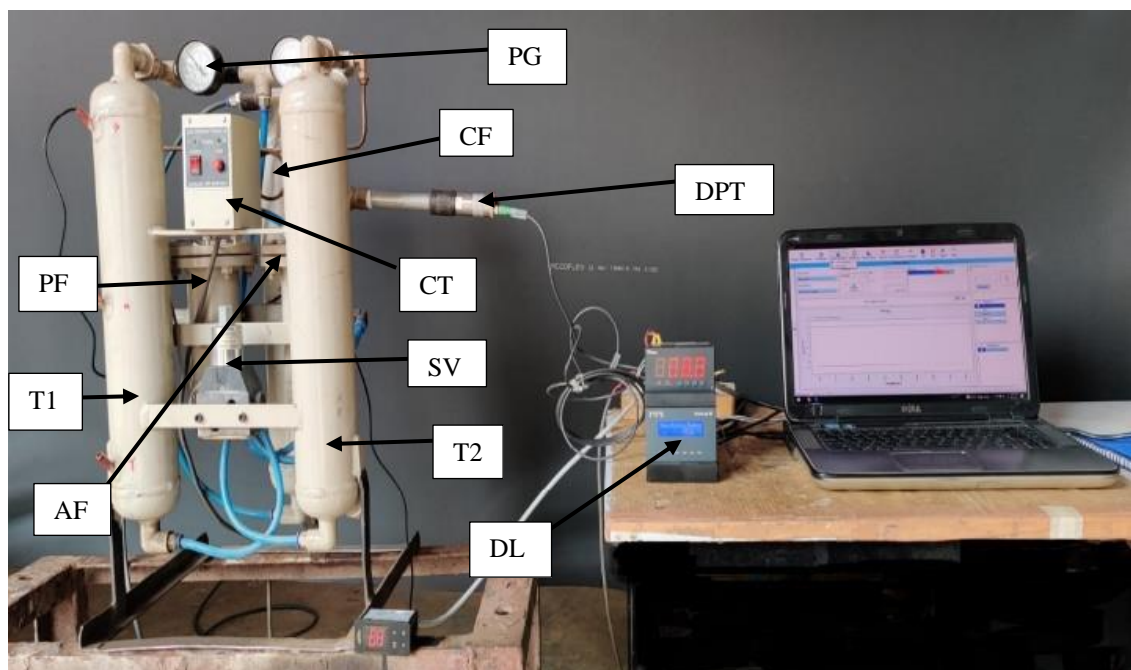


FIGURE 3. 11 Experimental test rig diagram



PG: Pressure Gauge  
CT: Control Timer  
CF: Carbon Filter  
SV: Solenoid Valve  
AF: After Filter

DPT: Dew Point Transmitter  
DL: Data Logger  
T2: Tower B  
T1: Tower A  
PF: Pre-Filter

FIGURE 3. 12 Detailed view of the experimental set up with Laptop and Data Logger attached.

### **3.2.2 Various components of the experimental set up**

The heatless air dryer consists of two packed bed towers which are constructed using a 4-inch diameter pipe cut of material SA 1239 across a length of 18 inch as can be seen in Figure 3.13 having a thickness of 4mm. Each tower undergoes adsorption and regeneration process as the cycle oscillates the direction of flow of the compressed air.



FIGURE 3. 13 Image of 4" diameter, 18 " height, 4mm thickness, SA1239 pipe used for tower fabrication.



FIGURE 3. 14 External image showing crown of the tower with wire mesh seal to prevent desiccant carryover in the process line



FIGURE 3. 15 Internal image showing crown of the tower with wire mesh seal to prevent desiccant carryover in the process line





FIGURE 3. 16 Image of the sub assembly fabrication

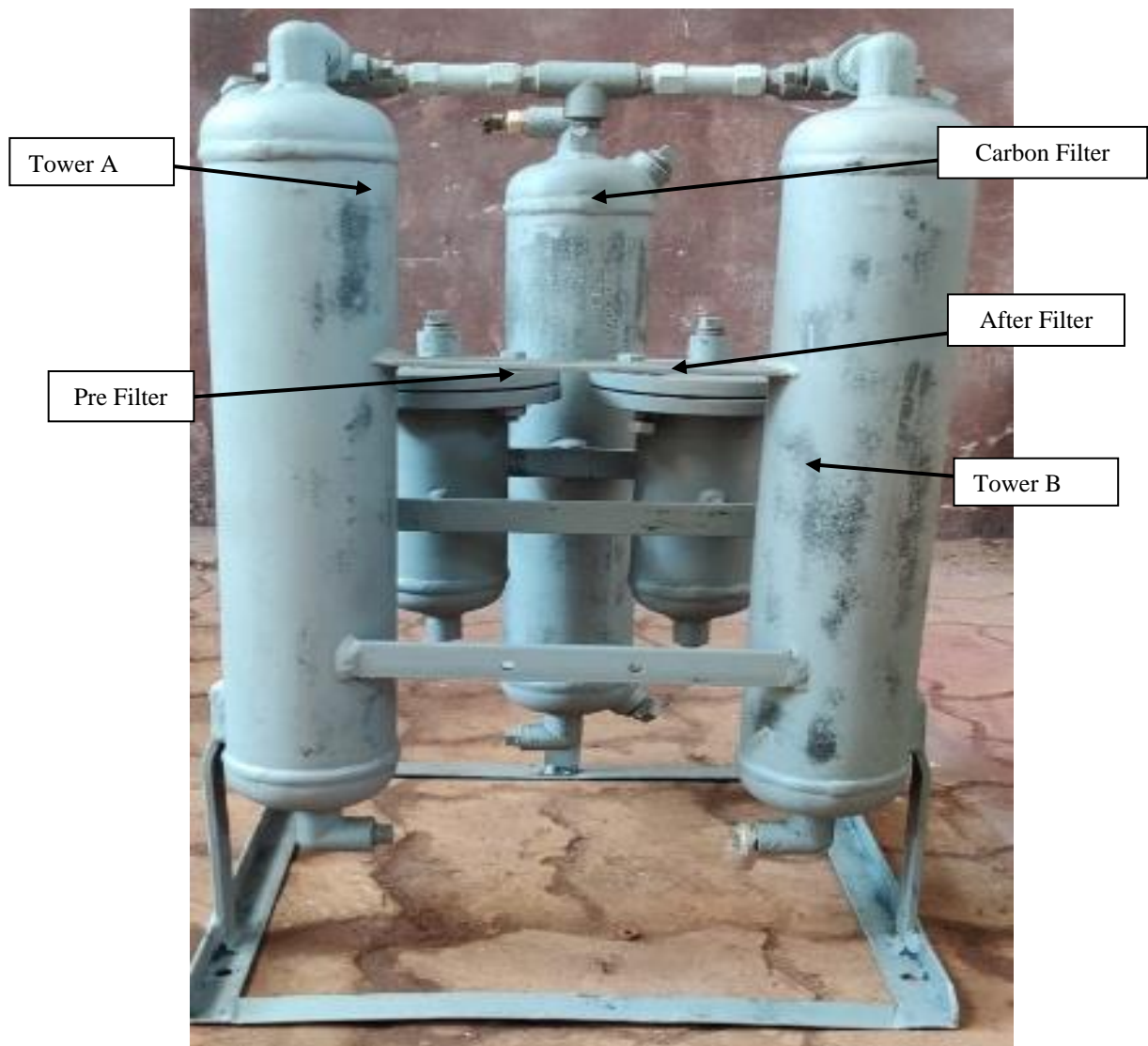


FIGURE 3. 17 Image depicting the fabricated test rig assembly of the desiccant towers with the pre filter , after filter and carbon filter.

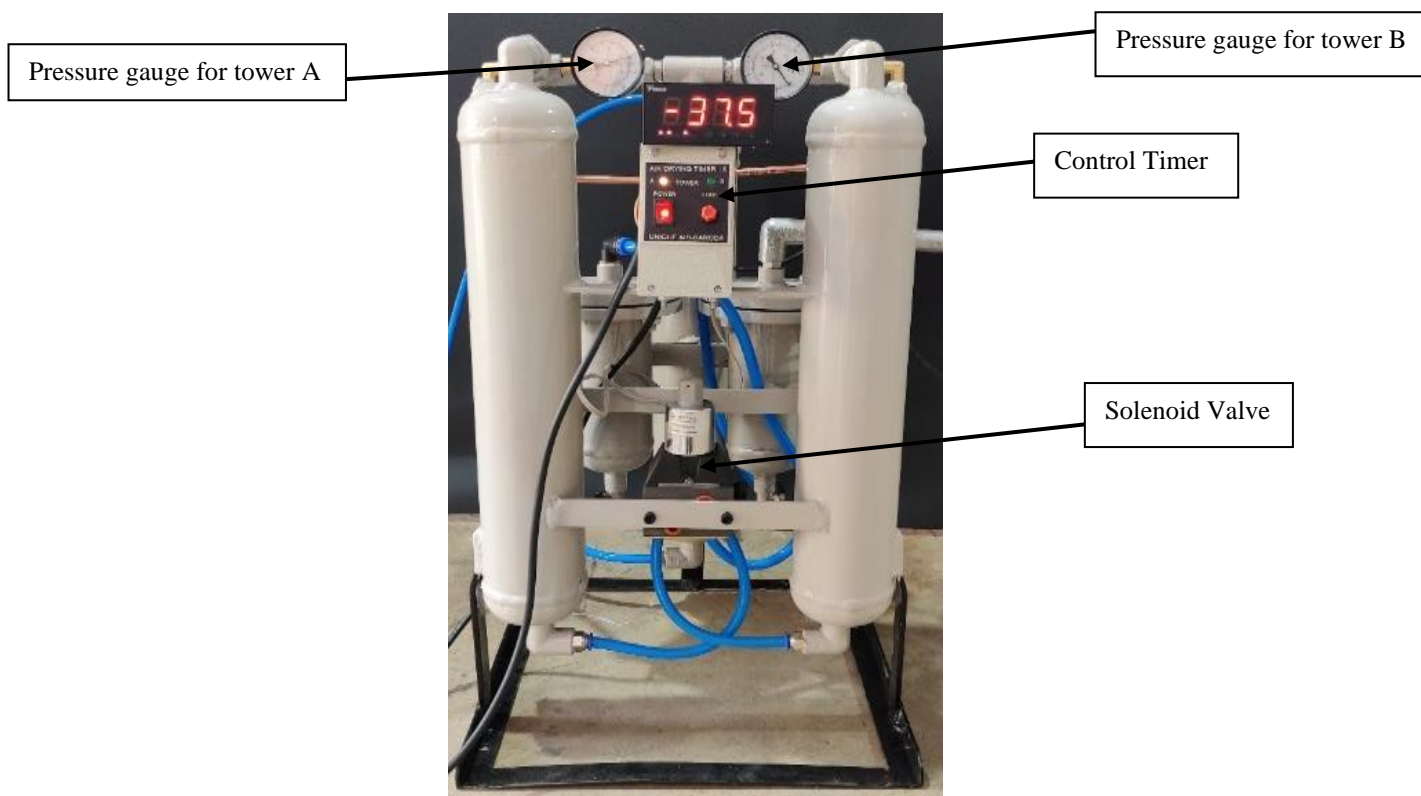


FIGURE 3. 18 Image depicting the test rig assembly with the control panels, pressure gauges and solenoid valve.



FIGURE 3. 19 Dew point meter for testing outlet air dew point temperature

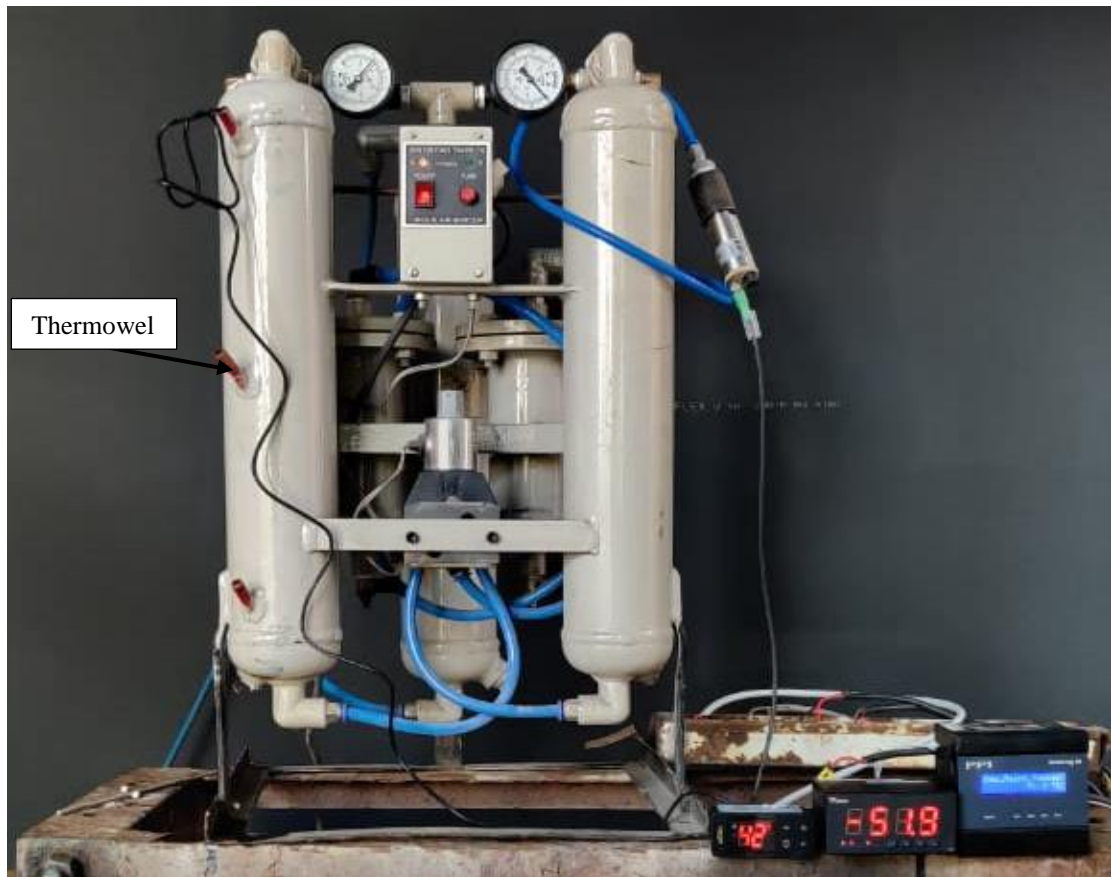


FIGURE 3. 20 Image of the final test rig with the thermowell testing facility across the length of the tower.

Three thermo wells were constructed on Tower A to study the variation in temperature along the length of the tower. Since the cycle oscillates from adsorption to regeneration in each tower. Thermo wells were constructed only on one tower.



FIGURE 3. 21 Assembly and testing





FIGURE 3. 22 Dew point transmitter



FIGURE 3. 23 Dew point Transmitter with Digital Indicator





FIGURE 3. 24 Data logger with RS435 to USB converter.



FIGURE 3. 25 Temperature Indicator with sensing probe



FIGURE 3. 26 Hygrometer for measuring Humidity

### 3.3 Performance parameters

Calculating the moisture removal rate and efficacy of the desiccant dehumidifier to evaluate its performance. The following equation is used to find the rate of moisture removal to the surface of the desiccant from the air:

$$X = m_a (Z_1 - Z_2) \quad (5)$$

Where,

$m_a$  = the mass flow rate of the compressed air at the inlet of the dehumidification tower.

$Z_1$ = the compressed air humidity ratios at the input.

$Z_2$ = the compressed air humidity ratios at the output.

The dehumidification tower's effectiveness  $\varepsilon_{DW}$  is calculated as the ratio of the change in real air humidity ratio to the highest feasible change in humidity ratio.

$$\varepsilon_{DW} = \frac{(Z_1 - Z_2)}{(Z_1 - Z_{2\text{ ideal}})} \quad (6)$$

### 3.4 Uncertainty Analysis

It is quite difficult to get accurate readings when measuring physical quantities. When measuring any physical quantity, there will always be some degree of uncertainty because of the shortcomings of both the measuring instruments and the humans using them. The computation of uncertainty analysis is accomplished with the use of Klein's Method, which can be formulated as follows.

$$w_r = \left[ \left( \frac{\partial R}{\partial x_1} w_1 \right)^2 + \left( \frac{\partial R}{\partial x_2} w_2 \right)^2 + \dots + \left( \frac{\partial R}{\partial x_n} w_n \right)^2 \right]^{\frac{1}{2}} \quad (6)$$

In this case, R is a fixed function of the independent variables  $x_1, x_2, \dots, x_n$ , and the values of  $w_1, w_2, \dots, w_n$  represent the degrees of uncertainty associated with those variables. Temperature and relative humidity readings have the potential to vary by as much as  $\pm 0.2$  °C and  $\pm 2\%$ , respectively, due to measurement errors.

It has been determined that a maximum uncertainty of  $\pm 7.18\%$  is related with the moisture rate. The calculation about the analysis of the degree of uncertainty is presented in detail in Annexure E.

### 3.5 Summary

Experimental test rig was carefully designed to investigate the use of different solid desiccants in a heatless air dryer. The heatless air drier with a capacity of 10 CFM has been

designed and built so that various solid desiccants, such as silica gel, Molecular Sieve 4A, Molecular Sieve 3A, Molecular Sieve 13x, and activated alumina, can be experimentally tested. The dryer makes use of compressed air, which is supplied by a reciprocating air compressor that has a capacity of 10 cubic feet per minute (CFM). A total of 10 cases were undertaken. For each case, experiments were performed and results were recorded with the help of a data logger. Experiments were performed using silica gel, activated alumina, Molecular Sieve 3A, Molecular Sieve 4A and Molecular Sieve 13x and heterogeneous mixtures obtained by mixing two of the previously mentioned desiccants. Thermowells were made along the tower A to observe the temperature gradient during adsorption process to study the heat released during adsorption. Performance parameters such as moisture removal rate and dehumidifier effectiveness are considered. The maximum uncertainty associated with the adsorption rate is found to be  $\pm 7.18\%$ .

## CHAPTER - 4

### Results and Discussion

Experiments were conducted on a heatless air dryer test rig designed for a 10 CFM capacity. Test runs were conducted for solid desiccants such as silica gel, activated alumina, Molecular Sieve 4A, Molecular Sieve 13x and its heterogeneous mixtures. Each experimental investigation for a particular desiccant was considered as one case. A total of 10 cases is studied experimentally and compared.

The results obtained experimentally are validated using ANN. Temperature gradient along the adsorption tower and regeneration tower were recorded to investigate the need for external cooling to control the heat of adsorption. However, from the results depicted below it can be clearly seen that no external cooling is essential owing to a temperature gradient not exceeding 5°C.

Following cases were considered for the experimental investigation:

*Case I:* Activated Alumina is experimentally investigated as a working medium in the heatless air dryer with a flow rate of 10 CFM.

*Case II:* Molecular Sieve 13x is experimentally investigated as a working medium in the heatless air dryer with a flow rate of 10 CFM.

*Case III:* Mixture of Molecular Sieve 13x and activated alumina is experimentally investigated as a working medium in the heatless air dryer with a flow rate of 10 CFM.

*Case IV:* Silica gel is experimentally investigated as a working medium in the heatless air dryer with a flow rate of 10 CFM.

*Case V:* Molecular Sieve 4A is experimentally investigated as a working medium in the heatless air dryer with a flow rate of 10 CFM.

*Case VI:* Mixture of Silica gel and Molecular Sieve 4A is experimentally investigated as a working medium in the heatless air dryer with a flow rate of 10 CFM.

*Case VII:* Mixture of Molecular Sieve 13x and Molecular Sieve 4A is experimentally investigated as a working medium in the heatless air dryer with a flow rate of 10 CFM.

*Case VIII:* Mixture of Activated Alumina and Molecular Sieve 4A is experimentally investigated as a working medium in the heatless air dryer with a flow rate of 10 CFM.

*Case IX:* Mixture of Silica Gel and Molecular Sieve 13x is experimentally investigated as a working medium in the heatless air dryer with a flow rate of 10 CFM.

*Case X:* Mixture of Silica gel and Activated Alumina is experimentally investigated as a working medium in the heatless air dryer with a flow rate of 10 CFM.

The dew point temperature is a direct measure of the dryness of air. The drier the air, the lower the dew point temperature. Using a dew point transmitter the dew point temperatures were recorded for each case. The readings recorded are depicted from Figure 4.1 to Figure 4.10. The summary of the moisture removal rate achieved in each case is given in table 4.1.

#### **4.1 Experimental investigation results of solid desiccants used in heatless air dryer**

*Case I:* Activated Alumina is experimentally investigated as a working medium in the heatless air dryer with a flow rate of 10 CFM. Compressed air having dew point 12.8°C was dried to a dew point of -39.8°C as can be seen in Figure 4.1, moisture removal rate of the dehumidifier achieved was 22.74 gm/hr while the effectiveness of the dehumidifier was 50.93%.



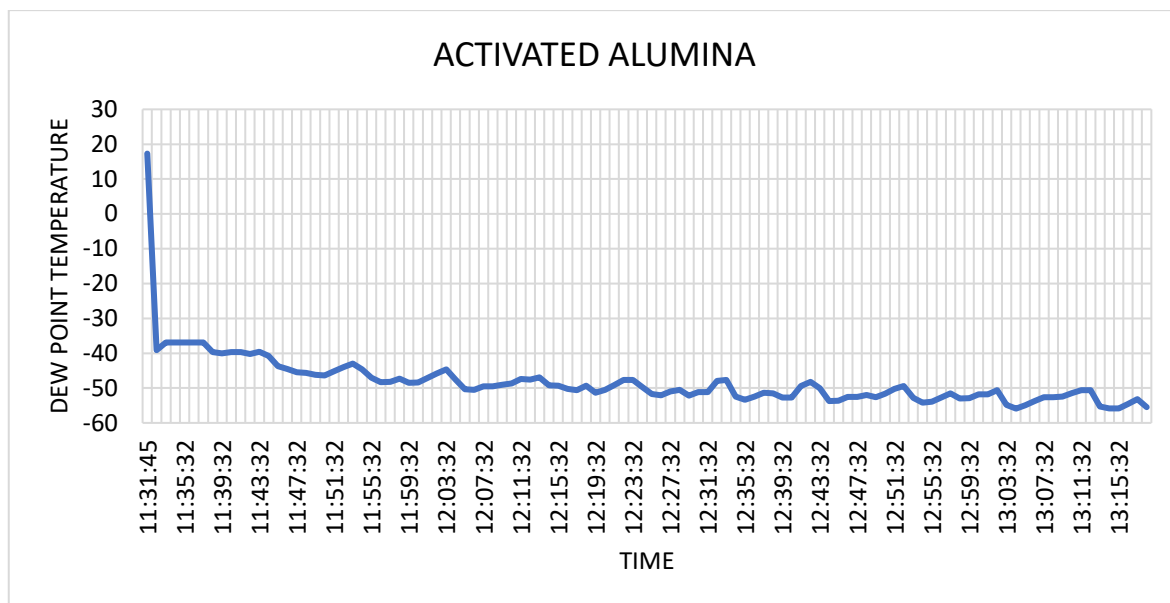


FIGURE 4. 1 Plot depicting variation of dew point temperature with time recorded by data logger when Activated Alumina is is used in the heatless air dryer.

*Case II:* Molecular Sieve 13x is experimentally investigated as a working medium in the heatless air dryer with a flow rate of 10 CFM. Compressed air having dew point 16.1°C was dried to a dew point of -70.0°C as can be seen in Figure4.2, moisture removal rate of the dehumidifier achieved was 54.63 gm/hr while the effectiveness of the dehumidifier was 80.55%.

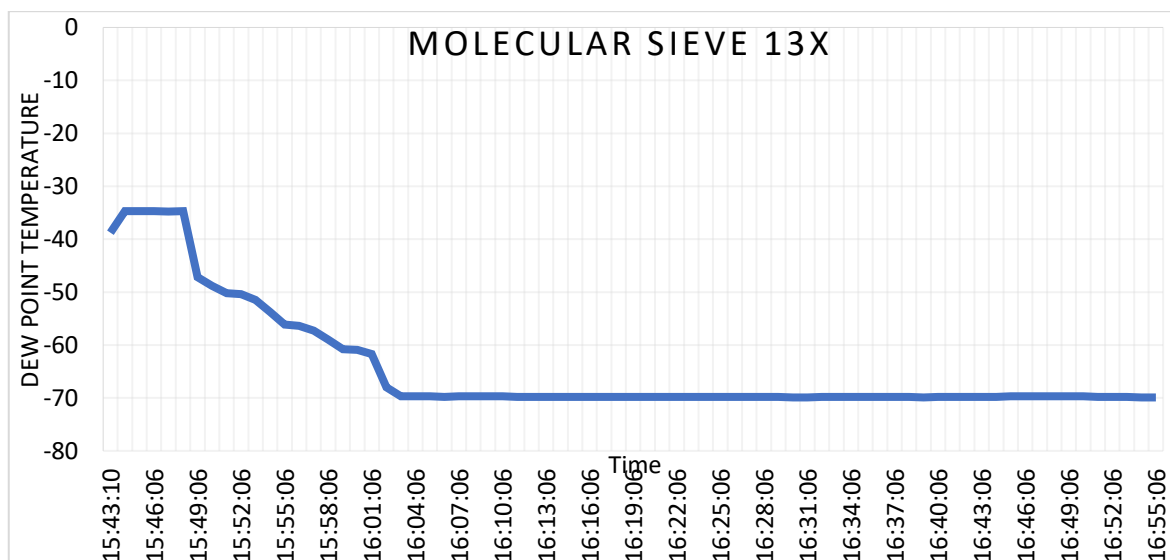


FIGURE 4. 2 Plot depicting variation of dew point temperature with time recorded by data logger when Molecular Sieve 13x is used in the heatless air dryer.

*Case III:* Mixture of Molecular Sieve 13x and activated alumina is experimentally investigated as a working medium in the heatless air dryer with a flow rate of 10 CFM.



Compressed air having dew point  $15.2^{\circ}\text{C}$  was dried to a dew point of  $-55^{\circ}\text{C}$  as can be seen in Figure 4.3, moisture removal rate of the dehumidifier achieved was  $49.81\text{ gm/hr}$  while the effectiveness of the dehumidifier was  $49.29\%$ .

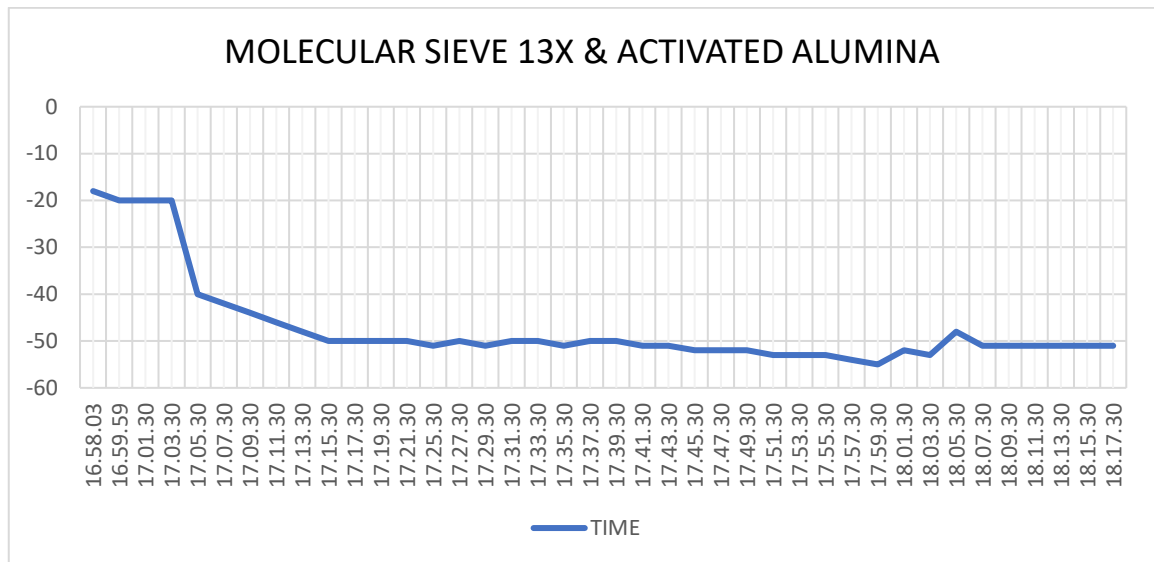


FIGURE 4. 3 Plot depicting variation of dew point temperature with time recorded by data logger when mixture of Molecular Sieve 13x and activated alumina is used in the air dryer.

*Case IV:* Silica gel is experimentally investigated as a working medium in the heatless air dryer with a flow rate of 10 CFM. Compressed air having dew point  $5.5^{\circ}\text{C}$  was dried to a dew point of  $-55^{\circ}\text{C}$  as can be seen in Figure 4.4, moisture removal rate of the dehumidifier achieved was  $22.51\text{ gm/hr}$  while the effectiveness of the dehumidifier was  $47.18\%$ .

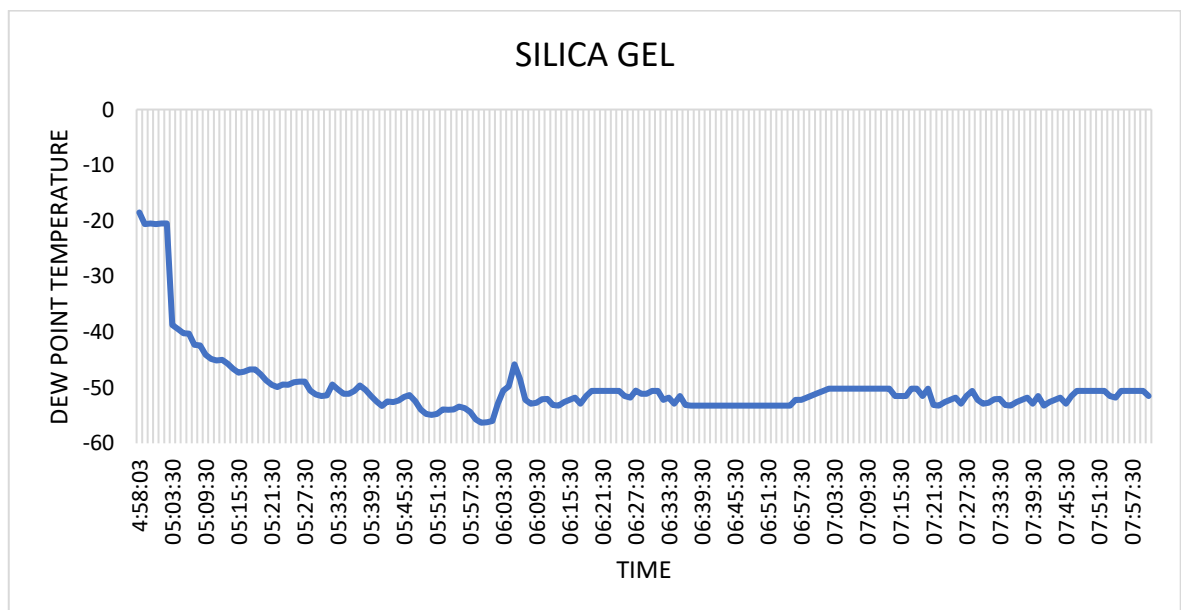


FIGURE 4. 4 Plot depicting variation of dew point temperature with time recorded by data logger when silica gel is used in the heatless air dryer.

*Case V:* Molecular Sieve 4A is experimentally investigated as a working medium in the heatless air dryer with a flow rate of 10 CFM. Compressed air having dew point 7.7°C was dried to a dew point of -63.4°C as can be seen in Figure4.5, moisture removal rate of the dehumidifier achieved was 39.58 gm/hr while the effectiveness of the dehumidifier was 81.68%.

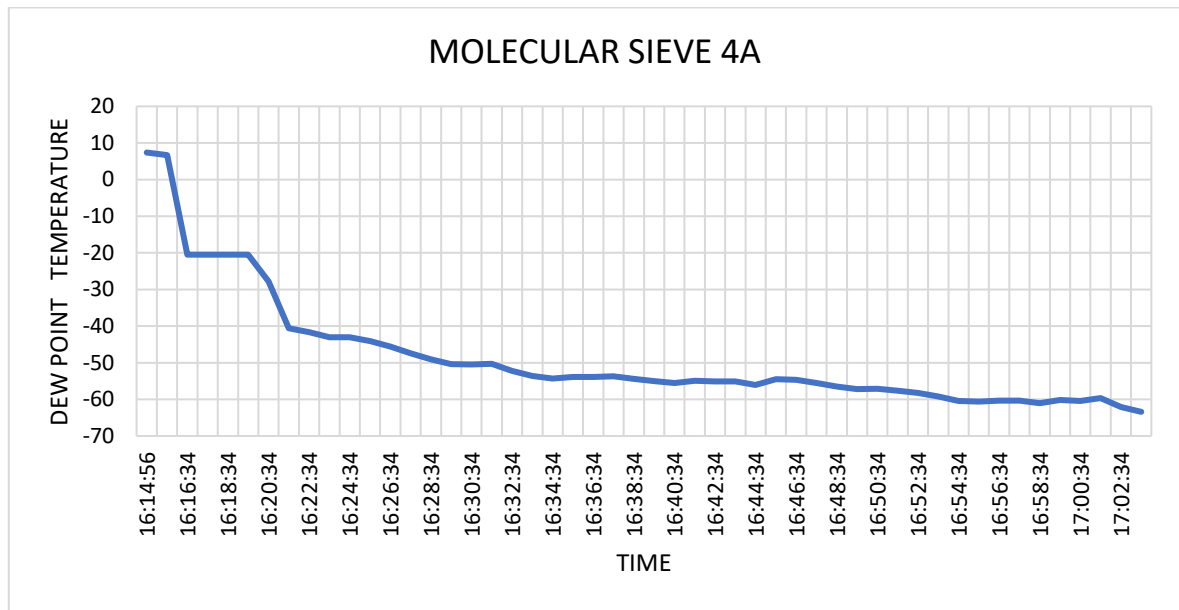


FIGURE 4. 5 Plot depicting variation of dew point temperature with time recorded by data logger when Molecular Sieve 4A is used in the heatless air dryer.

*Case VI:* Mixture of Silica gel and Molecular Sieve 4A is experimentally investigated as a working medium in the heatless air dryer with a flow rate of 10 CFM. Compressed air having dew point 19.9°C was dried to a dew point of -40.0°C as can be seen in Figure4.6, moisture removal rate of the dehumidifier achieved was 43.96 gm/hr while the effectiveness of the dehumidifier was 37.86%.

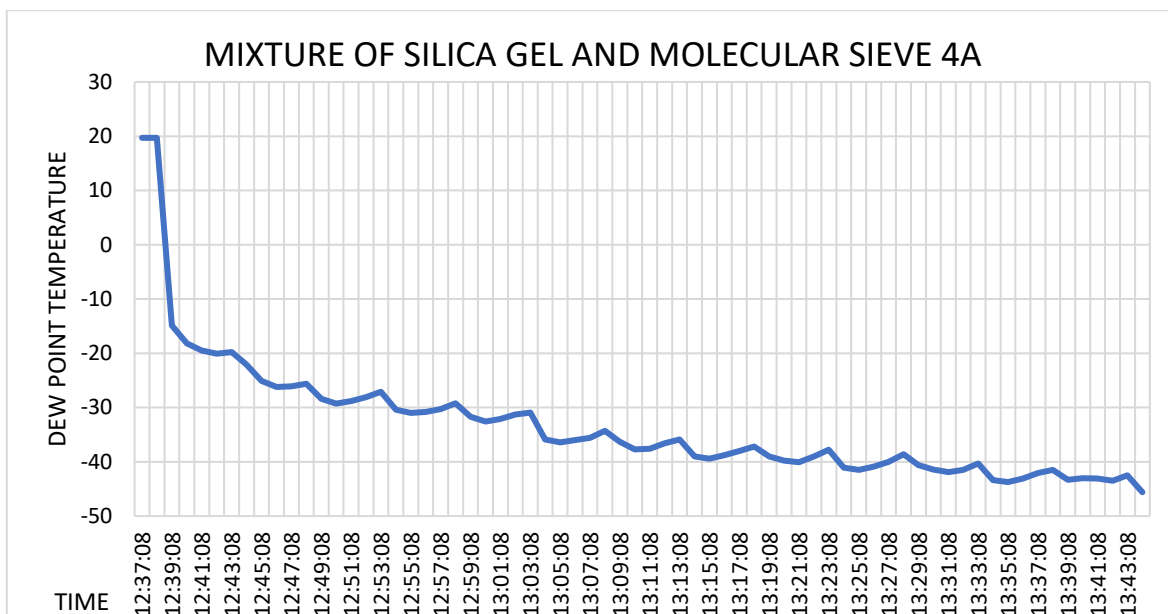


FIGURE 4. 6 Plot depicting variation of dew point temperature with time recorded by data logger when mixture of Silica gel and Molecular Sieve 4A is used in the heatless air dryer.

*Case VII:* Mixture of Molecular Sieve 13x and Molecular Sieve 4A is experimentally investigated as a working medium in the heatless air dryer with a flow rate of 10 CFM. Compressed air having dew point 19.3°C was dried to a dew point of -52°C as can be seen in Figure4.7, moisture removal rate of the dehumidifier achieved was 67.50 gm/hr while the effectiveness of the dehumidifier was 52.61%.

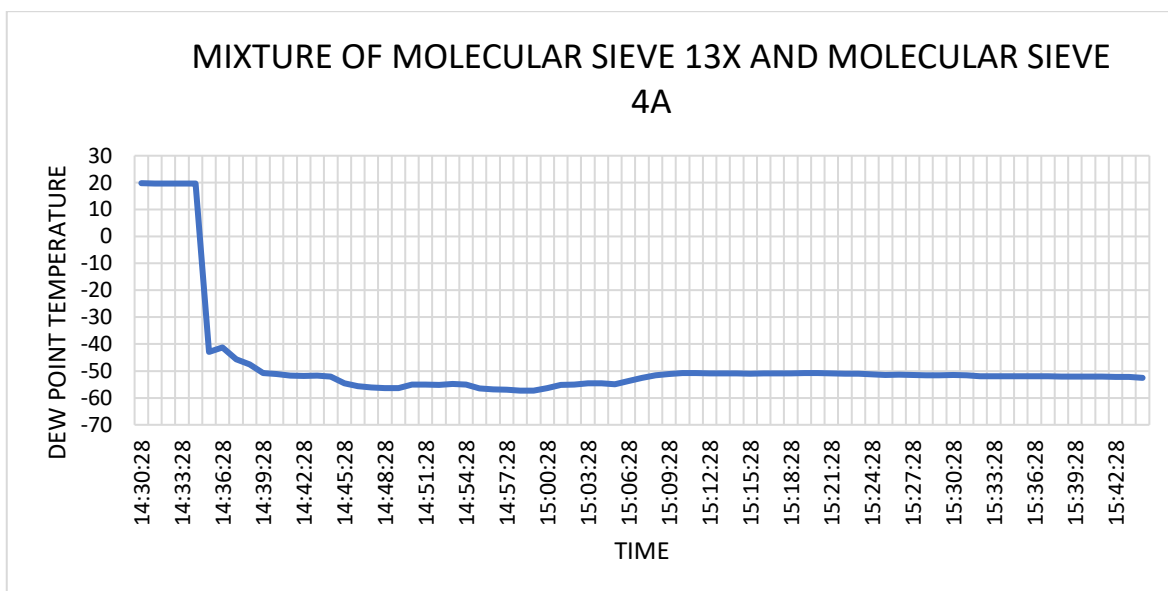


FIGURE 4. 7 Plot depicting variation of dew point temperature with time recorded by data logger when mixture of Molecular Sieve 13x and Molecular Sieve 4A is used in the heatless air dryer.

*Case VIII:* Mixture of Activated Alumina and Molecular Sieve 4A is experimentally investigated as a working medium in the heatless air dryer with a flow rate of 10 CFM. Compressed air having dew point 19.3°C was dried to a dew point of -45°C as can be seen in Figure 4.8, moisture removal rate of the dehumidifier achieved was 13.91 gm/hr while the effectiveness of the dehumidifier was 13.69%.

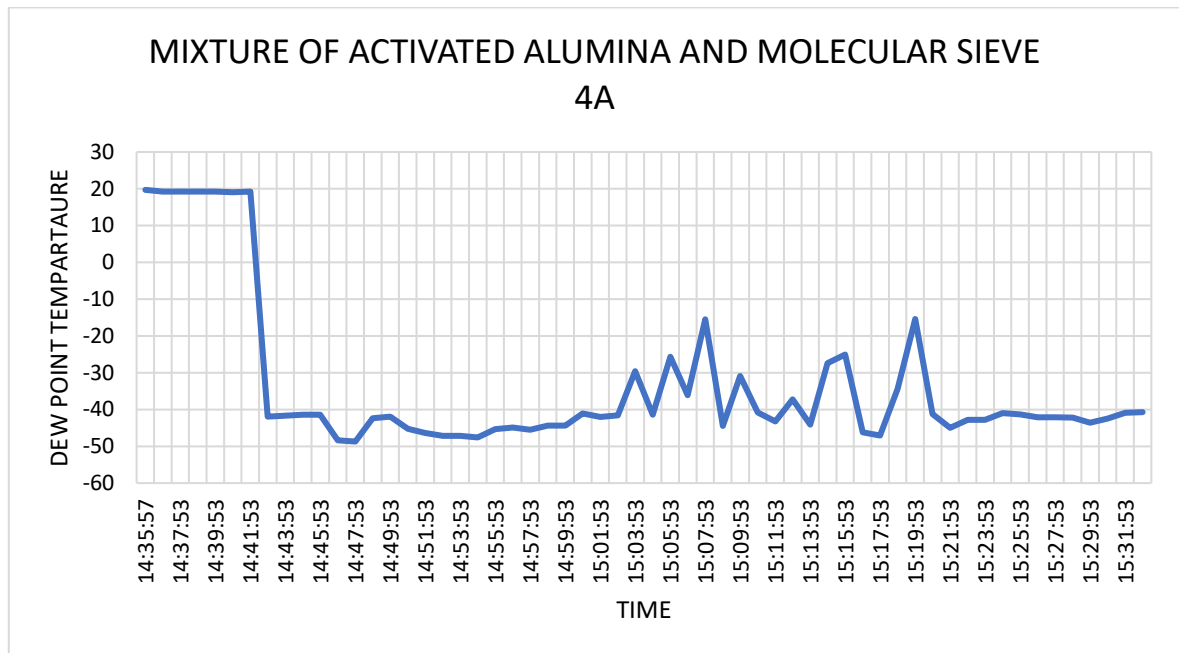


FIGURE 4. 8 Plot depicting variation of dew point temperature with time recorded by data logger when mixture of Activated Alumina and Molecular Sieve 4A is used in the heatless air dryer.

*Case IX:* Mixture of Silica Gel and Molecular Sieve 13x is experimentally investigated as a working medium in the heatless air dryer with a flow rate of 10 CFM. Compressed air having dew point 19.9°C was dried to a dew point of -57.4°C as can be seen in Figure 4.9, moisture removal rate of the dehumidifier achieved was 108.19 gm/hr while the effectiveness of the dehumidifier was 80.04%.

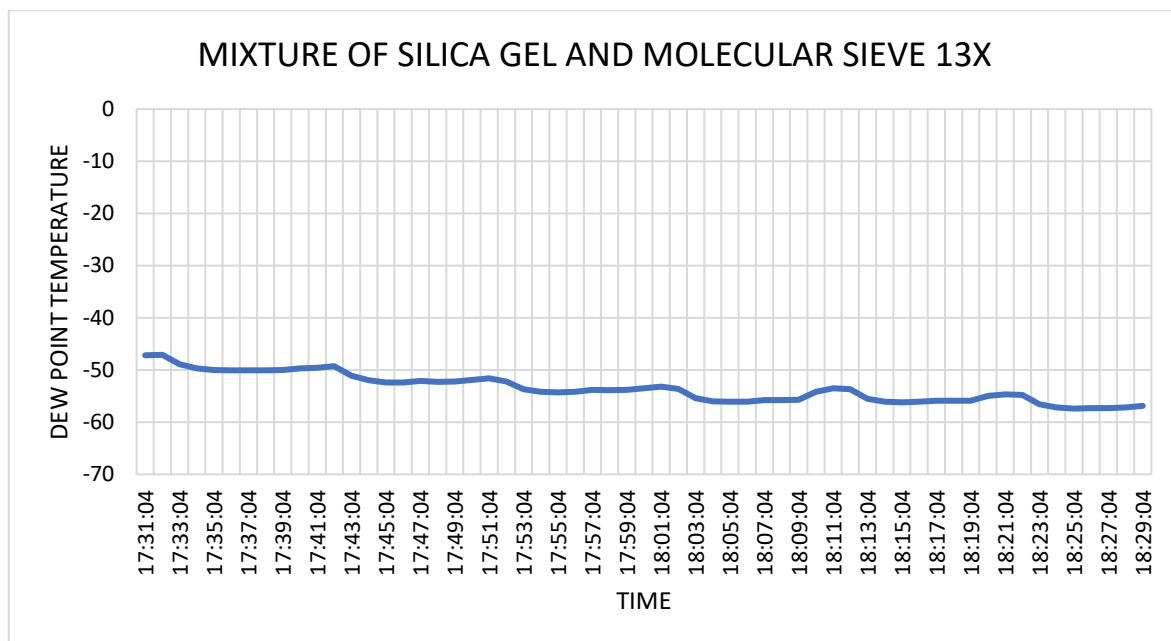


FIGURE 4. 9 Plot depicting variation of dew point temperature with time recorded by data logger when mixture of Silica Gel and Molecular Sieve 13x is used in the heatless air dryer.

*Case X:* Mixture of Silica gel and Activated Alumina is experimentally investigated as a working medium in the heatless air dryer with a flow rate of 10 CFM. Compressed air having dew point 6.3°C was dried to a dew point of -34.6°C as can be seen in Figure4.10, moisture removal rate of the dehumidifier achieved was 17.95 gm/hr while the effectiveness of the dehumidifier was 30.37%.

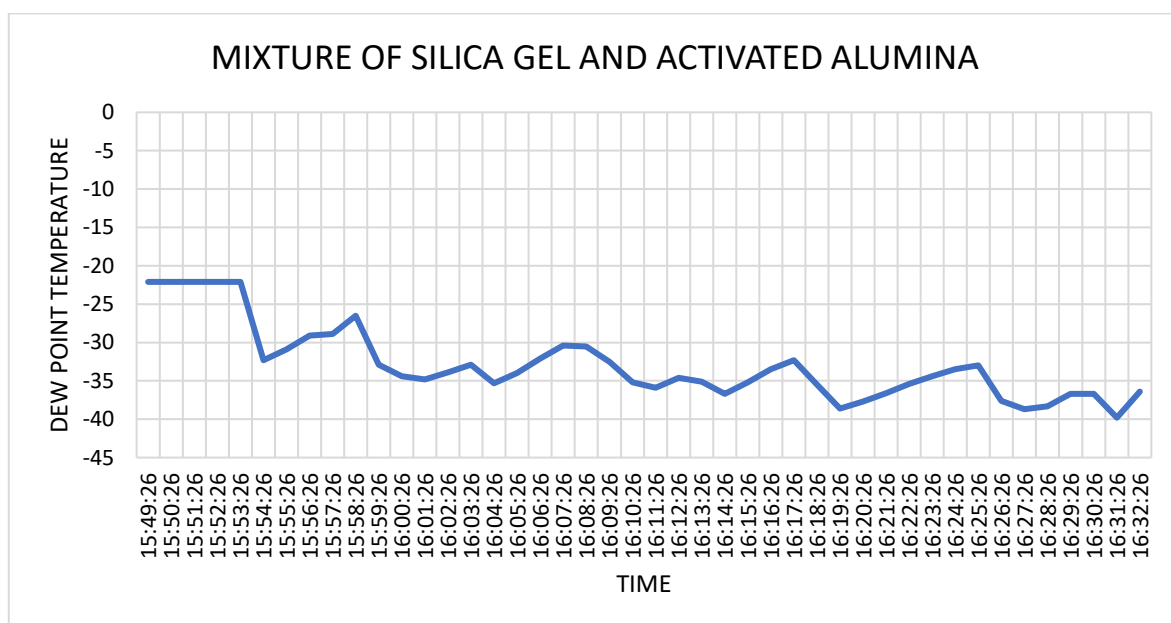


FIGURE 4. 10 Plot depicting variation of dew point temperature with time recorded by data logger when mixture of Silica gel and Activated Alumina is used in the heatless air dryer.

Parameters	Silica gel	Molecular Sieve 4A	Molecular Sieve 13X	Activated Alumina	Silica gel & AA	Silica gel & MS 4A	Silica gel & 13x	AA & MS 4A	AA & 13x	MS4A & 13x
Moisture removal rate in gm/hr	22.51	39.58	54.63	22.74	17.95	43.96	108.9	13.91	49.81	67.50
Effectiveness of dehumidifier in %	47.18	81.68	80.55	50.93	30.37	37.86	80.04	13.69	49.29	52.61

Table 4. 1 Results table of experimental test for case 1 to 10.

The preceding findings came about as a consequence of testing performed in the heatless air dryer on a variety of solid desiccants. Other variables, like flow rate, bed length, and so on, remained unchanged throughout the experiment. Experiments were conducted with the sole purpose of measuring the outcome of the change in desiccants that occurred in a heatless air dryer. Molecular Sieve 3A and Molecular Sieve 4A gave very similar results. Hence only Molecular Sieve 4A was considered for the investigation while Molecular Sieve 3A was dropped after preliminary investigation.

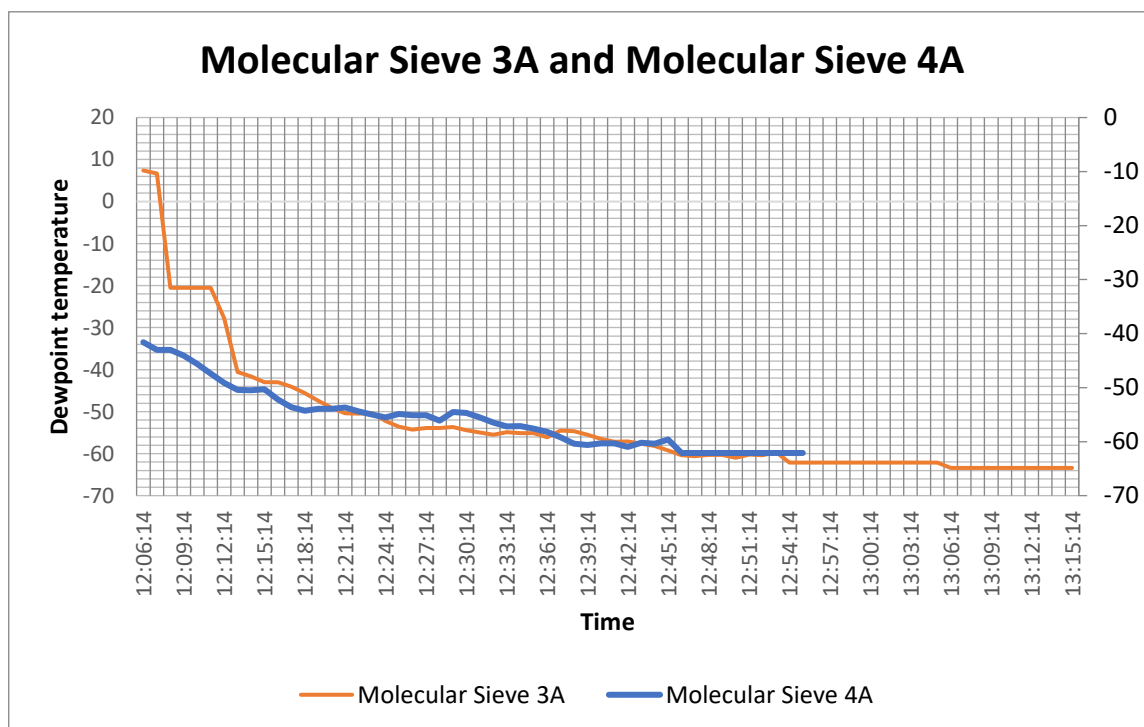


FIGURE 4. 11 Plot depicting comparative analysis of variation of dew point temperature with time for Molecular Sieve 3A and Molecular Sieve 4A used in the heatless air dryer.

## 4.2 Investigation results for heat of adsorption released across the tower for each case.

It was observed during adsorption process the adsorption tower would increase in temperature. To investigate the heat of adsorption released in each case, to avoid overheating, three thermowells were constructed at equal distance along the tower and temperature gradient was recorded. The thermowells were constructed only on one tower as the adsorption and regeneration cycle alternates in an interval of five minutes. The results of the temperature readings recorded in the thermowell are as shown in Fig 4.12 to Figure 4.32 for each case.

*Case I:* Activated Alumina is experimentally investigated as a working medium in the heatless air dryer with a flow rate of 10 CFM.

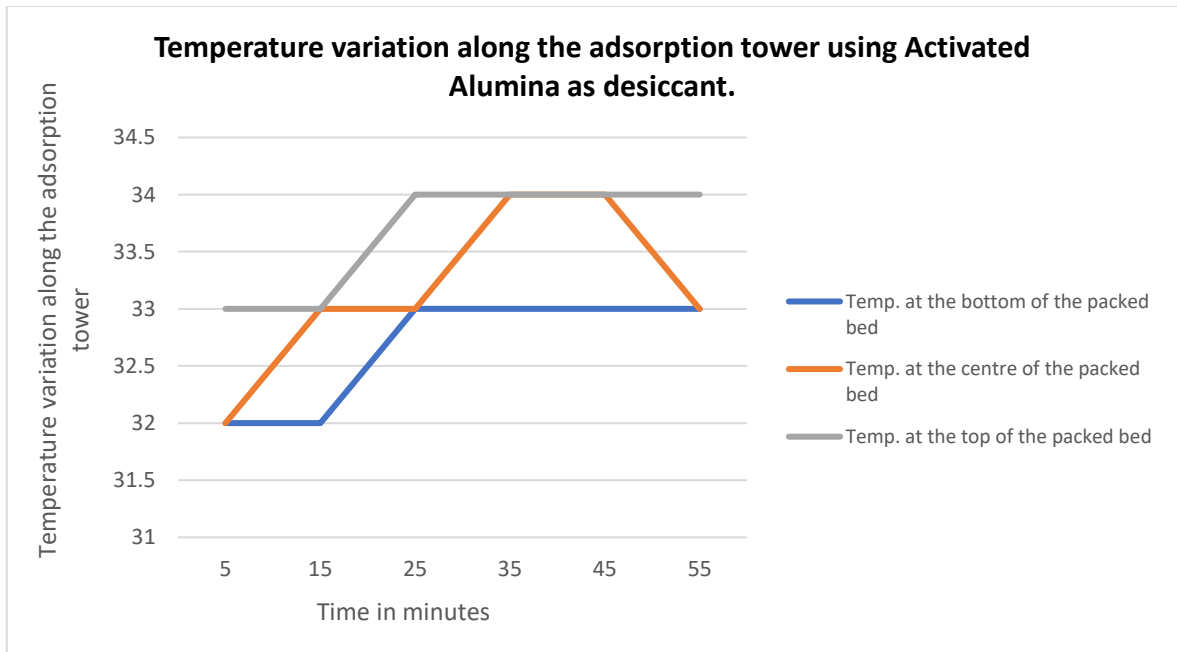


FIGURE 4. 12 Temperature variation along the adsorption tower using Activated Alumina as desiccant.

It can be clearly seen from Figure 4.12 that there is temperature rise when adsorption takes place in the adsorption tower during the testing of activated alumina. However, the  $\Delta T$  does not exceed 2°C. It is also observed that the temperature at the top of the packed bed is higher when compared to the bottom part of the bed. This is an indication that the desiccant at the top part of the packed bed is more actively involved in the phenomenon of adsorption. This could be due to the direction of the process air entering from the bottom of the bed and then

exiting into the process line from the top of the bed.

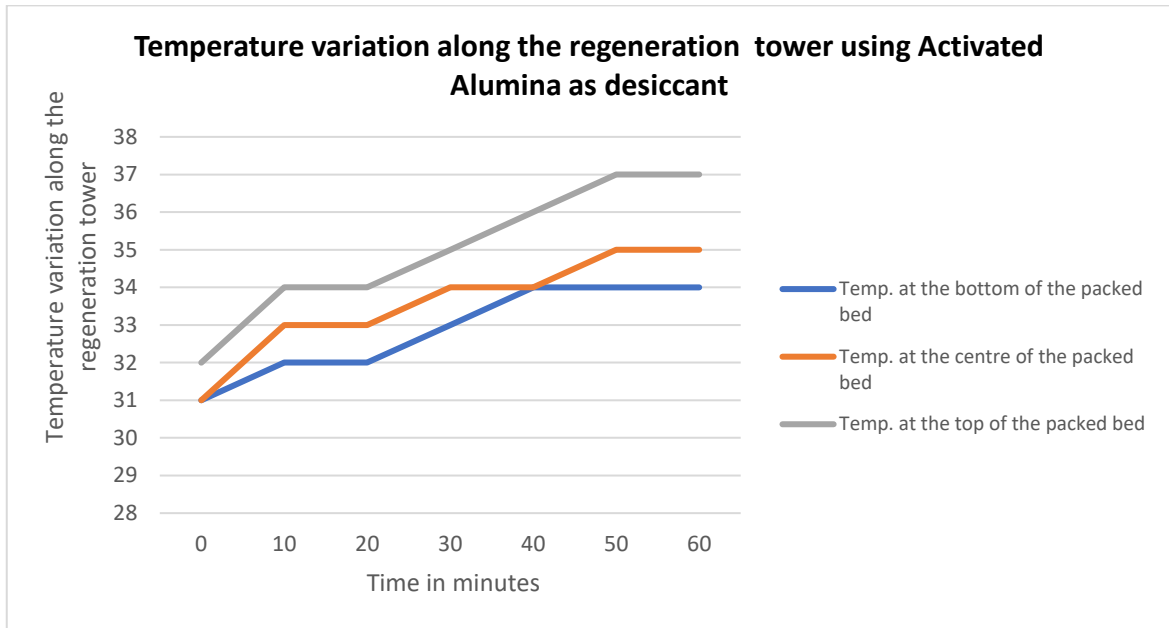


FIGURE 4. 13 Temperature variation along the regeneration tower using Activated Alumina as desiccant

Similarly, in Figure 4.13 when the regeneration tower was investigated with activated alumina as the desiccant, it was observed that a temperature rise of  $\Delta T$  at  $6^{\circ}\text{C}$  on the topmost side of the packed bed was observed while  $\Delta T$  of  $4^{\circ}\text{C}$  is observed at the bottom of the regeneration tower. Hence a decline in temperature gradient is observed as the regeneration occurs from top of the packed bed towards the bottom.

*Case II:* Molecular Sieve 13x is experimentally investigated as a working medium in the heatless air dryer with a flow rate of 10 CFM.



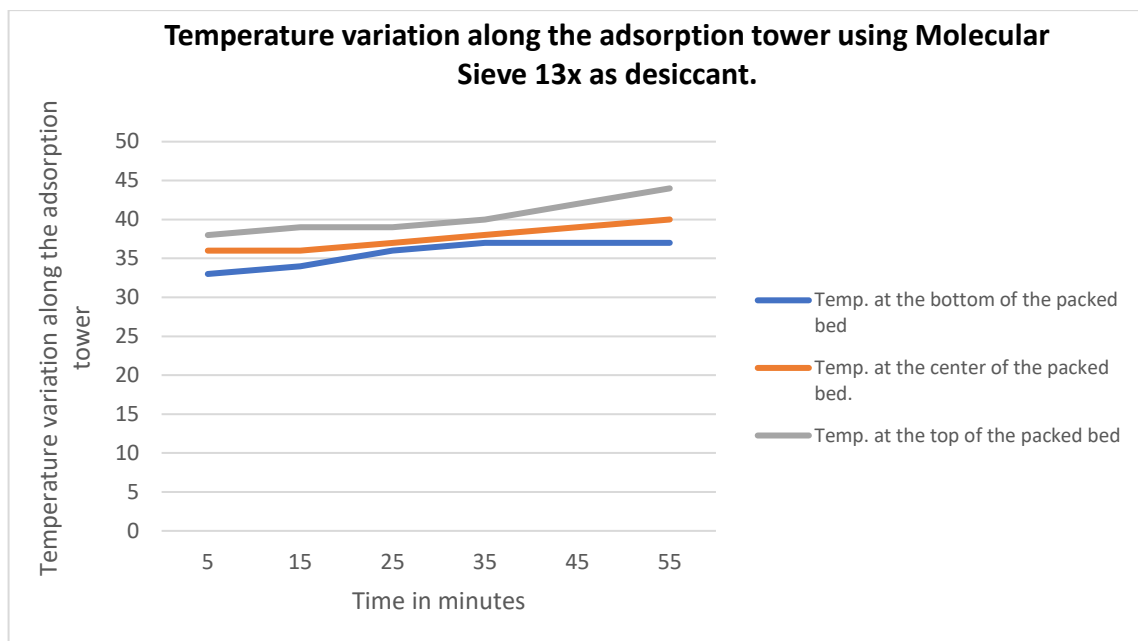


FIGURE 4. 14 Temperature variation along the adsorption tower using Molecular Sieve 13x as desiccant.

A  $\Delta T$  of  $4^{\circ}\text{C}$  was observed as shown in Figure 4.14 when the temperature gradient in the adsorption tower was recorded for Molecular Sieve 13x as desiccant in the heatless air dryer.  $\Delta T$  was uniform for the entire packed bed.

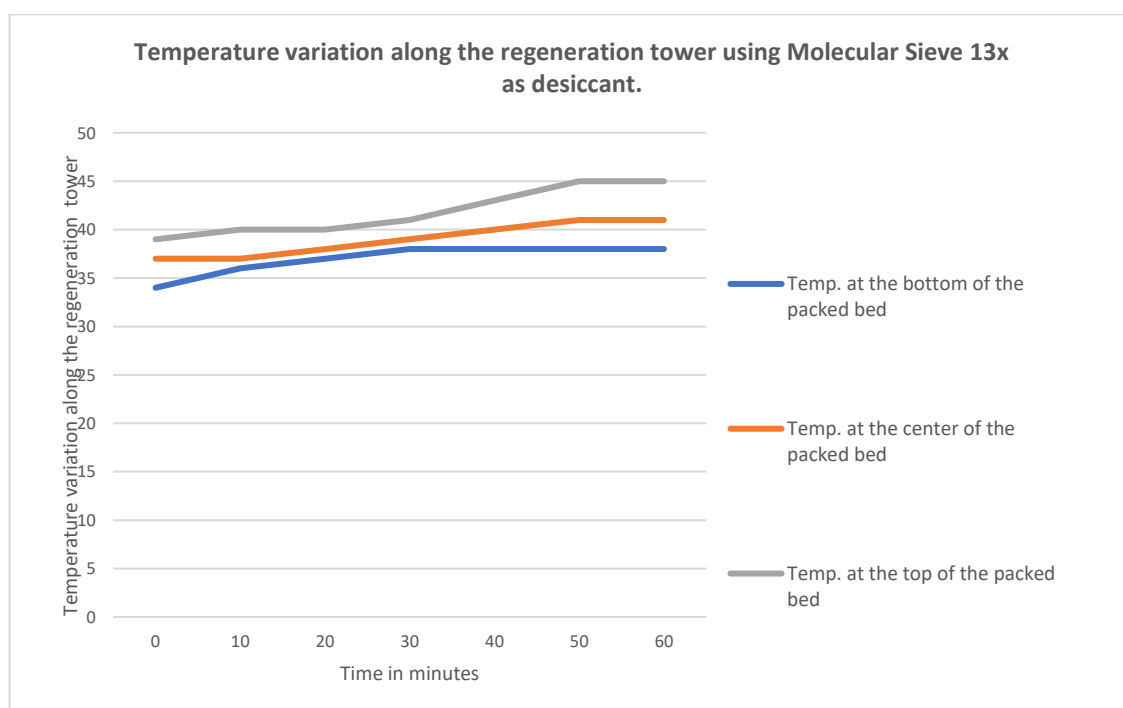


FIGURE 4. 15 Temperature variation along the regeneration tower using Molecular Sieve 13x as desiccant.

A  $\Delta T$  of  $4^{\circ}\text{C}$  was observed when the temperature gradient in the bottom of the regeneration tower was recorded for Molecular Sieve 13x as desiccant in the heatless air dryer. While  $\Delta T$  of  $6^{\circ}\text{C}$  was recorded at the bottom of the packed bed as can be seen in Fig.4.15.

*Case III:* Mixture of Molecular Sieve 13x and activated alumina is experimentally investigated as a working medium in the heatless air dryer with a flow rate of 10 CFM.

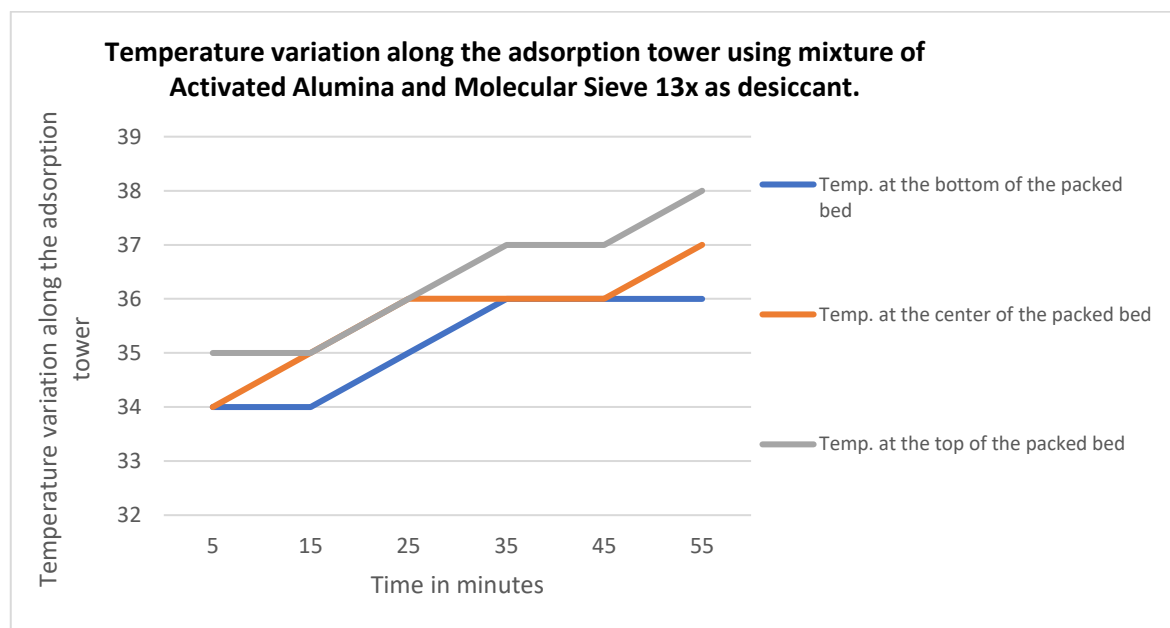


FIGURE 4. 16 Temperature variation along the adsorption tower using mixture of Activated Alumina and Molecular Sieve 13x as desiccant.

In Case III, a heterogeneous mixture of Activated Alumina and Molecular Sieve 13x is tested as a desiccant in the heatless air dryer. It is observed from Figure 4.16 that the temperature gradient at the bottom of the tower is  $2^{\circ}\text{C}$  while a  $\Delta T$  of  $3^{\circ}\text{C}$  was observed at the top most part of the packed bed during the adsorption process

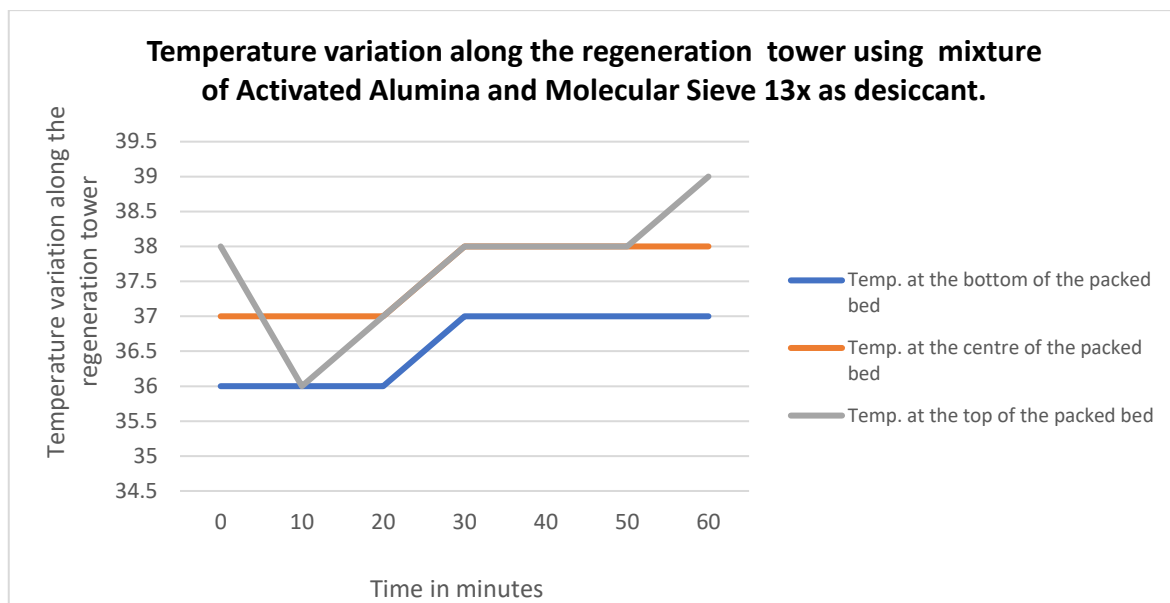


FIGURE 4. 17 Temperature variation along the regeneration tower using mixture of Activated Alumina and Molecular Sieve 13x as desiccant.

In the regeneration tower for Case III it is observed from Figure 4.17 that a minuscule temperature gradient of 1°C is recorded throughout the regeneration tower.

*Case IV:* Silica gel is experimentally investigated as a working medium in the heatless air dryer with a flow rate of 10 CFM.

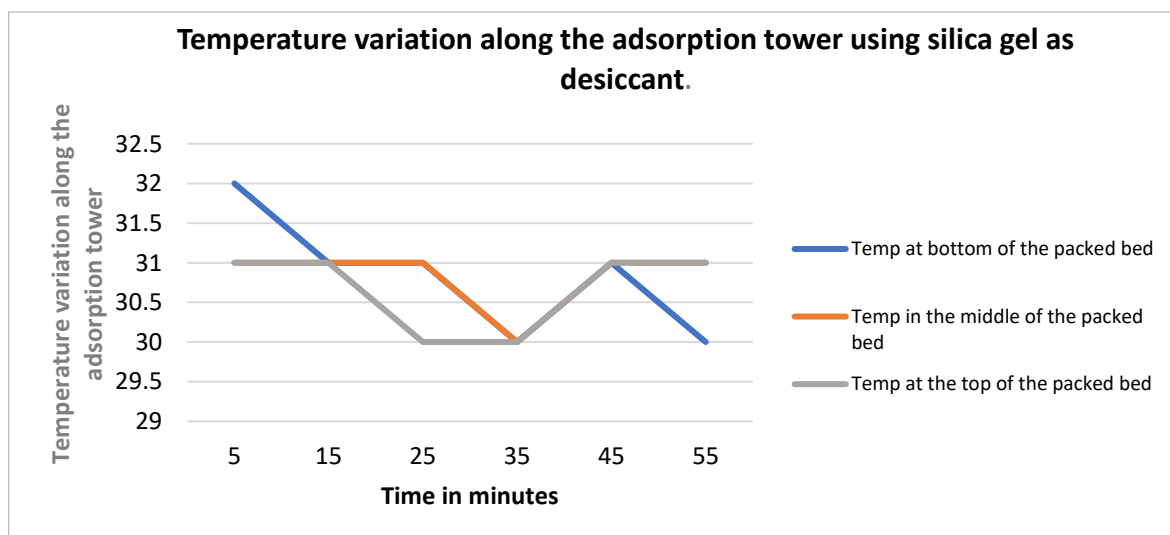


FIGURE 4. 18 Temperature variation along the adsorption tower using silica gel as desiccant.

As seen in Figure 4.18 the  $\Delta T$  during adsorption observed during testing of silica gel as a desiccant in the heatless air dryer was found to be -2°C at the bottom of the bed while a drop

of 1°C was observed in the mid-section of the tower while the temperature on the top most portion of the adsorption bed remained almost constant. This indicates there was no significant heat of adsorption released during the adsorption process for silica gel. Similarly, as can be seen in Figure 4.19 during the regeneration process a loss of 4°C is observed at the bottom of the regeneration tower while a drop of 2°C is noted at the top and middle portion of the packed bed.

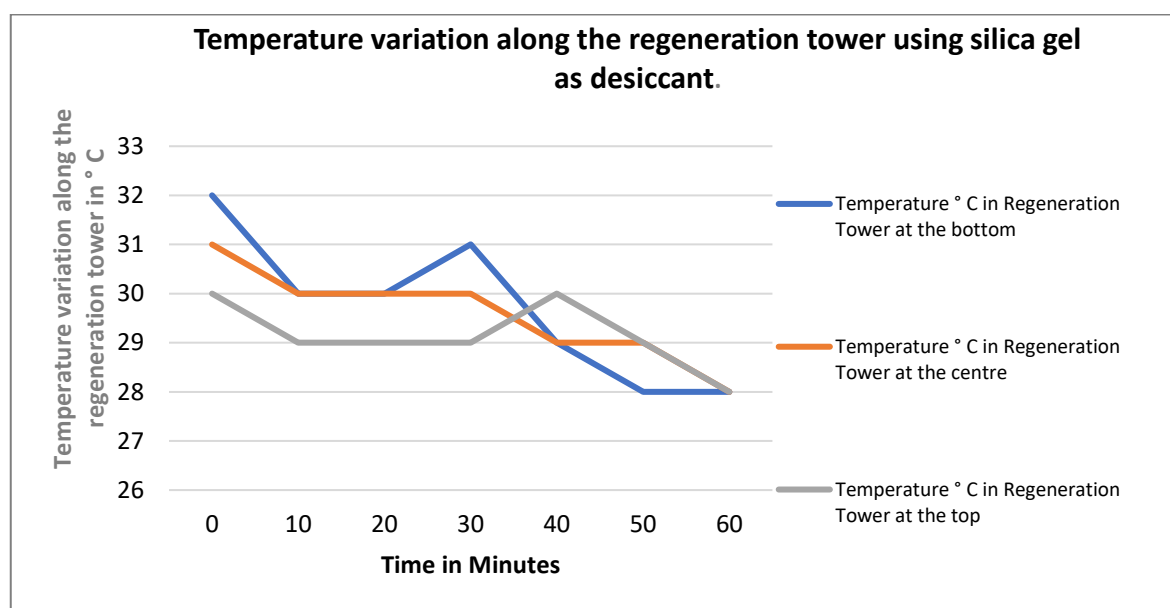


FIGURE 4. 19 Temperature variation along the regeneration tower using silica gel as desiccant.

*Case V:* Molecular Sieve 4A is experimentally investigated as a working medium in the heatless air dryer with a flow rate of 10 CFM.

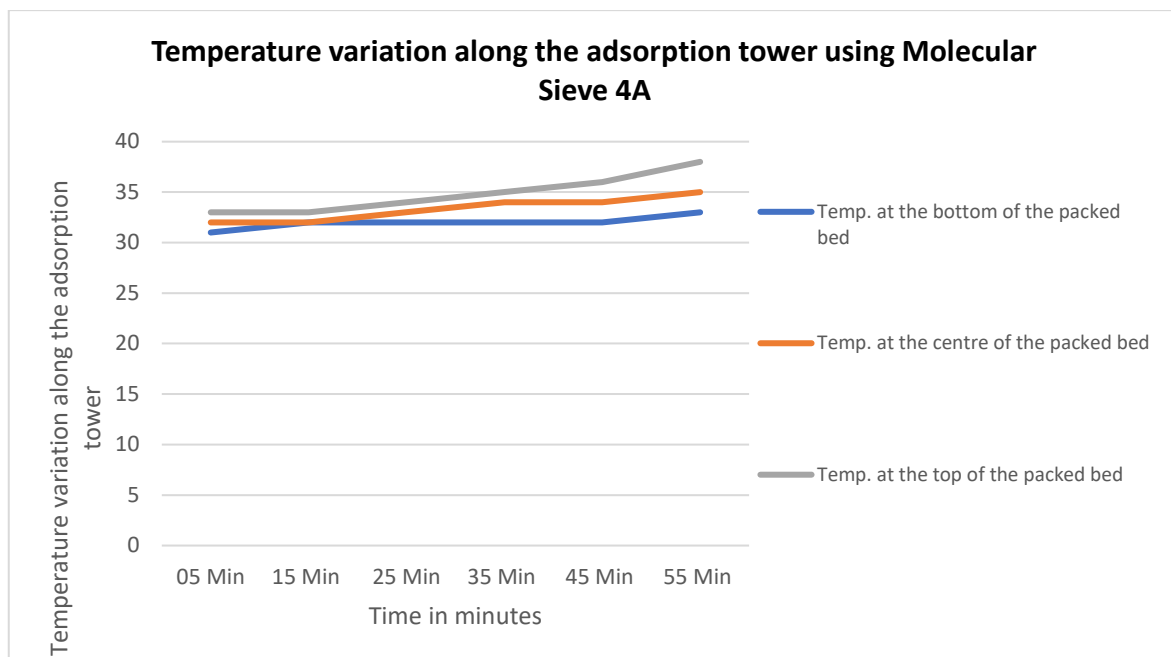


FIGURE 4. 20 Temperature variation along the adsorption tower using Molecular Sieve 4A

When Molecular Sieve 4A was tested in a heatless air dryer  $\Delta T$  of 5°C was recorded in the top of the packed bed during adsorption as well as regeneration as seen in Figure 4.20. Indicating active participation of the desiccants in the top most part of the packed bed.

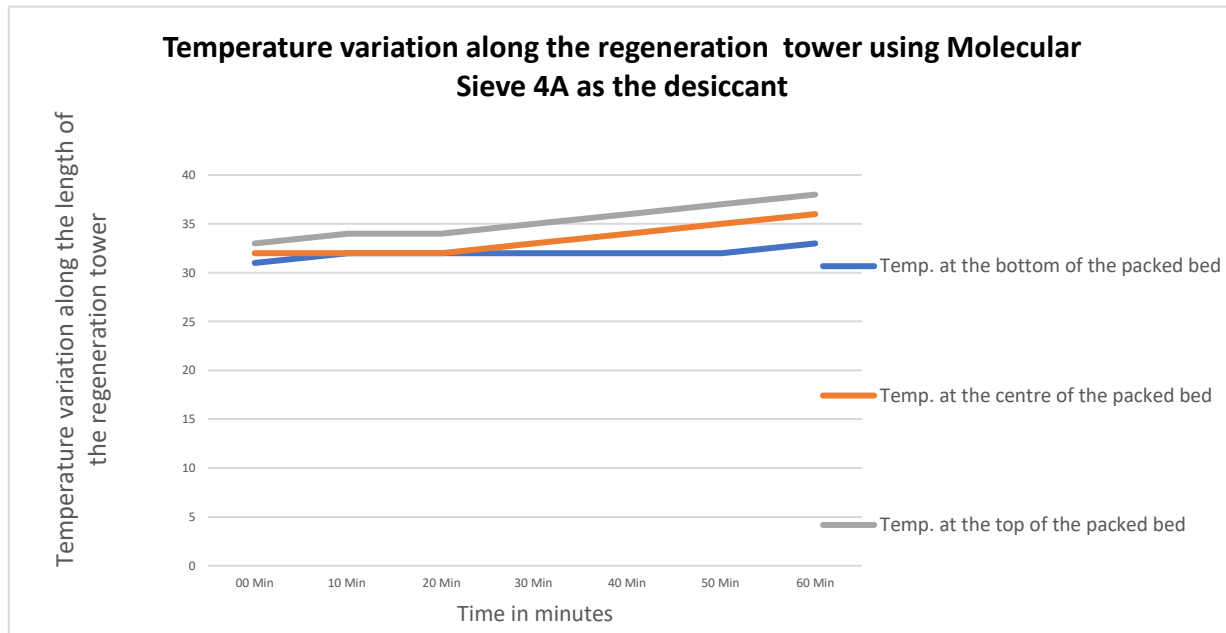


FIGURE 4. 21 Temperature variation along the regeneration tower using Molecular Sieve 4A as the desiccant

*Case VI:* Mixture of Silica gel and Molecular Sieve 4A is experimentally investigated as a working medium in the heatless air dryer with a flow rate of 10 CFM.

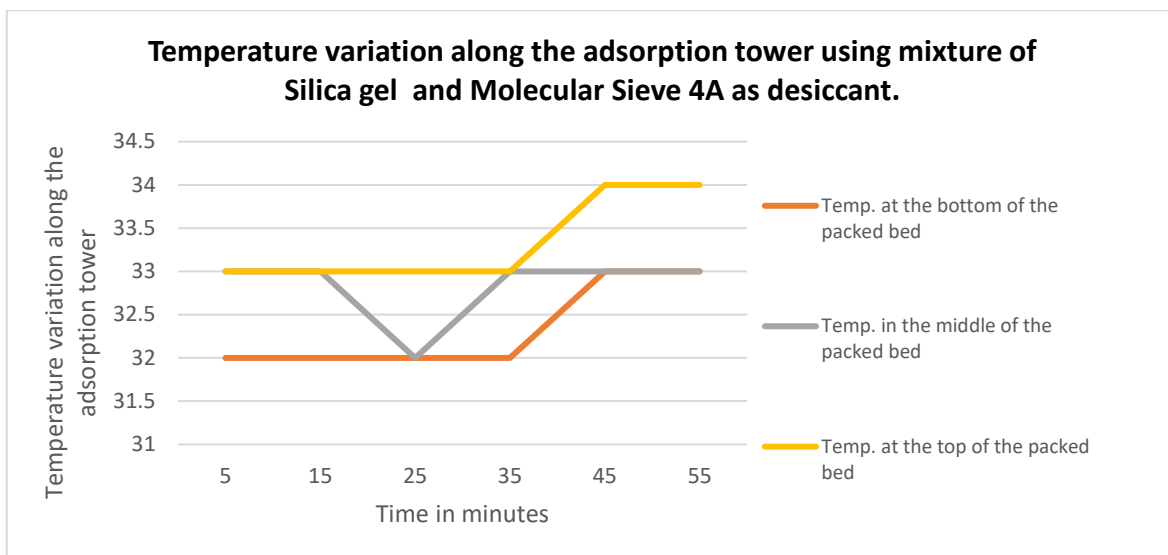


FIGURE 4. 22 Temperature variation along the adsorption tower using mixture of Silica gel and Molecular Sieve 4A as desiccant.

During the adsorption and regeneration processes, when using the mixture of silica gel and Molecular Sieve 4A, it was noted that a maximum of 1°C increase in temperature was recorded in the adsorption tower as shown in Figure 4.22. This was discovered by observing the temperature variation along the packed bed throughout these processes. As shown in Figure 4.23, a rise in temperature of 4 °C was noticed while the regeneration process was in progress.

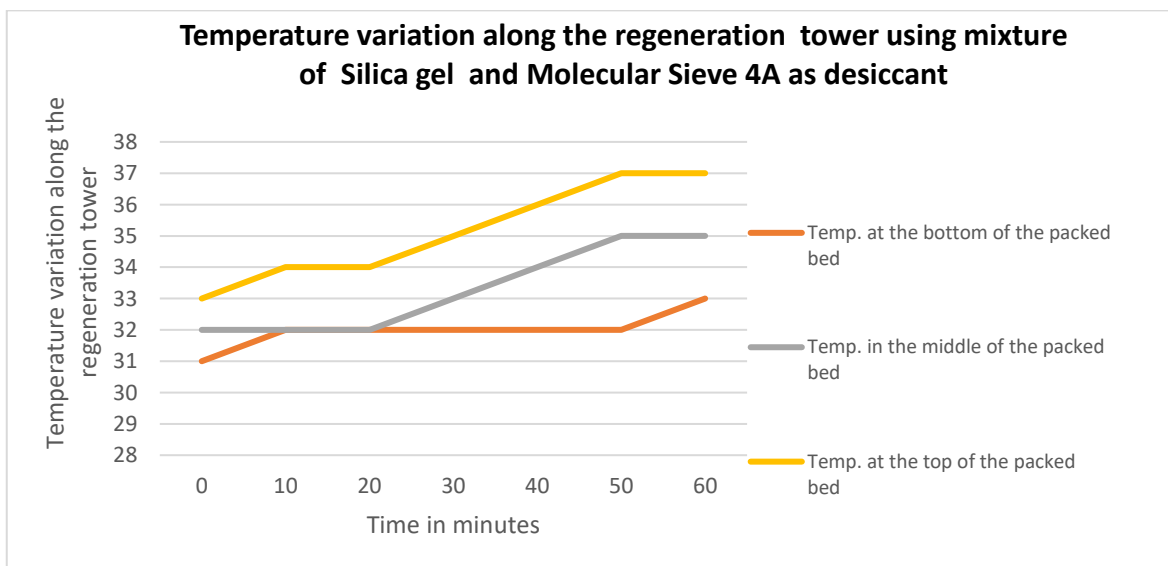


FIGURE 4. 23 Temperature variation along the regeneration tower using mixture of Silica gel and Molecular Sieve 4A as desiccant.

*Case VII:* Mixture of Molecular Sieve 13x and Molecular Sieve 4A is experimentally investigated as a working medium in the heatless air dryer with a flow rate of 10 CFM.

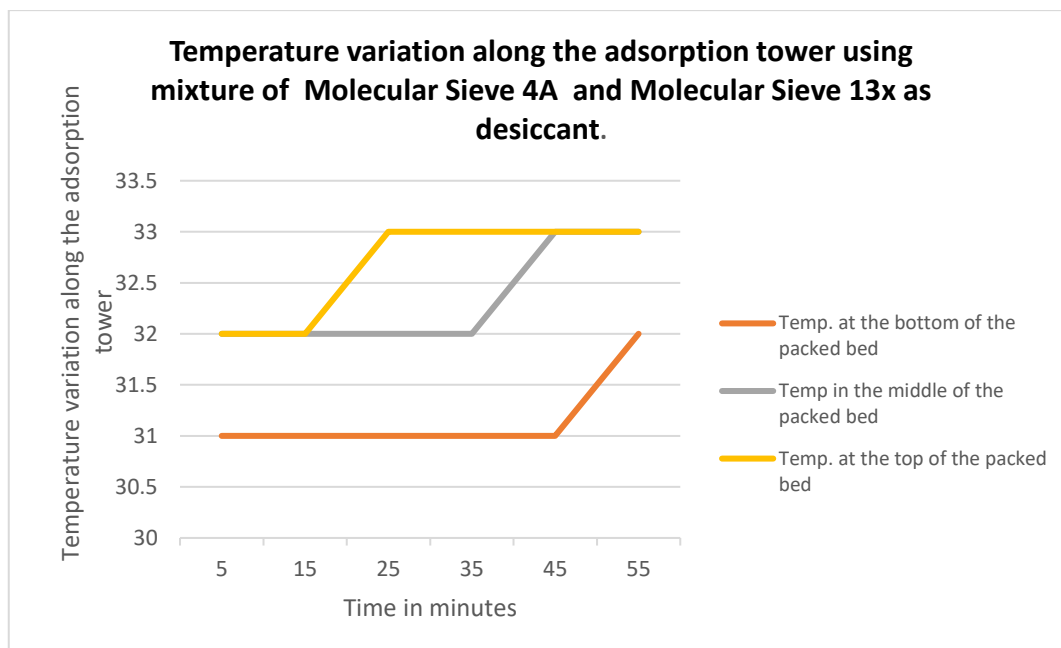


FIGURE 4. 24 Temperature variation along the adsorption tower using mixture of Molecular Sieve 4A and Molecular Sieve 13x as desiccant.

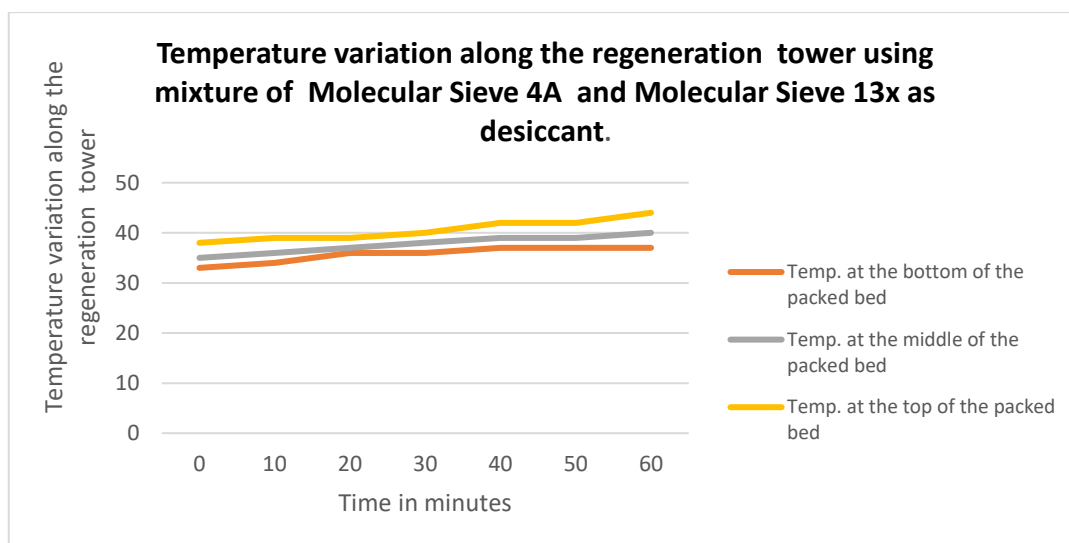


FIGURE 4. 25 Temperature variation along the regeneration tower using mixture of Molecular Sieve 4A and Molecular Sieve 13x as desiccant.

Figure 4.24 and Figure 4.25 depict the rise in temperature of the packed bed during the adsorption and regeneration process respectively when mixture of Molecular Sieve 4A and Molecular Sieve 13x is used in the heatless desiccant air dryer. A maximum  $\Delta T$  of  $2^{\circ}\text{C}$  is recorded during adsorption and  $\Delta T$  of  $4^{\circ}\text{C}$  is recorded during regeneration process.

*Case VIII:* Mixture of Activated Alumina and Molecular Sieve 4A is experimentally investigated as a working medium in the heatless air dryer with a flow rate of 10 CFM.

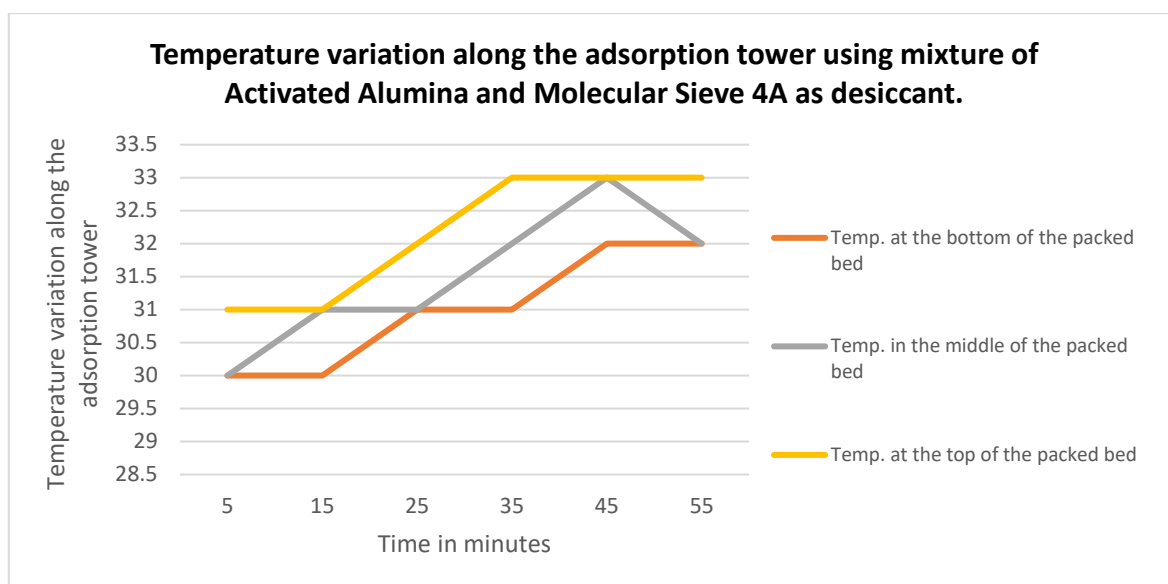


FIGURE 4. 26 Temperature variation along the adsorption tower using mixture of Activated Alumina and Molecular Sieve 4A as desiccant.

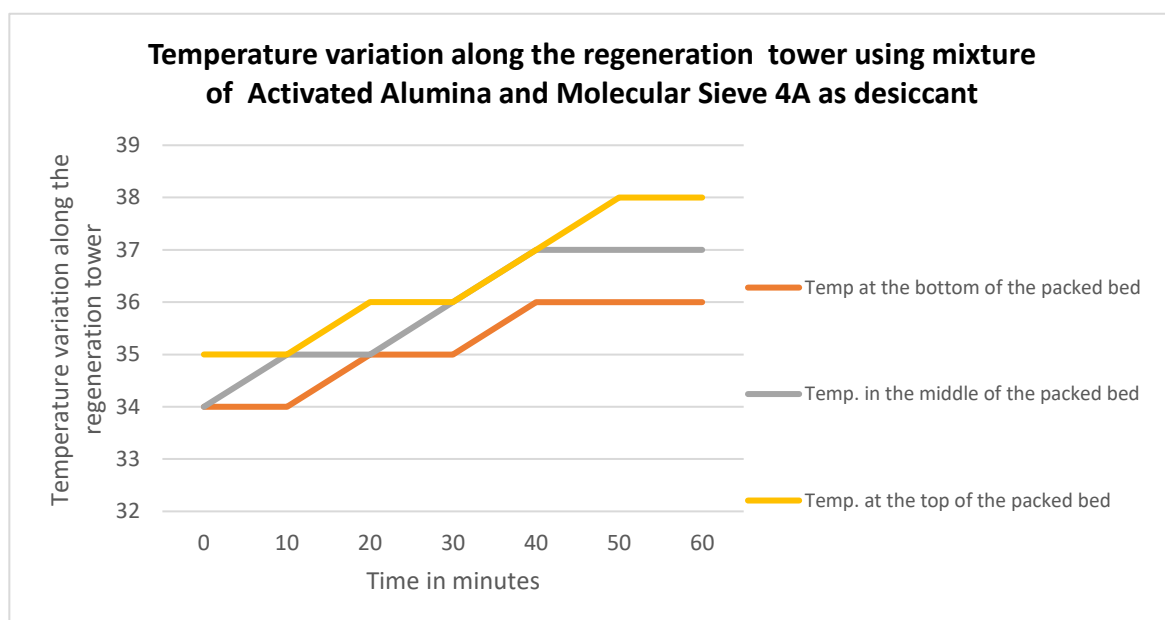


FIGURE 4. 27 Temperature variation along the regeneration tower using mixture of Activated Alumina and Molecular Sieve 4A as desiccant.

When utilised in the heatless air dryer, a mixture of activated alumina and Molecular Sieve 4A produced a  $\Delta T$  of 3°C along the length of the packed bed as seen in Figure 4.26 and Figure 4.27 during adsorption and regeneration processes.

*Case IX:* Mixture of Silica Gel and Molecular Sieve 13x is experimentally investigated as a working medium in the heatless air dryer with a flow rate of 10 CFM.



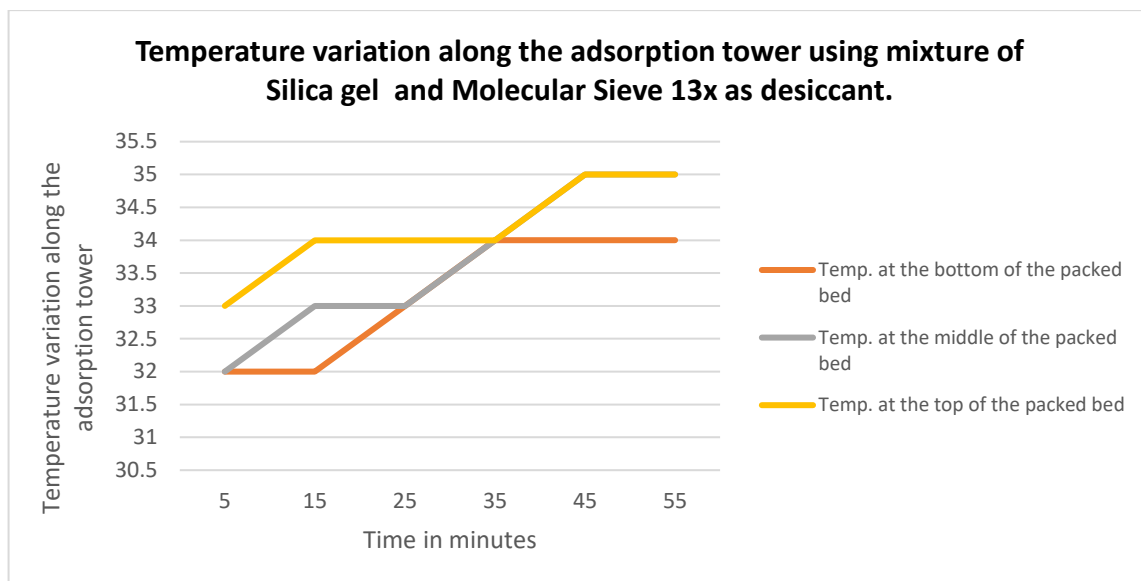


FIGURE 4. 28 Temperature variation along the adsorption tower using mixture of Silica gel and Molecular Sieve 13x as desiccant.

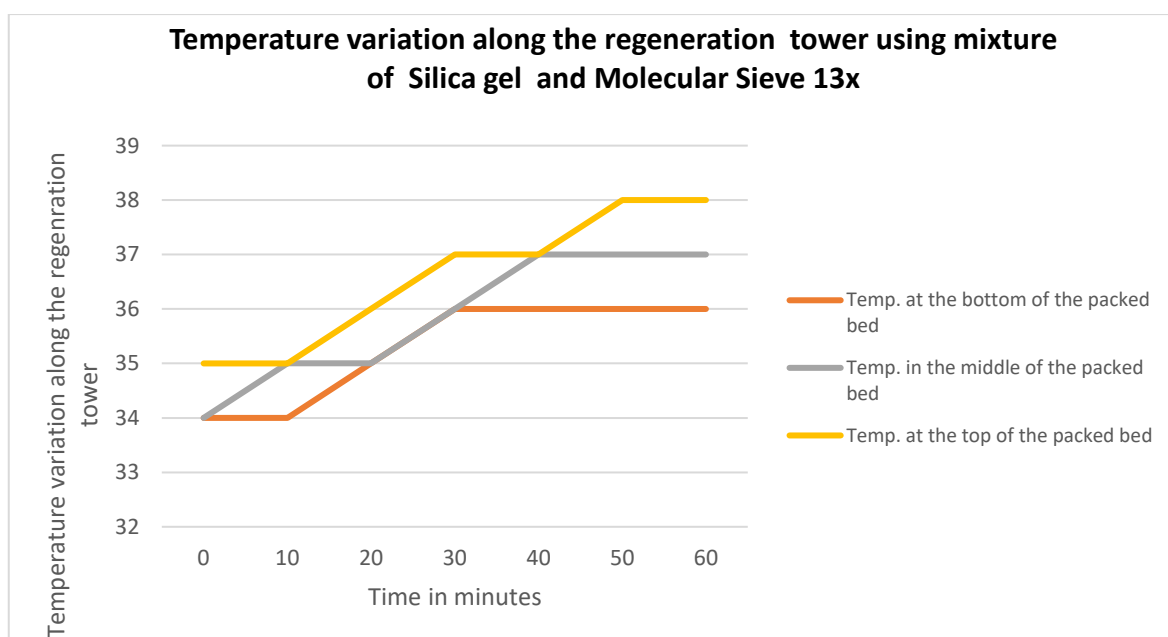


FIGURE 4. 29 Temperature variation along the regeneration tower using mixture of Silica gel and Molecular Sieve 13x

In the adsorption tower when the mixture of silica gel and Molecular Sieve 13x were tested, a 2°C rise in the temperature at the bottom of the bed was noted over a period of 1 hour as seen in Figure 4.28. While similarly a rise of 3 °C was recorded for the top of the packed bed during regeneration process as seen in Figure 4.29.

*Case X:* Mixture of Silica gel and Activated Alumina is experimentally investigated as a working medium in the heatless air dryer with a flow rate of 10 CFM.

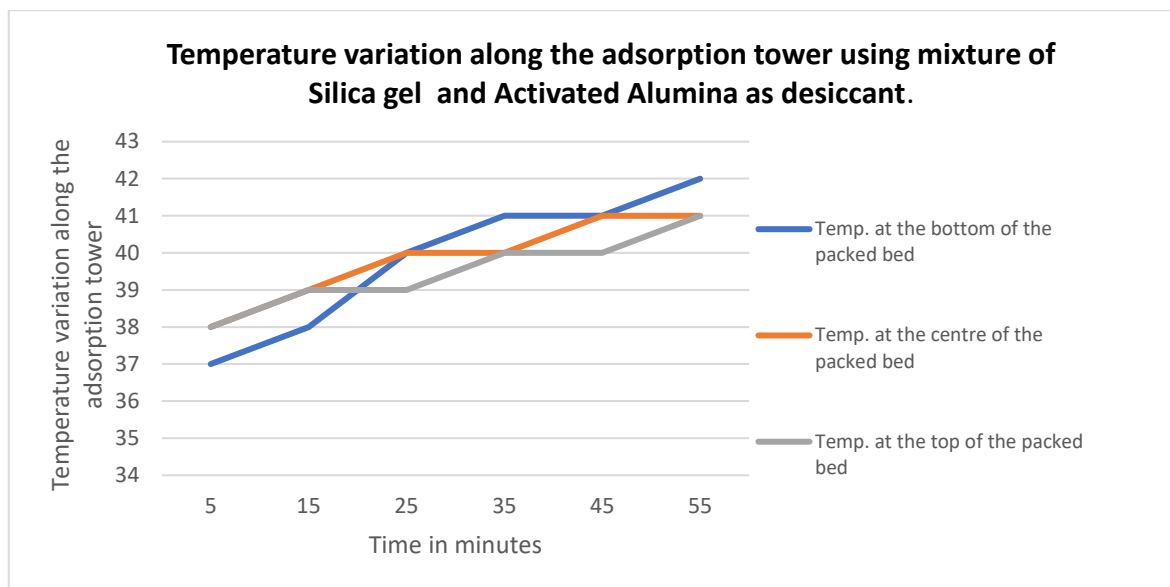


FIGURE 4. 30 Temperature variation along the adsorption tower using mixture of Silica gel and Activated Alumina as desiccant.

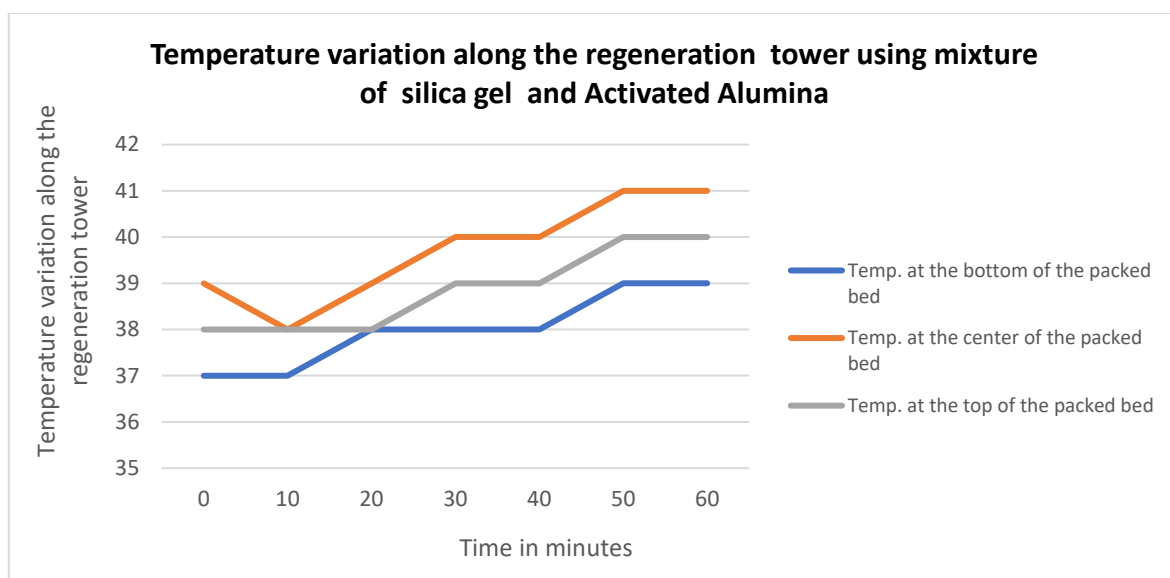


FIGURE 4. 31 Temperature variation along the regeneration tower using mixture of silica gel and Activated Alumina

Figure 4.30 and Figure 4.31 depict the temperature variation along the adsorption and regeneration tower respectively when silica gel and activated alumina is used a desiccant in the heatless air dryer. It can be observed that a temperature gradient of 5°C at the bottom of the packed bed during adsorption is recorded. While a rise of 2°C through out the packed bed is observed during the regeneration process.

#### 4.4 Validation of experimental work using Artificial Neural Network

The training and testing process of the ANN model was based on experimentally measured data procured from testing silica gel solid desiccant in the heatless air dryer. Effects of duration, relative humidity, dry bulb temperature and wet bulb temperature of the inlet air on the moisture removal rate, effectiveness, outlet dew point temperature and outlet relative humidity were predicted. The Figure 4.32 below depicts a graphical representation of the network architecture.

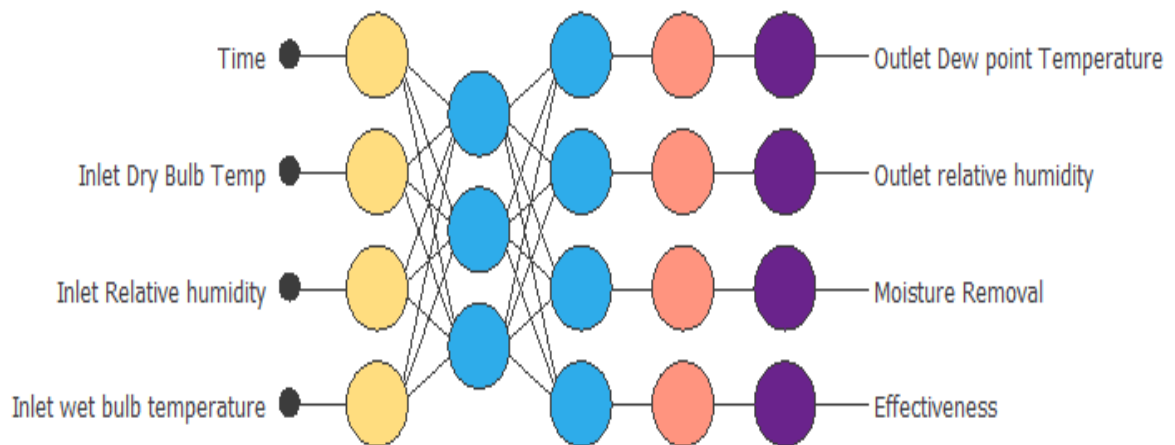


FIGURE 4. 32 Graphical representation of the neural network architecture

The performance of the ANN model is measured using the correlation coefficient ( $R$ ) and the mean square error (MSE). The ANN model performs well statistically, with a correlation coefficient of 0.96 and 0.90 for effectiveness and moisture removal rate respectively that is very close to unity and MSE values for ANN training and predictions that are very low when compared to the range of experiments evaluated for a heatless air dryer. The results obtained using the ANN are depicted below.

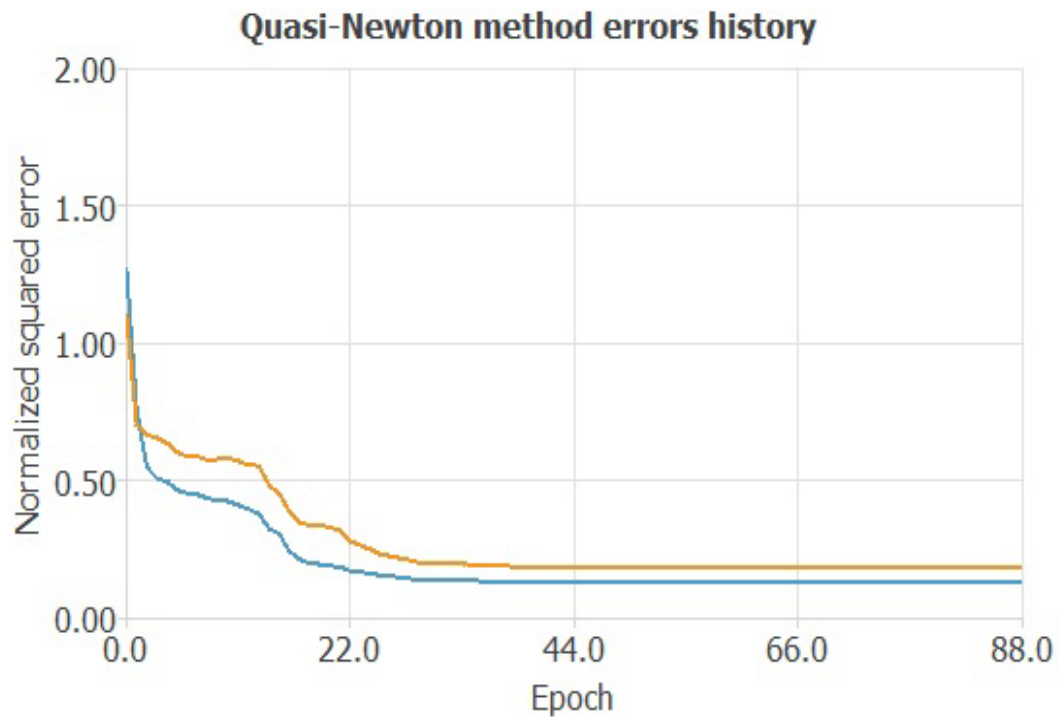


FIGURE 4. 33 Plot depicting training and selection error.

The created neural network displayed a high degree of resemblance with the findings of the experiment. The training and selection errors for each iteration are depicted in the following plot, which can be seen in Figure 4.33. Both the training error and the selection error are depicted by the two lines: the blue line represents the training error, while the orange line depicts the selection error. The training error begins with a value of 1.26967 and ends with a value of 0.129613 after 88 iterations of the training process. The selection mistake starts out with a value of 1.09951, and after 88 iterations, it reaches its final value of 0.183657.

The errors statistics take into account the least amount of error, the most amount of error, the average amount of error, and the standard deviation of the errors that occur between the neural network and the testing samples in the data set. They are an effective method for determining the overall quality of a model. The following table illustrates the absolute and percentage mistakes produced by the neural network for the testing data. Also included are the errors' minimum, maximum, and mean values, as well as their standard deviations.

	Minimum	Maximum	Mean	Deviation
<b>Absolute error</b>	0.000469208	23.9746	0.61919	2.60824
<b>Relative error</b>	6.62723e-6	0.338624	0.00874563	0.0368395
<b>Percentage error</b>	0.000662723	33.8624	0.874563	3.68395

Table 4. 2 Digressions of the absolute and percentage errors of the neural network for the testing data

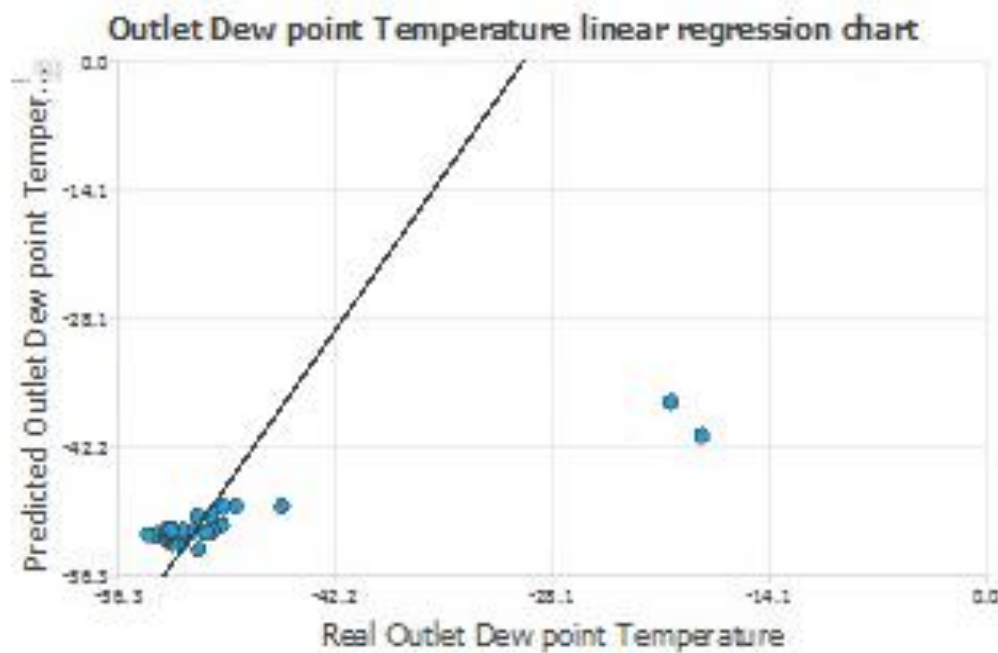


FIGURE 4. 3411 Comparisons between ANN predictions for outlet dew point temperature with experimental results

A linear regression analysis between the scaled neural network outputs and the associated targets for an independent testing subset is the traditional way for testing a model's loss. For each output variable, this approach yields three parameters. The y-intercept would be 0 for the first two parameters a and b, correlating to it. If the correlation coefficient is 1, then the outputs of the neural network and the targets in the testing subset are perfectly correlated.

The linear regression for the output process air dew point temperature is displayed in the following chart in graphical form. Each circle on the graph displays a predicted value in comparison to the actual value. The value of the correlation is 0.95, which is extremely close to one, indicating that the output predicted by the ANN and that produced through

experiments are in high agreement. This can be seen in Figure 4.45, which also demonstrates that the grey line represents the best linear fit.

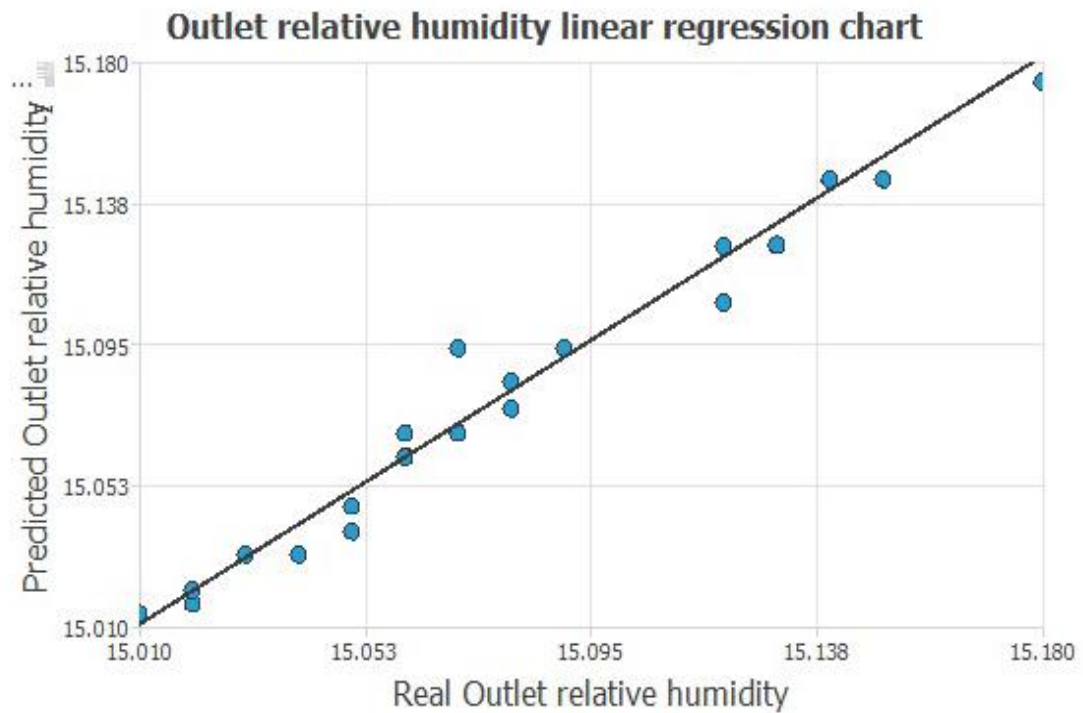


FIGURE 4. 35 Comparisons between the ANN predictions and experimental results for relative humidity at the outlet of the dryer.

Similarly, a correlation of 0.99 can be detected between the value that was predicted for the outlet relative humidity and the experimental readings, as shown in Figure 4.35. The correlation between the values that were predicted for the moisture removal rate and the values that were actually achieved through experimentation is 0.90, as can be shown in Figure 4.36. As shown in Figure 4.37, there was a correlation of 0.96 between the effectiveness that was projected and the effectiveness that was actually achieved. Because all of these correlation values are so close to having the value one, it is clear that the outcomes predicted by the neural network are in good agreement with the results of the experiments.

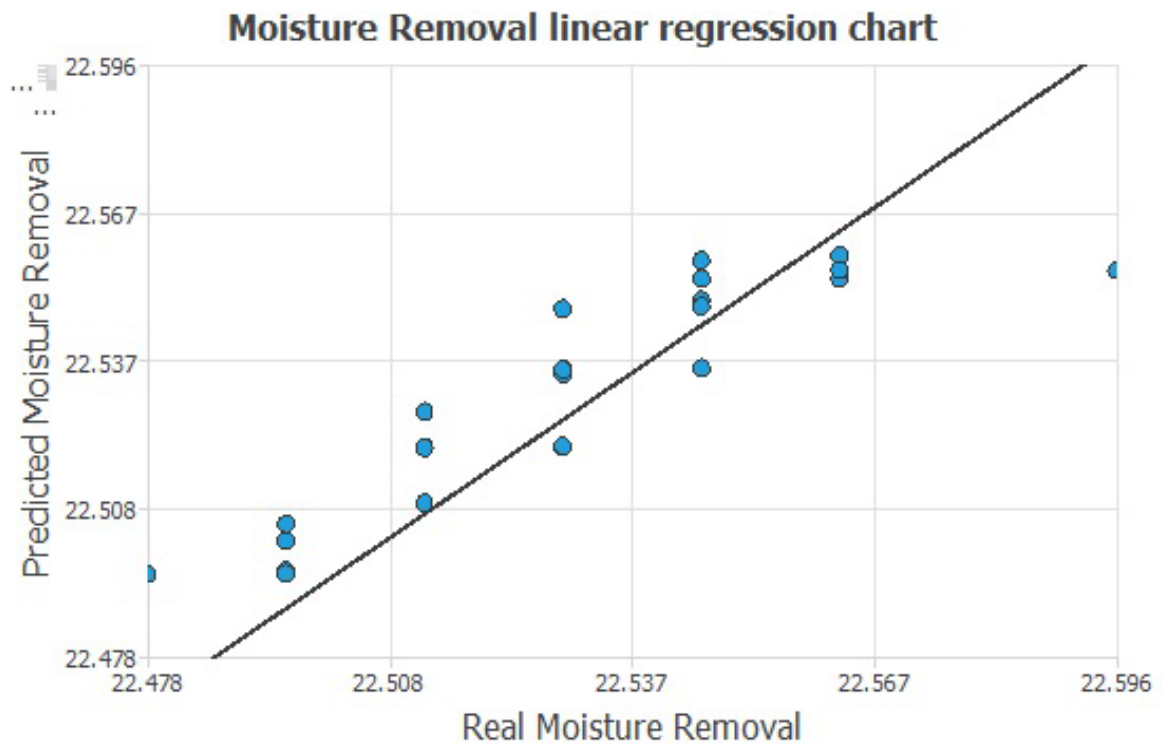


FIGURE 4. 126 Comparisons between the ANN predictions and experimental results for the rate of moisture removal of the dryer.

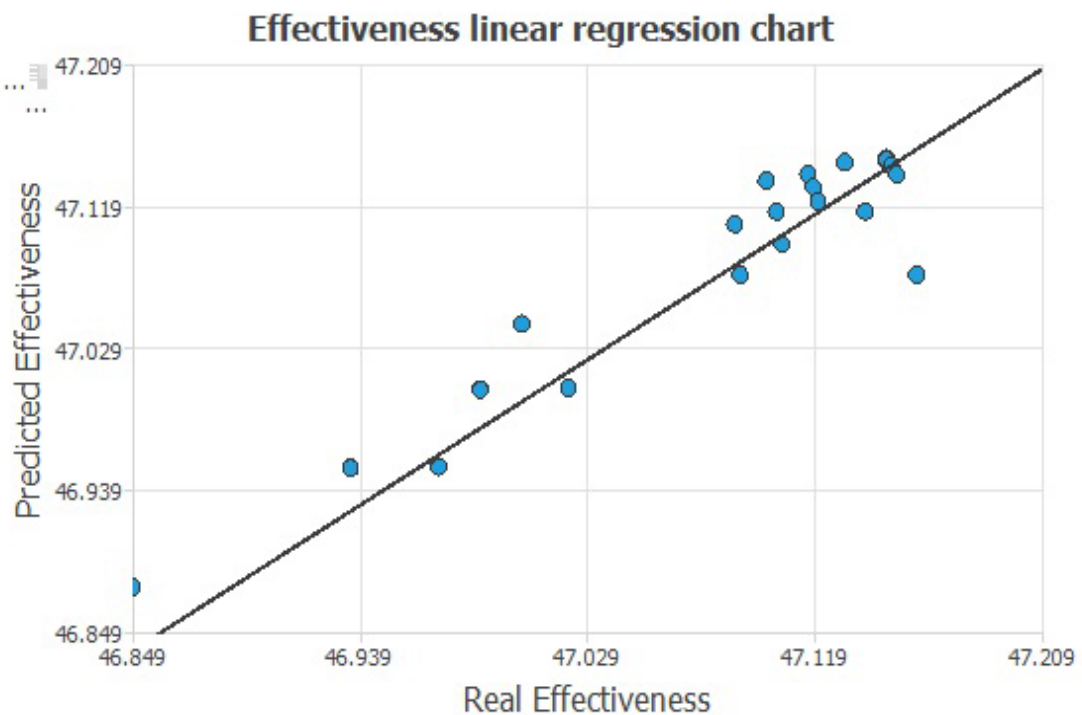


FIGURE 4. 137 Comparisons between the ANN predictions and experimental results for the effectiveness of the dryer.

The experimental results indicated outlet dew point temperature of  $-55^{\circ}\text{C}$  for 60 minutes trial

time and the ANN model predicted  $-56.3^{\circ}\text{C}$  for 900 minutes trial time. It is observed from Figure 4.34 to Figure 4.37 that the correlation for the ANN predicted results and the experimental test results are approaching unity which shows good agreement between the two.

## 4.5 Discussion

The dew point temperature can be used as a measurement to determine how dry the compressed air is. The experimental examination for case II with Molecular Sieve 13x demonstrated that the heatless air dryer was able to achieve a dew point of  $-70^{\circ}\text{C}$ , and the achievable moisture removal rate obtained was 54.63 gm/hr. This was seen in Figure 4.2. In addition, the scanning electron microscope images that was taken during the preliminary research for Molecular Sieve 13x reveals that the solid desiccant has a uniform distribution of pores. Because of this, it is recommended to make use of Molecular Sieve 13x in circumstances when it is necessary to have exceptionally dry air. The experimental examination from case study IX demonstrated that the heterogeneous mixture of silica gel and Molecular Sieve 13x offered the greatest result for moisture removal with an adsorption rate of 108.19 gm/hr. This is the case in spite of the fact that Molecular Sieve 13x has the most expensive price of all of the desiccants that were investigated, but silica gel was discovered to be the least expensive of all of the desiccants. In case study VIII, utilising a blend of activated alumina and Molecular Sieve 4A resulted in the lowest adsorption rate of 13.91 gm/hr. After testing each unique desiccant, it was determined that silica gel had the lowest adsorption rate, coming in at 22.51 gm/hr with a dew point of  $-55^{\circ}\text{C}$ . As a consequence of these findings, the importance of the desiccant component of a heatless air dryer has been brought to light by the experimental test. Even if one does not modify any of the other settings, but instead makes a change to the desiccant that is used in the heatless air dryer, they will be able to achieve the necessary amount of dryness.

In each of the cases, researchers looked at how the adsorption and regeneration processes affected the temperature distribution across the packed bed. It was investigated to determine whether or not the adsorption tower required additional cooling from the outside in order to maximize its adsorption capability. It has also been discovered that the temperature at the top of the packed bed is higher compared to the temperature at the lower half of the bed in each and every instance. This indicates that the desiccant at the top of the packed bed is more



actively involved in the process of adsorption than the desiccant that is lower down in the bed. This might be because the process air enters from the bottom of the bed and subsequently exits into the process line from the top of the bed. Hence impact of direction of flow change into better utilisation of the desiccant in a packed bed needs to be further investigated. Therefore, one may conclude, based on Figure 4.12 to Figure 4.31, that the temperature variation did not exceed 6°C. Hence external cooling was concluded to be not necessary as the tower does not over heat.

The verification is carried out with the assistance of an artificial neural network. Because of the employment of the neural designer software, time, effort, and countless manhours were saved throughout the prediction process, which, without the software, would have been incredibly time consuming. The neural network was trained with the help of experimental data from Case IV, which involved the use of silica gel as a desiccant in a heatless air dryer. The results of the experiment indicated that the outflow dew point temperature was -55 degrees Celsius for a trial time of 60 minutes, while the ANN model projected -56.3 degrees Celsius for a trial length of 900 minutes. It is observed from Figure 4.34 to Figure 4.37 that the correlation for the ANN predicted results and the experimental test results are approaching unity which shows good agreement between the two.

# CHAPTER - 5

## Conclusion

- The experimental investigations of Molecular Sieve 13x, Molecular Sieve 4A, Silica gel, and Activated Alumina, as well as their heterogeneous mixes, were carried out effectively.
- According to the findings of the experiment, the most effective desiccant was Molecular Sieve 13x when it was employed by itself in the heatless drier. It was able to remove moisture at a rate of 54.63 gm/hr and had an efficiency of 80%.
- However, the heterogeneous mixture of silica gel and Molecular Sieve 13x produced the relatively best results, with a Moisture Removal Rate (MRR) of 108.19 gm/hr and an efficiency of 80%.
- Due to the fact that silica gel is available at a lower cost than MS13x, the price of the desiccant might be decreased as a result of the combination. On the other hand, it ought to be utilised in situations in which low-pressure compressed air needs to be dried.
- The heat of adsorption and regeneration was also examined for both towers. Due to the poor crushing strength of silica gel in comparison to MS13x. It was discovered that because there was not a substantial difference in temperature over the length of the packed bed, it was not necessary to employ any form of external cooling on the packed bed.
- In the preliminary investigation, the Molecular Sieve 3A was chosen as the object of the inquiry. Following the completion of the experiments, it was discovered, as shown in Figure and Figure, that the outcomes produced by Molecular Sieve 3A and Molecular Sieve 4A were quite similar. As a result, Molecular Sieve 4A was selected as the single candidate for additional research, as no major change in result was recorded for Molecular Sieve 3A.
- The ANN was used to verify the results of the experimental work. Software called a

neural designer was used for the same purpose. The results of the experiments conducted using silica gel were utilised in the training of the neural network, and the outcomes that were predicted showed a high level of agreement with the results that were actually tested.

- ANN was also used to predict the desiccant performance over a period of time. Hence it can be effectively used as a prediction tool for solid desiccant saving tedious calculations and man hours.
- Based on the study of the relevant literature that was done, it is possible to state with absolute certainty that no other researcher has ever conducted an investigation like this. This research will serve as a roadmap for the industry, allowing them to select the suitable desiccant according to the level of dryness required rather than adjusting the size of the heatless air dryer.

## **5.1 Suggestions for future work**

- A composite desiccant engineered for use in heatless air dryer, specifically, can be developed.
- Molecular Sieve 13x and silica gel can be further investigated for use in heatless air dryer to increase the performance of the heatless air dryer.
- Investigation should be carried on the cycle switch over time and its impact on the cycle along with the heat of adsorption released and its effect on the adsorption rate.
- Investigation should be carried out in heatless air dryer to minimize the use of purge air for regeneration, as compressed air is used for purging and after that it is released in the atmosphere to be lost.
- ANN (Artificial Neural Network) should be trained and used to predict the life of desiccant in the heatless air dryer, this will save potential cost of time and extensive amount of manhours to monitor the life expectancy of a solid desiccant.
- Investigation on the temperature variation in the adsorption tower and regeneration tower due to the exothermic reaction that takes place during adsorption revealed that the

desiccant in the upper part of the tower has higher temperature when compared to the desiccant in lower tower. This was an indication that better utilization of desiccant was taking place in the upper part when the flow of process air was unidirectional. Hence investigation needs to be carried out in packed bed to study the impact of bidirectional flow on the desiccants in a packed bed.

## List of References

- [1] A. Ertas, E. E. Anderson, and I. Kiris, “Properties of a New Liquid Desiccant Solution- Lithium Chloride and Calcium Chloride Mixture,” *Solar Energy*, vol. 49, no. 3, pp. 205–212, 1992, doi: 10.1016/0038-092X(92)90073-J.
- [2] K. S. Rambhad, P. V. Walke, and D. J. Tidke, “Solid desiccant dehumidification and regeneration methods - A review,” *Renewable and Sustainable Energy Reviews*, vol. 59, pp. 73–83, 2016, doi: 10.1016/j.rser.2015.12.264.
- [3] M. Sultan, I. I. El-Sharkawy, T. Miyazaki, B. B. Saha, and S. Koyama, “An overview of solid desiccant dehumidification and air conditioning systems,” *Renewable and Sustainable Energy Reviews*, vol. 46, pp. 16–29, 2015, doi: 10.1016/j.rser.2015.02.038.
- [4] A. Lowenstein, “Review of Liquid Dessciant Technology for HVAC applications,” *HVAC&R Res*, vol. 14, no. 6, p. 22, 2008, doi: 10.1080/10789669.2008.10391042.
- [5] H. Fu and X. Liu, “Review of the impact of liquid desiccant dehumidification on indoor air,” *Build Environ*, vol. 116, no. 1, pp. 158–172, 2017, doi: 10.1016/j.buildenv.2017.02.014.
- [6] M. M. Rafique, P. Gandhidasan, and H. M. S. Bahaidarah, “Liquid desiccant materials and dehumidifiers - A review,” *Renewable and Sustainable Energy Reviews*, vol. 56, pp. 179–195, 2016, doi: 10.1016/j.rser.2015.11.061.
- [7] P. Gandhidasan, “Quick performance prediction of liquid desiccant regeneration in a packed bed,” *Solar Energy*, vol. 79, no. 1, pp. 47–55, 2005, doi: 10.1016/j.solener.2004.10.002.
- [8] S. Misha, S. Mat, M. H. Ruslan, and K. Sopian, “Review of solid/liquid desiccant in the drying applications and its regeneration methods,” *Renewable and Sustainable Energy Reviews*, vol. 16, no. 7, pp. 4686–4707, 2012, doi: 10.1016/j.rser.2012.04.041.
- [9] A. Giampieri, Z. Ma, A. Smallbone, and A. P. Roskilly, “Thermodynamics and economics of liquid desiccants for heating, ventilation and air-conditioning – An overview,” *Appl Energy*, vol. 220, no. December 2017, pp. 455–479, 2018, doi: 10.1016/j.apenergy.2018.03.112.
- [10] D. B. Jani, M. Mishra, and P. K. Sahoo, “Solid desiccant air conditioning - A state of the art review,” *Renewable and Sustainable Energy Reviews*, vol. 60, pp. 1451–1469, 2016, doi: 10.1016/j.rser.2016.03.031.

- [11] R. P. Singh, V. K. Mishra, and R. K. Das, “Desiccant materials for air conditioning applications - A review,” *IOP Conf Ser Mater Sci Eng*, vol. 404, no. 1, 2018, doi: 10.1088/1757-899X/404/1/012005.
- [12] T. K. Ghosh and A. L. Hines, *Solid desiccant dehumidification systems*, vol. 120 A. Elsevier Masson SAS, 1999. doi: 10.1016/s0167-2991(99)80575-8.
- [13] A. Zouaoui, L. Zili-Ghedira, and S. Ben Nasrallah, “Open solid desiccant cooling air systems: A review and comparative study,” *Renewable and Sustainable Energy Reviews*, vol. 54, pp. 889–917, 2016, doi: 10.1016/j.rser.2015.10.055.
- [14] G. Panaras, E. Mathioulakis, and V. Belessiotis, “Achievable working range for solid all-desiccant air-conditioning systems under specific space comfort requirements,” *Energy Build*, vol. 39, no. 9, pp. 1055–1060, 2007, doi: 10.1016/j.enbuild.2006.10.015.
- [15] G. Panaras, E. Mathioulakis, and V. Belessiotis, “Solid desiccant air-conditioning systems - Design parameters,” *Energy*, vol. 36, no. 5, pp. 2399–2406, 2011, doi: 10.1016/j.energy.2011.01.022.
- [16] U. Eicker *et al.*, “Experimental investigations on desiccant wheels,” *Appl Therm Eng*, vol. 42, pp. 71–80, 2012, doi: 10.1016/j.applthermaleng.2012.03.005.
- [17] G. Angrisani, C. Roselli, and M. Sasso, “Effect of rotational speed on the performances of a desiccant wheel,” *Appl Energy*, vol. 104, pp. 268–275, 2013, doi: 10.1016/j.apenergy.2012.10.051.
- [18] Z. Guidara, M. Elleuch, and H. ben Bacha, “New solid desiccant solar air conditioning unit in Tunisia: Design and simulation study,” *Appl Therm Eng*, vol. 58, no. 1–2, pp. 656–663, 2013, doi: 10.1016/j.applthermaleng.2013.05.005.
- [19] R. Narayanan, W. Y. Saman, and S. D. White, “A non-adiabatic desiccant wheel: Modeling and experimental validation,” *Appl Therm Eng*, vol. 61, no. 2, pp. 178–185, 2013, doi: 10.1016/j.applthermaleng.2013.07.007.
- [20] Y. Guan, Y. Zhang, Y. Sheng, X. Kong, and S. Du, “Feasibility and economic analysis of solid desiccant wheel used for dehumidification and preheating in blast furnace: A case study of steel plant, Nanjing, China,” *Appl Therm Eng*, vol. 81, pp. 426–435, 2015, doi: 10.1016/j.applthermaleng.2015.02.006.
- [21] M. Intini, M. Goldsworthy, S. White, and C. M. Joppolo, “Experimental analysis and numerical modelling of an AQSOA zeolite desiccant wheel,” *Appl Therm Eng*, vol. 80, pp. 20–30, 2015, doi: 10.1016/j.applthermaleng.2015.01.036.

- [22] S. Misha, S. Mat, M. H. Ruslan, E. Salleh, and K. Sopian, "Performance of a solar assisted solid desiccant dryer for kenaf core fiber drying under low solar radiation," *Solar Energy*, vol. 112, pp. 194–204, 2015, doi: 10.1016/j.solener.2014.11.029.
- [23] R. Tu, X. H. Liu, and Y. Jiang, "Irreversible processes and performance improvement of desiccant wheel dehumidification and cooling systems using exergy," *Appl Energy*, vol. 145, pp. 331–344, 2015, doi: 10.1016/j.apenergy.2015.02.043.
- [24] D. B. Jani, M. Mishra, and P. K. Sahoo, "Experimental investigation on solid desiccant-vapor compression hybrid air-conditioning system in hot and humid weather," *Appl Therm Eng*, vol. 104, pp. 556–564, 2016, doi: 10.1016/j.applthermaleng.2016.05.104.
- [25] D. B. Jani, M. Mishra, and P. K. Sahoo, "Performance prediction of solid desiccant - Vapor compression hybrid air-conditioning system using artificial neural network," *Energy*, vol. 103, pp. 618–629, 2016, doi: 10.1016/j.energy.2016.03.014.
- [26] S. Misha, S. Mat, M. H. Ruslan, E. Salleh, and K. Sopian, "Performance of a solar-assisted solid desiccant dryer for oil palm fronds drying," *Solar Energy*, vol. 132, pp. 415–429, 2016, doi: 10.1016/j.solener.2016.03.041.
- [27] A. Zendehboudi, "Implementation of GA-LSSVM modelling approach for estimating the performance of solid desiccant wheels," *Energy Convers Manag*, vol. 127, pp. 245–255, 2016, doi: 10.1016/j.enconman.2016.08.070.
- [28] K. F. Fong and C. K. Lee, "New perspectives in solid desiccant cooling for hot and humid regions," *Energy Build*, vol. 158, pp. 1152–1160, 2018, doi: 10.1016/j.enbuild.2017.11.016.
- [29] K. F. Fong and C. K. Lee, "Impact of adsorbent characteristics on performance of solid desiccant wheel," *Energy*, vol. 144, pp. 1003–1012, 2018, doi: 10.1016/j.energy.2017.12.113.
- [30] G. Goodarzia, N. Thirukonda, S. Heidari, A. Akbarzadeh, and A. Date, "Performance Evaluation of Solid Desiccant Wheel Regenerated by Waste Heat or Renewable Energy," *Energy Procedia*, vol. 110, no. December 2016, pp. 434–439, 2017, doi: 10.1016/j.egypro.2017.03.165.
- [31] D. B. Jani, M. Mishra, and P. K. Sahoo, "Application of artificial neural network for predicting performance of solid desiccant cooling systems – A review," *Renewable and Sustainable Energy Reviews*, vol. 80, no. May, pp. 352–366, 2017, doi: 10.1016/j.rser.2017.05.169.

- [32] R. Narayanan, "Investigation of Geometry Effects of Channels of a Silica-gel Desiccant Wheel," *Energy Procedia*, vol. 110, no. December 2016, pp. 20–25, 2017, doi: 10.1016/j.egypro.2017.03.099.
- [33] D. B. Jani, M. Mishra, and P. K. Sahoo, "A critical review on application of solar energy as renewable regeneration heat source in solid desiccant – vapor compression hybrid cooling system," *Journal of Building Engineering*, vol. 18, pp. 107–124, 2018, doi: 10.1016/j.job.2018.03.012.
- [34] D. B. Jani, M. Mishra, and P. K. Sahoo, "Performance analysis of a solid desiccant assisted hybrid space cooling system using TRNSYS," *Journal of Building Engineering*, vol. 19, pp. 26–35, 2018, doi: 10.1016/j.job.2018.04.016.
- [35] R. Tu, Y. Hwang, T. Cao, M. Hou, and H. Xiao, "Investigation of adsorption isotherms and rotational speeds for low temperature regeneration of desiccant wheel systems," *International Journal of Refrigeration*, vol. 86, pp. 495–509, 2018, doi: 10.1016/j.ijrefrig.2017.11.008.
- [36] A. Zendehboudi, G. Angrisani, and X. Li, "Parametric studies of silica gel and molecular sieve desiccant wheels: Experimental and modeling approaches," *International Communications in Heat and Mass Transfer*, vol. 91, pp. 176–186, 2018, doi: 10.1016/j.icheatmasstransfer.2017.12.002.
- [37] X. Zhou, M. Goldsworthy, and A. Sproul, "Performance investigation of an internally cooled desiccant wheel," *Appl Energy*, vol. 224, no. January, pp. 382–397, 2018, doi: 10.1016/j.apenergy.2018.05.011.
- [38] H. H. Wang, T. S. Ge, X. L. Zhang, and Y. Zhao, "Experimental investigation on solar powered self-cooled cooling system based on solid desiccant coated heat exchanger," *Energy*, vol. 96, pp. 176–186, 2016, doi: 10.1016/j.energy.2015.12.067.
- [39] M. Rajamani, V. R. Mishra, and S. M. Maliyekkal, "Bundled-firewood like  $\text{AlOOH}$ - $\text{CaCl}_2$  nanocomposite desiccant," *Chemical Engineering Journal*, vol. 323, no. April, pp. 171–179, 2017, doi: 10.1016/j.cej.2017.04.084.
- [40] X. Zheng, T. S. Ge, Y. Jiang, and R. Z. Wang, "Experimental study on silica gel- $\text{LiCl}$  composite desiccants for desiccant coated heat exchanger," *International Journal of Refrigeration*, vol. 51, pp. 24–32, 2015, doi: 10.1016/j.ijrefrig.2014.11.015.
- [41] Y. Jiang, T. Ge, and R. Wang, "Performance simulation of a joint solid desiccant heat pump and variable refrigerant flow air conditioning system in EnergyPlus," *Energy Build*, vol. 65, pp. 220–230, 2013, doi: 10.1016/j.enbuild.2013.06.005.



- [42] J. Nie *et al.*, “Theoretical study on volatile organic compound removal and energy performance of a novel heat pump assisted solid desiccant cooling system,” *Build Environ*, vol. 85, pp. 233–242, 2015, doi: 10.1016/j.buildenv.2014.11.034.
- [43] R. Tu, X. H. Liu, and Y. Jiang, “Performance analysis of a new kind of heat pump-driven outdoor air processor using solid desiccant,” *Renew Energy*, vol. 57, pp. 101–110, 2013, doi: 10.1016/j.renene.2013.01.038.
- [44] R. Tu, Y. Hwang, and F. Ma, “Performance analysis of a new heat pump driven multi-stage fresh air handler using solid desiccant plates,” *Appl Therm Eng*, vol. 117, pp. 553–567, 2017, doi: 10.1016/j.applthermaleng.2017.02.005.
- [45] N. Lior and H. S. Al-Sharqawi, “Exergy analysis of flow dehumidification by solid desiccants,” *Energy*, vol. 30, no. 6, pp. 915–931, 2005, doi: 10.1016/j.energy.2004.04.029.
- [46] R. Tu, X. H. Liu, Y. Hwang, and F. Ma, “Performance analysis of ventilation systems with desiccant wheel cooling based on exergy destruction,” *Energy Convers Manag*, vol. 123, pp. 265–279, 2016, doi: 10.1016/j.enconman.2016.06.013.
- [47] B. Li, Q. Y. Lin, and Y. Y. Yan, “Development of solid desiccant dehumidification using electro-osmosis regeneration method for HVAC application,” *Build Environ*, vol. 48, no. 1, pp. 128–134, 2012, doi: 10.1016/j.buildenv.2011.09.008.
- [48] R. Qi, C. Tian, and S. Shao, “Experimental investigation on possibility of electro-osmotic regeneration for solid desiccant,” *Appl Energy*, vol. 87, no. 7, pp. 2266–2272, 2010, doi: 10.1016/j.apenergy.2010.02.005.
- [49] R. Qi, C. Tian, S. Shao, M. Tang, and L. Lu, “Experimental investigation on performance improvement of electro-osmotic regeneration for solid desiccant,” *Appl Energy*, vol. 88, no. 8, pp. 2816–2823, 2011, doi: 10.1016/j.apenergy.2011.01.055.
- [50] S. K. Yeboah and J. Darkwa, “A critical review of thermal enhancement of packed beds for water vapour adsorption,” *Renewable and Sustainable Energy Reviews*, vol. 58. Elsevier Ltd, pp. 1500–1520, May 01, 2016. doi: 10.1016/j.rser.2015.12.134.
- [51] A. Ramzy, H. Abdelmeguid, and W. M. Elawady, “A novel approach for enhancing the utilization of solid desiccants in packed bed via intercooling,” *Appl Therm Eng*, vol. 78, pp. 82–89, 2015, doi: 10.1016/j.applthermaleng.2014.12.035.
- [52] A. K. Ramzy, R. Kadoli, and T. P. Ashok Babu, “Experimental and theoretical investigations on the cyclic operation of TSA cycle for air dehumidification using packed beds of silica gel particles,” *Energy*, vol. 56, pp. 8–24, Jul. 2013, doi: 10.1016/j.energy.2013.03.048.

- [53] A. Ramzy K., R. Kadoli, and T. P. Ashok Babu, "Improved utilization of desiccant material in packed bed dehumidifier using composite particles," *Renew Energy*, vol. 36, no. 2, pp. 732–742, 2011, doi: 10.1016/j.renene.2010.06.038.
- [54] B. Shelpuk, "The technical challenges for solid desiccant cooling," *Heat Recovery Systems and CHP*, vol. 13, no. 4, pp. 321–328, 1993, doi: 10.1016/0890-4332(93)90056-2.
- [55] J.-Y. San, C.-C. Ni, and S.-H. Hsu, "Validity of solid-side mass diffusivity in simulation of water vapor adsorbed by silica gel in packed beds," 2002.
- [56] A. A. Pesarant and A. F. Mills, "Moisture transport in silica gel packed beds-4 Experimental study," 1987.
- [57] B. Baghapour, M. Rouhani, A. Sharafian, S. B. Kalhori, and M. Bahrami, "A pressure drop study for packed bed adsorption thermal energy storage," *Appl Therm Eng*, vol. 138, pp. 731–739, Jun. 2018, doi: 10.1016/j.applthermaleng.2018.03.098.
- [58] P. Gandhidasan, A. A. Al-Farayedhi, and A. A. Al-Mubarak, "Dehydration of natural gas using solid desiccants," *Energy*, vol. 26, no. 9, pp. 855–868, 2001, doi: 10.1016/S0360-5442(01)00034-2.

# Annexure-A: Calibration Certificates

## A.1. Calibration certificate of dew point meter



1 (1)  
Certificate report no. H49-20500438

## CALIBRATION CERTIFICATE

**Instrument** Dewpoint transmitter DMT143  
**Serial number** S4940566  
**Order code** DMT143 G1G1B1A0A0ASX  
**Manufacturer** Vaisala Oyj, Finland  
**Calibration date** 4th December 2020  
**Test procedure** doc210447-a

The above instrument was calibrated by comparing the dewpoint output to a reference dewpoint meter.

The measurement results are traceable to the international system of units (SI) through national metrology institutes (NIST USA, MIKES Finland, or equivalent) or via ISO/IEC 17025 accredited calibration laboratories.

### Calibration results

Reference dewpoint <sup>1)</sup> °C	Observed dewpoint <sup>1)</sup> °C	Difference °C	Permissible difference °C	Measurement uncertainty <sup>2)</sup> °C
-56.5	-56.5	0.0	± 1.8	± 0.6
-39.8	-39.6	0.2	± 1.8	± 0.5
-10.0	-9.9	0.1	± 1.8	± 0.5
3.6	3.7	0.1	± 1.8	± 0.5

1) Frostpoint in the range below 0 °C

2) 95 % confidence level, k=2 (repeatability of the calibrated instrument included)

### Analog output calibration results

Output forced to mA	Observed output mA	Difference mA	Permissible difference mA
12.000	11.999	-0.001	±0.20

### Equipment used in calibration

Type	Serial number	Calibration date	Certificate number
373 LX	08-0325	2020-02-05	M-20H002
AT 34970A	EM 13589	2020-01-10	1250-307108274
E3236A	16202	2019-01-21	1250-307099953

**Ambient conditions** / Humidity 35 ± 5%RH, Temperature 21 ± 2 °C, Pressure 1012 ± 20 hPa.




\_\_\_\_\_  
Technician


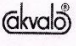


*This report shall not be reproduced except in full, without the written approval of Vaisala.*

DOC225880-C


Vaisala Oyj | PO Box 26, FI-00421 Helsinki, Finland  
Phone +358 9 894 91 | Fax +358 9 8949 2227  
Email [firstname.lastname@vaisala.com](mailto:firstname.lastname@vaisala.com) | [www.vaisala.com](http://www.vaisala.com)  
Domicile Vantaa, Finland | VAT FI01244162 | Business ID 0124416-2

## A.2.Calibration Certificate for Pressure Gauge

	<small>AN ISO 9001:2008 COMPANY</small> <b>AKVALO INSTRUMENTS PVT. LTD</b> <small>MEASURING TECHNOLOGIES</small>																																	
<b>TEST AND CALIBRATION CERTIFICATE</b> <small>QA/F/05 REV.00</small>																																		
Certificate No: <b>42176</b> Date: <b>07/02/2020</b> O.C. Number: <b>9LA42068</b> Date: <b>19/12/2019</b>																																		
<table border="1" style="width: 100%; border-collapse: collapse;"> <tr> <th colspan="3" style="text-align: center;">CALIBRATION CHART</th> </tr> <tr> <th style="width: 20%;">Test Gauge</th> <th style="width: 20%;">Sr. No</th> <th style="width: 60%;">9L 08215</th> </tr> <tr> <th>Reading Kg /cm<sup>2</sup></th> <th>UP</th> <th>Down</th> </tr> <tr> <td>0</td> <td>0.00</td> <td>0.00</td> </tr> <tr> <td>4</td> <td>4.02</td> <td>4.02</td> </tr> <tr> <td>8</td> <td>8.03</td> <td>8.04</td> </tr> <tr> <td>12</td> <td>12.01</td> <td>12.10</td> </tr> <tr> <td>14</td> <td>14.00</td> <td>14.00</td> </tr> <tr><td> </td><td> </td><td> </td></tr> <tr><td> </td><td> </td><td> </td></tr> <tr><td> </td><td> </td><td> </td></tr> </table>	CALIBRATION CHART			Test Gauge	Sr. No	9L 08215	Reading Kg /cm <sup>2</sup>	UP	Down	0	0.00	0.00	4	4.02	4.02	8	8.03	8.04	12	12.01	12.10	14	14.00	14.00										Test equipment Used  Brand Master Gauge Make : Akvalo Instruments Pvt Ltd. Gandhinagar Sr. No: <b>1037783</b> Range: <b>25 Kg /cm<sup>2</sup></b> Accuracy : $\pm 0.25$ % FSD Traceability : NABL This is Certify that Above Tested Instrument is within Specified Accuracy $\pm 2$ % FSD As per Standards and Permissible Error at any point shall be : <b>0.28 Kg /cm<sup>2</sup></b>
CALIBRATION CHART																																		
Test Gauge	Sr. No	9L 08215																																
Reading Kg /cm <sup>2</sup>	UP	Down																																
0	0.00	0.00																																
4	4.02	4.02																																
8	8.03	8.04																																
12	12.01	12.10																																
14	14.00	14.00																																
<div style="display: flex; justify-content: space-around; align-items: center;">  <div style="text-align: right;">               Q C Department           </div> </div>																																		

	<small>AN ISO 9001:2008 COMPANY</small> <b>AKVALO INSTRUMENTS PVT. LTD</b> <small>MEASURING TECHNOLOGIES</small>																																	
<b>TEST AND CALIBRATION CERTIFICATE</b> <small>QA/F/05 REV.00</small>																																		
Certificate No: <b>42177</b> Date: <b>07/02/2020</b> O.C. Number: <b>9LA42068</b> Date: <b>19/12/2019</b>																																		
<table border="1" style="width: 100%; border-collapse: collapse;"> <tr> <th colspan="3" style="text-align: center;">CALIBRATION CHART</th> </tr> <tr> <th style="width: 20%;">Test Gauge</th> <th style="width: 20%;">Sr. No</th> <th style="width: 60%;">9L 08216</th> </tr> <tr> <th>Reading Kg /cm<sup>2</sup></th> <th>UP</th> <th>Down</th> </tr> <tr> <td>0</td> <td>0.00</td> <td>0.00</td> </tr> <tr> <td>4</td> <td>4.01</td> <td>4.03</td> </tr> <tr> <td>8</td> <td>8.03</td> <td>8.05</td> </tr> <tr> <td>12</td> <td>12.11</td> <td>12.01</td> </tr> <tr> <td>14</td> <td>14.02</td> <td>14.02</td> </tr> <tr><td> </td><td> </td><td> </td></tr> <tr><td> </td><td> </td><td> </td></tr> <tr><td> </td><td> </td><td> </td></tr> </table>	CALIBRATION CHART			Test Gauge	Sr. No	9L 08216	Reading Kg /cm <sup>2</sup>	UP	Down	0	0.00	0.00	4	4.01	4.03	8	8.03	8.05	12	12.11	12.01	14	14.02	14.02										Test equipment Used  Brand Master Gauge Make : Akvalo Instruments Pvt Ltd. Gandhinagar Sr. No: <b>1037783</b> Range: <b>25 Kg /cm<sup>2</sup></b> Accuracy : $\pm 0.25$ % FSD Traceability : NABL This is Certify that Above Tested Instrument is within Specified Accuracy $\pm 2$ % FSD As per Standards and Permissible Error at any point shall be : <b>0.28 Kg /cm<sup>2</sup></b>
CALIBRATION CHART																																		
Test Gauge	Sr. No	9L 08216																																
Reading Kg /cm <sup>2</sup>	UP	Down																																
0	0.00	0.00																																
4	4.01	4.03																																
8	8.03	8.05																																
12	12.11	12.01																																
14	14.02	14.02																																
<div style="display: flex; justify-content: space-around; align-items: center;">  <div style="text-align: right;">               Q C Department           </div> </div>																																		

### A.3 Calibration Certificate for Hygrometer.

<div style="text-align: center;"> <small>SINCE 1982</small></div> <div><b>CERTIFICATE OF CALIBRATION</b> We hereby certify that this product has been calibrated and found to be in accordance with the applicable SPECIFICATIONS and MECO STANDARDS. Accuracies of the standard equipment used in this calibration are traceable to the National Standards.</div> <div style="text-align: center;"><b>MECO METERS PVT. LTD.</b> Plot No. EL-60, MIDC Electronic Zone, TTC Industrial Area, Mahape, Navi Mumbai - 400710 (INDIA) Tel: 0091-22-27673311-16, 27673300 (Board) Fax: 0091-22-27673310, 27673330 E-mail: sales@mecoinst.com Web: www.mecoinst.com</div> <div style="text-align: center;"></div> <div>SR. NO. : <u>2019/224614</u> CHECKED BY : <u>[Signature]</u> DATE : <u>28-1-19</u> MODEL NO. : <u>920P</u></div> <div style="text-align: center;"><small>Copyright MECO METERS PVT. LTD. All rights reserved.</small></div> <div style="text-align: center;">8</div>	<div style="text-align: center;"> <small>SINCE 1982</small></div> <div style="text-align: center;"><b>HUMIDITY &amp; TEMPERATURE METER MODEL - 920P</b></div> <div style="text-align: center;"></div> <div style="text-align: center;"><b>Operation Manual</b></div>
--	---



## Annexure-B: Test Certificates

### B.1 Test Certificate for Activated Alumina

M/s.GUJARAT OXIDES, VILLAGE:TUNDAV,TAL:SAVLI

DIST: VADODARA-391770

Mail: [ace.savli@gmail.com](mailto:ace.savli@gmail.com) (M) 09924089676

#### CERTIFICATE OF ANALYSIS

5.6.2019

To : M/s. UNIQUE AIR PRODUCTS, VADODARA

PRODUCT: Activated Alumina

GRADE: A-101

PARTICLE SIZE: 5-8mm

ITEM CODE: 1000003663

BATCH No.: 0205/34006

P.O No.: UA-PO-11/19-20/ 30.5.19

DATE OF MFG.: MAY 2019

DATE OF EXPIRY: APRIL. 2022

Sr. No.	PROPERTIES	RESULTS
(A)	<b>MECHANICAL</b>	
1.	Bed crushing strength - %	95.0%
	Ind. Ball crush strength, point load basis, in kgs.	14.3
2.	Loss on attrition - %	
	By tumbling	0.10%
	By rotation - %	0.10%
(B)	<b>PHYSICAL</b>	
1.	Free Moisture at 300oC - %	1.5%
2.	Tapped bulk density , kg/m3	820
3.	Loss on ignition, (250-1000oC) - %	6.1%
4.	Pore volume(Total) cc/gm	0.41
5.	Surface area, m2/gm	360
6.	Water adsorption capacity at 60% RH & 30oC	20.0
7.	Water adsorption capacity at 15% RH & 30oC	5.2
(C)	<b>CHEMICAL</b>	
1.	Na2O - %	0.25
2.	Fe2O3 - %	0.01
3.	SiO2 - %	0.01
4.	Al2O3 - %	92.9%

#### ANALYTICAL REMARKS:

Material meets specifications for activated alumina adsorbent grade A-101

TEST METHOD: IS9700(1991), Confirming to Grade-I.

Size Distribution (Tyler Mesh): 5-8mm.

Undersize: Less than 2% Oversize: Less than 2%

**FOR GUJARAT OXIDES**

MANISH ARORA

Q.C.INCHARGE

## B.2 Test Certificate of Molecular Sieve 13X

### CERTIFICATE OF ANALYSIS

5.6.2019

To: M/s. UNIQUE AIR PRODUCTS, VADODARA  
PRODUCT: MOLECULAR SIEVES  
Type: 13X  
Item Code: MS-13  
Batch No.: 0205/30006  
Month of Mfg.: May 2019

Month of expiry: : April 2022

P.O.NO/ DATE : UA-PO-11/19-20/30.5.19

Sr. No.	PROPERTIES	RESULTS
(A)	MECHANICAL	
1.	Type:	13X
2.	Form:	Balls
3.	Size:	3-5mm
4.	Bed crushing strength: %	90%
5.	Loss on attrition: (Wear rate) Hard surface % (Tumbling & rotation method)	0.12%
6.	Ind. Crush strength 0n point load basis, kgs	30-50N
7.	pH	12
(B)	PHYSICAL	
1.	Water adsorption at 75%RH & 30oC. - %	21.7%
2.	Thermal stability at 600oC, adsorption - %	21.7%
3.	Water adsorption at 15%RH & 30oC - %	20.1%
3.	Benzene & other toxic gases adsorption capacity, - %	32
4.	Mercaptan removal - %	7
5.	CO 2 Removal - %	18
6.	Loss on ignition - %	1.8%
7.	Tapped Bulk density kg/m3	700

#### ANALYTICAL REMARKS:

The above material supplied meets the specifications of Grade MS-13.

Size qualification=96%.


All other parameters are in line with your specs.

MANISH ARORA

Q.C. INCHARGE



## B.3 Test Certificate for Molecular Sieve 4A

**SORBEAD INDIA**<sup>TM</sup>

**Office** : 306-307, Prayasha Complex,  
Next to Hyundai Motors, Chhani Naka,  
Vadodara-390024. (Gujarat) India.

**Phone** : +91-265-2761041 / 2761042

**Toll Free** : **1800-233-2677**

**E-mail** : [sales@sorbeadindia.com](mailto:sales@sorbeadindia.com)

**Website** : [www.sorbeadindia.com](http://www.sorbeadindia.com)

**Products We Manufacture :**  
Silica Gel-Blue, White & Orange Beads, Molecular Sieve-Beads,  
Pellets & Powder, Activated Alumina Balls, Aluminium Oxide Column  
Grades.

**Product We Serve :**  
**DMF / USFDA Grade :**  
Cotton, Rayon & Polyester Coils, Desiccants Pouches, LDPE Bags,  
laminated & Aluminium Tubes

**CERTIFICATE OF ANALYSIS**

Customer	: ALICE JUDE DSOUZA
PO No	: E Mail Dtd 22.01.22
Quantity	: 5 Kgs
Packing	: 1 Can X 5Kg
Invoice No	: GST/21-22/930 Dtd.25.01.2022
Batch No	: C20602O23
Product	: Molecular Sieve 4A Beads
Shape	: Beads
Size	: 1.6-2.7 mm
Bulk density	: 792 Kg/m <sup>3</sup>
Crushing strength (N)	: 21 N
Attrition Loss	: 0.03 %
Water Adsorption at 25°C at 60% RH.	: 21.10%
Residual moisture	: 0.90%

**\*Remarks: The products confirms to its standard specification**

For SORBEAD INDIA

*Rajendra*

Q. A. MANAGER




Factory Address : Plot No. 14, Swastik Industrial Estate & Plot No. 53, 54 A & 54 B - Navdurga Estate Park, Old N.H. No. 8, - SANKARDA - 391 350, Tal. & Dist. Vadodara (Gujarat), INDIA, Ph. No.: 9099020023





## B.4 Test Certificate for Silica Gel

**SORBEAD INDIA**<sup>TM</sup>

**Office** : 306-307, Prayasha Complex,  
Next to Hyundai Motors, Chhani Naka,  
Vadodara-390024. (Gujarat) India.

**Phone** : +91-265-2761041 / 2761042

**Toll Free** : **1800-233-2677**

**E-mail** : [sales@sorbeadindia.com](mailto:sales@sorbeadindia.com)

**Website** : [www.sorbeadindia.com](http://www.sorbeadindia.com)

**Products We Manufacture :**  
Silica Gel-Blue, White & Orange Beads, Molecular Sieve-Beads,  
Pellets & Powder, Activated Alumina Balls, Aluminium Oxide Column  
Grades.

**Product We Serve :**  
**DMF / USFDA Grade :**  
Cotton, Rayon & Polyester Coils, Desiccants Pouches, LDPE Bags,  
laminated & Aluminium Tubes

### CERTIFICATE OF ANALYSIS

Customer	: ALICE JUDE DSOUZA
PO No.	: E Mail Dtd 22.01.22
Invoice No.	: GST/21-22/930 Dtd.25.01.2022
Product	: Silica Gel White Beads
Batch No	: C11305O08
Quantity	: 5 Kg (1 Can X 5 Kg)
Appearance	: Spherical White Beads
Size	: 3-5 mm
PH	: 4.2
Bulk Density	: 0.766 gm/ml
Loss on Drying	: 1.25 %
Adsorption Capacity	
30% RH	: 17.89 %
60% RH	: 32.80 %
100% RH	: 39.50 %

Remarks: The products confirms to its standard specification.

For SORBEAD INDIA

*Rajendra*

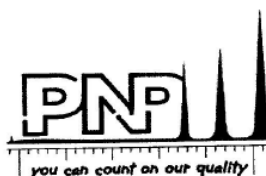
Q. A. MANAGER



Factory Address : Plot No. 14, Swastik Industrial Estate & Plot No. 53, 54 A & 54 B - Navdurga Estate Park, Old N.H. No. 8, - SANKARDA - 391 350, Tal. & Dist. Vadodara (Gujarat), INDIA. Ph. No.: 9099020023



## B.5 SEM analysis results



**PNP Analytical Solutions**

### RESULT OF ANALYSIS

Page 1 of 1

Report No. : PNP/AD/220223/R1

Report date : 22.02.2023

Name & Address of Client : Alice D'souza  
Research Scholar  
Gujarat Technological University

Sr. No	Batch No.	Results
1.	Sillica gel	SEM analysis data attached
2.	MS3A	SEM analysis data attached
3.	MS4A	SEM analysis data attached

Note : Analysis performed as per Inhouse method.

\*\*\*\*\* End of report \*\*\*\*\*

Authorised Signatory

**Note:**

- 1) Result listed in the report shall be applicable for sample submitted and the parameter of test applied.
- 2) Sample drawn and submitted by client for analysis.
- 3) The liability of our lab is limited to the invoiced amount.
- 4) This report cannot be replicate, wholly or in part, in any form of media without our permission.
- 5) Method of analysis for this test is developed inhouse based on standard & sample provided by client.
- 6) Analysis method parameter shall not be shared.

B-4/17 and 18 (Second floor), Krishna Industrial Estate, Opposite Gorwa BIDC, Gorwa, Vadodara, Gujarat, 390016.

(m): 9374831889 / 9106929989

Email: care@pnpanalytical.com

Web: www.pnpanalytical.com

# Annexure - C: Details of Purchase

## C.1 Invoice of Desiccant Purchase

**Factory & Ware House :** Plot No.14, Swastik Ind. Estate & Plot No. 53, 54A & 54B, Navdurga Estate Park, Old N.H. No. 8, Sankarda - 391350 Dist. Vadodara, (Gujarat) India.

**Regd. Office :** 306-307, Prayasha Complex, Next to Hyundai Motors, Chhani Naka, Vadodara - 390024, Gujarat, India  
Phone : + 91-265-2761041-42, E-mail : sales@sorbeadindia.com  
Website : www.sorbeadindia.com



**Products We Serve :** Silica Gel-Blue, White & Orange Beads, Molecular Sieve-Beads, Pellets & Powder, Activated Alumina Balls, Alumina Oxide Column Grades, DMF / FDA Grade : Desiccants Pouches, Cotton, Rayon, Polyester Coils, Laminated & Alumina Tubes, LDPE Bags.

**GSTIN :** 24AAQFS2930P12M

**PAN NO :** AAQFS2930P

### Tax Invoice

ORIGINAL FOR RECIPIENT

<b>Bill To:</b> <b>ALICE JUDE DSOUZA</b> Assistant Professor, Govt. Engineering College, Bharuch Pin:392002, K/A:Ms. Alice Jude Dsouza, MO:8511158280 State Name : Gujarat Code : 24 GSTIN No : PAN No :				<b>Place of Supply:</b> <b>UNIQUE AIR PRODUCTS</b> Plot No 193/B, Makarpura GIDC, Vadodara, K/A Ms. Alice Jude Dsouza, CELL NO.: 8511158280 Pin:390010, K/A: ,MO: State Name : Gujarat Code : 24 GSTIN No : PAN No :			
Invoice No : <b>GST/21-22/930</b> Dated : <b>25-Jan-22</b>		Terms Of Payment.: Due Date:		Transport: <b>SPECIAL VEHICLE (PAID BASIS)</b> / Vehicle No.:			
Order No. : <b>EMAIL</b> Order Dated : <b>22-Jan-22</b> Destination : <b>DOOR DELIVERY</b> Other Terms : <b>100% ADVANCE</b>							
Sr No	Item Description	HSN Code	Billed Qty Per	Rate	Gross Amount		
1	MOLECULAR SIEVES 4A BEADS 1.6-2.7 MM MOLECULAR SIEVE 4A BEADS 1.6 - 2.7 MM 01 CAN X 5 KGS = 5KGS	38249900	5.00 KGS.	650	3,250.00		
2	SILICA GEL WHITE BEADS 3-5MM SILICA GEL WHITE BEADS 3-5 MM 01 CAN X 5 KGS = 5KGS	38249900	5.00 KGS.	450	2,250.00		
<b>TOTAL</b>					<b>5,500.00</b>		
HSN/SAC 38249900		Taxable Value 5,500.00	Central Tax 9% 495.00	State Tax 9% 495.00	Total Tax Amount 990.00		
<b>Total</b>		<b>5,500.00</b>	<b>495.00</b>	<b>495.00</b>	<b>990.00</b>		
<b>Company's Bank Details</b> A/c Holder's Name: <b>Sorbead India</b> Bank Name : <b>ICICI BANK LTD.</b> A/c No. : <b>000305001589</b> Branch & IFS Code : <b>ICIC00000003</b> SWIFT Code : <b>ICICINBBCTS</b>				<b>CGST 9%</b> 495.00 <b>SGST 9%</b> 495.00			
<b>Amount In Words:</b> INR Six Thousand Four Hundred Ninety Only.				<b>Invoice Total</b>	<b>6,490.00</b>		
<b>MARINE CARGO OPEN POLICY : TATA AIG OPEN POLICY NO: 0891059771 VALID UPTO 28.04.2022</b> <b>TAX PAYABLE ON REVERSE CHARGE BASIS : NO</b>							
Declaration:- (01)-Goods once sold will not be taken back OR exchange.(02)-Any rejection will accepted within 30days from the date of invoice with prior approval.(03)-Any bill not paid within due will be charged interest @24% p.a.				<b>Sorbead India</b>  <b>Authorised Signatory</b>			

Subject To Vadodara Jurisdiction

## C.2 Invoice of Data Logger Purchase

PPI The Reliable Experts		PRO FORMA INVOICE									
<b>M/S.PROCESS PRECISION INSTRUMENTS</b> 101, Diamond Indl. Estate, Navghar Vasai Road (E), Dist. : Palghar - 401210 Tel : 0250- 2391722/33/37/42 VAT TIN : 27460013178 - V - w.e.f. 1-4-2006 CST TIN : 27460013178 - C - w.e.f. 1-4-2006 LBT/WARD NO. 65/11/2011  <b>GST TIN NO : 27AAAF0413C1Z0</b> <b>ARN NO : AA2712160181896</b>		<table border="1"> <tr> <td>Proforma No.</td> <td>PRF-444/2020-2021</td> </tr> <tr> <td>Date</td> <td>25.03.2021</td> </tr> <tr> <td>Challan ref</td> <td>E-MAIL</td> </tr> <tr> <td>Date</td> <td>19.03.2021</td> </tr> </table>		Proforma No.	PRF-444/2020-2021	Date	25.03.2021	Challan ref	E-MAIL	Date	19.03.2021
Proforma No.	PRF-444/2020-2021										
Date	25.03.2021										
Challan ref	E-MAIL										
Date	19.03.2021										
<b>CUSTOMER</b> Kind Attn: Mr. Nelvin Johny M/s. ALICE JUDE DSOUZA Mechanical Engineering Department, Government Engineering College, Bharuch. Mob No. 9979860338 E-mail: <a href="mailto:info@uniqueair.co.in">info@uniqueair.co.in</a>		<b>SHIP TO</b> Kind Attn: Mr. Nelvin Johny M/s. UNIQUE AIR PRODUCTS 193/B, GIDC Industrial Estate, Makarpura, Vadodara 390010. Mob No. 9979860338 E-mail: <a href="mailto:info@uniqueair.co.in">info@uniqueair.co.in</a>									
<b>SHIPPING DETAILS</b> <b>DESPATCH MODE</b> By SURFACE  <b>COURIER MODE</b> BY SHREE MAHAVIR		<b>PAYMENT</b> 100% ADVANCE									
SR.NO	QTY	RATE	TOTAL AMOUNT								
1)	1	6937.00	6,937.00								
MODEL.: SCANLOG-96 SINGLE CHANNEL , SOFTWARE VERSION INPUT : 4-20MA 2 ALARM RELAY											
2)	1	1446.00	1,446.00								
RS485 TO USB CONVERTOR											
3)	1	FREE	----								
PC SOFTWARE CD											
		Sub total	INR 8,383.00								
		Freight	INR 150.00								
		Sub total	INR 8,533.00								
		IGST@18%	INR 1,535.94								
		<b>TOTAL</b>	<b>INR 10,068.94</b>								
<b>BANK DETAILS FOR ECS MODE OF PAYMENT.</b> NAME OF THE COMPANY : PROCESS PRECISION INSTRUMENTS NAME OF THE BANK& : CENTRAL BANK OF INDIA ADDRESS : BORIBUNDER BRANCH ACCOUNT NO : 1318685748 BANK ACCOUNT TYPE : CC IFSC CODE[RTGS/ NEFT] : CBIN 0280606											
<b>TERMS &amp; CONDITIONS:</b> Delivery: <b>READY FOR DESPATCH.</b> Payment Terms: <b>100% advance against Profor</b> [cheque in the name of Process Precision Instruments or BY NEFT mode - BANK DETAILS AS ABOVE]											
I certify the above to be true and correct to the best of my knowledge.											
Thanking you and assuring you of our best attention, For PROCESS PRECISION INSTRUMENTS MR.SATISH P.BHAT [GM-SALES]											



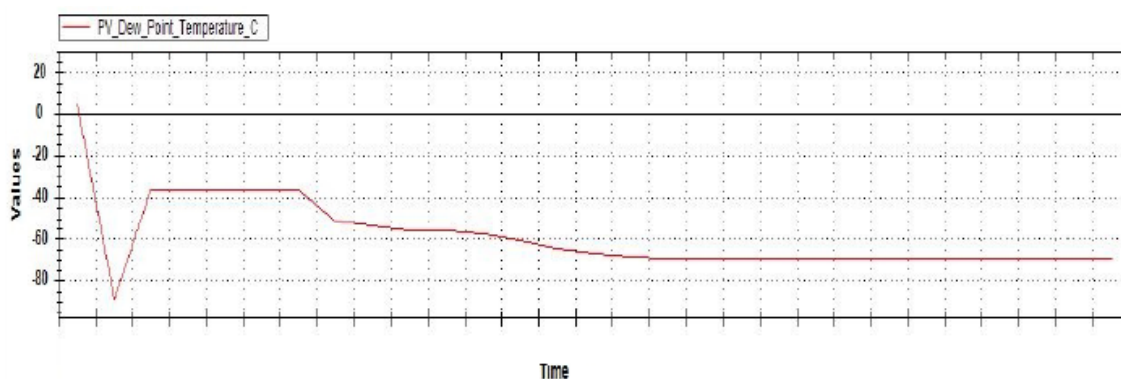
## Annexure-D: Experimental Data

### Experimental Data

Parameters	Unit	Silica gel	Molecular Sieve 4A	Molecular Sieve 13X	Activated Alumina	Silica gel & AA	Silica gel & MS 4A	Silica gel & 13x	AA & MS 4 A	AA & 13x	MS4A & 13x
<b>Inlet Dew point Temp T1</b>	° C	5.5	7.7	16.1	12.8	6.3	19.9	19.9	19.3	15.2	19.3
<b>Outlet Dew point Temp T2</b>	° C	-55	-63.4	-70.0	-39.8	-34.6	-51	-57.4	-45	-55	-52
<b>Inlet RH</b>	%	28.4	28.56	40.37	50.14	35.19	69.12	80.45	60.45	60.15	76.36
<b>Outlet RH</b>	%	15	5.23	7.85	24.6	24.5	42.95	16.05	52.17	30.5	36.18
<b>Reject Air RH</b>	%	25.5	18.21	36.81	33.77	31.7	76.24	79.68	76.70	45.22	89.19
<b>Atmospheric RH</b>	%	31.8	30.86	41.32	52.51	42.85	77.15	80.72	76.19	65.51	90.80
<b>Atmospheric WBT</b>	%	16.4	18.8	27.13	26.98	27.06	26.80	26.71	27.06	26.38	26.28
<b>Inlet WBT</b>	%	14.6	18.51	26.89	25.41	23.89	25.64	26.57	26.12	25.21	25.06
<b>Outlet WBT</b>	%	12.21	11.4	21.8	14.2	20.83	20.57	20.60	22.17	15.3	17.24
<b>Reject Air WBT</b>	%	14.9	14.5	27.31	26.95	26.4	27.05	25.99	27.14	26.55	26.49
<b>Moisture removal rate</b>	gm/hr	22.51	39.58	54.63	22.74	17.95	43.96	108.19	13.91	42.95	67.50
<b>Effectiveness of dehumidifier</b>	%	47.18	81.68	80.55	50.93	30.37	37.86	80.04	13.69	36.58	52.61



## Experimental readings of Molecular Sieve 13x recorded by the dew point transmitter



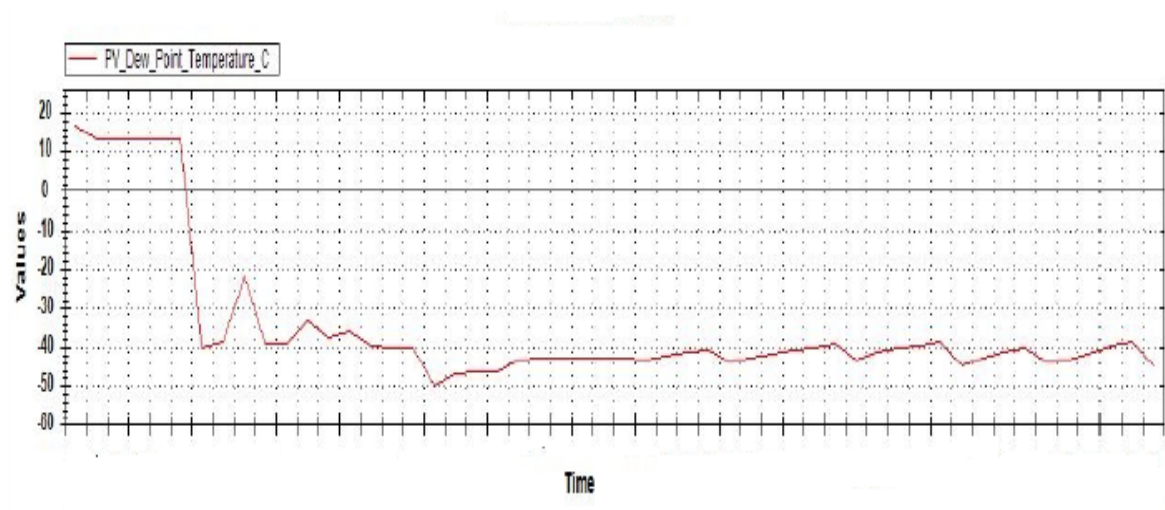
ChannelName	MIN	MAX	AVG
PV_Dew_Point_Temperature_C	-69.9	-34.7	-64.3

LogDateTime	PV_Dew_Point_Temperature_C
06-10-2022 15:43	-38.8
06-10-2022 15:44	-34.7
06-10-2022 15:45	-34.7
06-10-2022 15:46	-34.7
06-10-2022 15:47	-34.8
06-10-2022 15:48	-34.7
06-10-2022 15:49	-47.2
06-10-2022 15:50	-48.8
06-10-2022 15:51	-50.2
06-10-2022 15:52	-50.4
06-10-2022 15:53	-51.5
06-10-2022 15:54	-53.8
06-10-2022 15:55	-56.1
06-10-2022 15:56	-56.4
06-10-2022 15:57	-57.3
06-10-2022 15:58	-59
06-10-2022 15:59	-60.8
06-10-2022 16:00	-60.9
06-10-2022 16:01	-61.7
06-10-2022 16:02	-68
06-10-2022 16:03	-69.7
06-10-2022 16:04	-69.7
06-10-2022 16:05	-69.7
06-10-2022 16:06	-69.8
06-10-2022 16:07	-69.7

06-10-2022 16:08	-69.7
06-10-2022 16:09	-69.7
06-10-2022 16:10	-69.7
06-10-2022 16:11	-69.8
06-10-2022 16:12	-69.8
06-10-2022 16:13	-69.8
06-10-2022 16:14	-69.8
06-10-2022 16:15	-69.8
06-10-2022 16:16	-69.8
06-10-2022 16:17	-69.8
06-10-2022 16:18	-69.8
06-10-2022 16:19	-69.8
06-10-2022 16:20	-69.8
06-10-2022 16:21	-69.8
06-10-2022 16:22	-69.8
06-10-2022 16:23	-69.8
06-10-2022 16:24	-69.8
06-10-2022 16:25	-69.8
06-10-2022 16:26	-69.8
06-10-2022 16:27	-69.8
06-10-2022 16:28	-69.8
06-10-2022 16:29	-69.8
06-10-2022 16:30	-69.9
06-10-2022 16:31	-69.9
06-10-2022 16:32	-69.8
06-10-2022 16:33	-69.8
06-10-2022 16:34	-69.8
06-10-2022 16:35	-69.8
06-10-2022 16:36	-69.8
06-10-2022 16:37	-69.8
06-10-2022 16:38	-69.8
06-10-2022 16:39	-69.9
06-10-2022 16:40	-69.8
06-10-2022 16:41	-69.8
06-10-2022 16:42	-69.8
06-10-2022 16:43	-69.8
06-10-2022 16:44	-69.8
06-10-2022 16:45	-69.7
06-10-2022 16:46	-69.7
06-10-2022 16:47	-69.7
06-10-2022 16:48	-69.7
06-10-2022 16:49	-69.7
06-10-2022 16:50	-69.7
06-10-2022 16:51	-69.8
06-10-2022 16:52	-69.8

06-10-2022 16:53	-69.8
06-10-2022 16:54	-69.9
06-10-2022 16:55	-69.9

### Experimental readings of Activated Alumina recorded by the dew point transmitter



ChannelName	MIN	MAX	AVG
PV_Dew_Point_Temperature_C	-55.9	17.3	-48.3

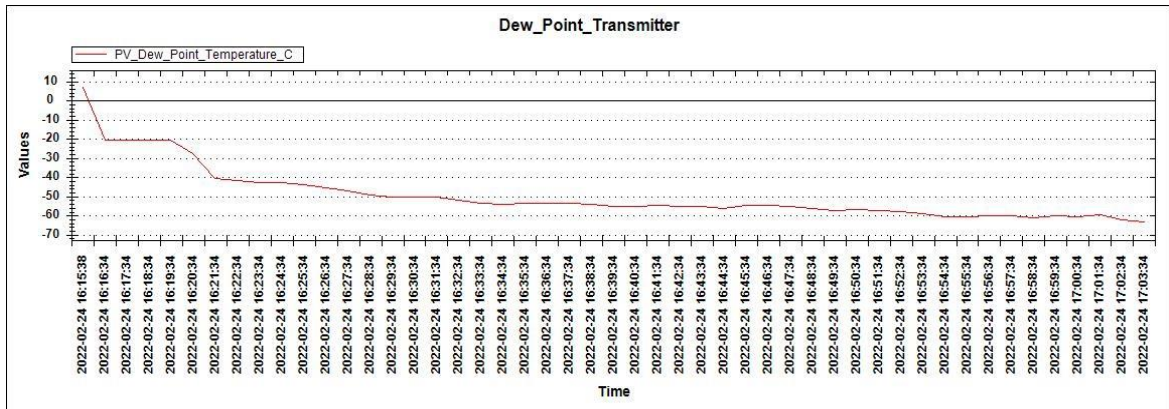
LogDateTime	PV_Dew_Point_Temperature_C
06-10-2022 11:31	17.3
06-10-2022 11:32	-39.1
06-10-2022 11:33	-36.9
06-10-2022 11:34	-36.9
06-10-2022 11:35	-36.9
06-10-2022 11:36	-36.9
06-10-2022 11:37	-36.9
06-10-2022 11:38	-39.7
06-10-2022 11:39	-40
06-10-2022 11:40	-39.7
06-10-2022 11:41	-39.7
06-10-2022 11:42	-40.2
06-10-2022 11:43	-39.6
06-10-2022 11:44	-40.8
06-10-2022 11:45	-43.7
06-10-2022 11:46	-44.5
06-10-2022 11:47	-45.5
06-10-2022 11:48	-45.6



06-10-2022 11:49	-46.2
06-10-2022 11:50	-46.4
06-10-2022 11:51	-45.2
06-10-2022 11:52	-44
06-10-2022 11:53	-43
06-10-2022 11:54	-44.6
06-10-2022 11:55	-47
06-10-2022 11:56	-48.3
06-10-2022 11:57	-48.2
06-10-2022 11:58	-47.3
06-10-2022 11:59	-48.5
06-10-2022 12:00	-48.4
06-10-2022 12:01	-47.1
06-10-2022 12:02	-45.8
06-10-2022 12:03	-44.6
06-10-2022 12:04	-47.6
06-10-2022 12:05	-50.3
06-10-2022 12:06	-50.5
06-10-2022 12:07	-49.5
06-10-2022 12:08	-49.5
06-10-2022 12:09	-49
06-10-2022 12:10	-48.7
06-10-2022 12:11	-47.4
06-10-2022 12:12	-47.6
06-10-2022 12:13	-46.9
06-10-2022 12:14	-49.2
06-10-2022 12:15	-49.3
06-10-2022 12:16	-50.2
06-10-2022 12:17	-50.6
06-10-2022 12:18	-49.3
06-10-2022 12:19	-51.3
06-10-2022 12:20	-50.5
06-10-2022 12:21	-49.1
06-10-2022 12:22	-47.7
06-10-2022 12:23	-47.7
06-10-2022 12:24	-49.7
06-10-2022 12:25	-51.7
06-10-2022 12:26	-52.1
06-10-2022 12:27	-51
06-10-2022 12:28	-50.5
06-10-2022 12:29	-52.2
06-10-2022 12:30	-51.2
06-10-2022 12:31	-51.2
06-10-2022 12:32	-47.9
06-10-2022 12:33	-47.7

06-10-2022 12:34	-52.4
06-10-2022 12:35	-53.4
06-10-2022 12:36	-52.4
06-10-2022 12:37	-51.3
06-10-2022 12:38	-51.5
06-10-2022 12:39	-52.7
06-10-2022 12:40	-52.7
06-10-2022 12:41	-49.4
06-10-2022 12:42	-48.2
06-10-2022 12:43	-50.1
06-10-2022 12:44	-53.7
06-10-2022 12:45	-53.6
06-10-2022 12:46	-52.5
06-10-2022 12:47	-52.5
06-10-2022 12:48	-52
06-10-2022 12:49	-52.6
06-10-2022 12:50	-51.6
06-10-2022 12:51	-50.2
06-10-2022 12:52	-49.4
06-10-2022 12:53	-52.8
06-10-2022 12:54	-54.2
06-10-2022 12:55	-53.9
06-10-2022 12:56	-52.7
06-10-2022 12:57	-51.5
06-10-2022 12:58	-53
06-10-2022 12:59	-52.9
06-10-2022 13:00	-51.8
06-10-2022 13:01	-51.8
06-10-2022 13:02	-50.6
06-10-2022 13:03	-54.8
06-10-2022 13:04	-55.9
06-10-2022 13:05	-54.9
06-10-2022 13:06	-53.7
06-10-2022 13:07	-52.6
06-10-2022 13:08	-52.6
06-10-2022 13:09	-52.4
06-10-2022 13:10	-51.4
06-10-2022 13:11	-50.6
06-10-2022 13:12	-50.6
06-10-2022 13:13	-55.3
06-10-2022 13:14	-55.8
06-10-2022 13:15	-55.8
06-10-2022 13:16	-54.6
06-10-2022 13:17	-53.2

## Experimental readings of Silica gel recorded by the dew point transmitter



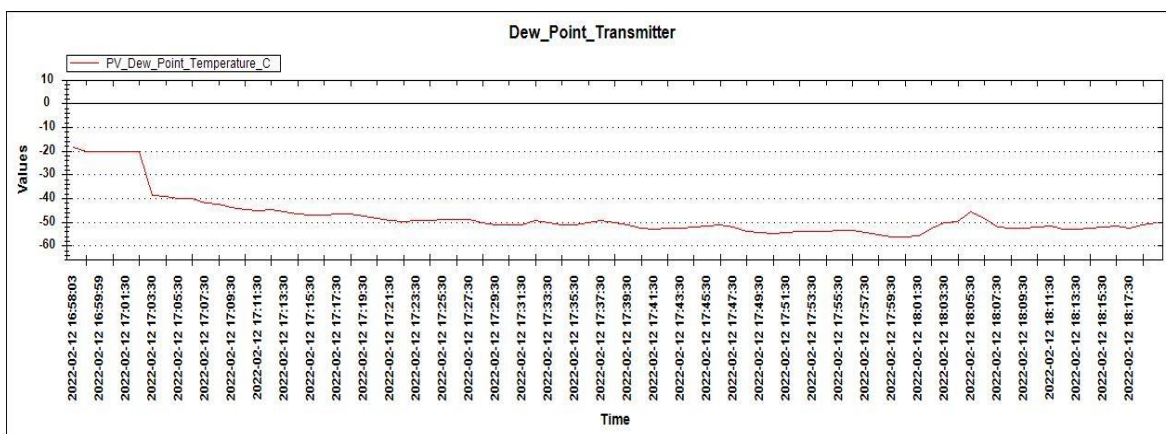
ChannelName	MIN	MAX	AVG
PV_Dew_Point_Temperature_C	-56.3	-18.5	-48

LogDateTime	PV_Dew_Point_Temperature_C
02-12-2022 16:58	-18.5
02-12-2022 16:58	-20.6
02-12-2022 16:59	-20.5
02-12-2022 17:00	-20.6
02-12-2022 17:01	-20.5
02-12-2022 17:02	-20.5
02-12-2022 17:03	-38.7
02-12-2022 17:04	-39.5
02-12-2022 17:05	-40.2
02-12-2022 17:06	-40.3
02-12-2022 17:07	-42.3
02-12-2022 17:08	-42.4
02-12-2022 17:09	-44.1
02-12-2022 17:10	-44.8
02-12-2022 17:11	-45.1
02-12-2022 17:12	-45
02-12-2022 17:13	-45.7
02-12-2022 17:14	-46.6
02-12-2022 17:15	-47.3
02-12-2022 17:16	-47.1
02-12-2022 17:17	-46.7
02-12-2022 17:18	-46.7
02-12-2022 17:19	-47.6
02-12-2022 17:20	-48.7
02-12-2022 17:21	-49.5

02-12-2022 17:22	-49.9
02-12-2022 17:23	-49.4
02-12-2022 17:24	-49.5
02-12-2022 17:25	-49
02-12-2022 17:26	-48.9
02-12-2022 17:27	-48.9
02-12-2022 17:28	-50.5
02-12-2022 17:29	-51.2
02-12-2022 17:30	-51.5
02-12-2022 17:31	-51.4
02-12-2022 17:32	-49.4
02-12-2022 17:33	-50.3
02-12-2022 17:34	-51.1
02-12-2022 17:35	-51.1
02-12-2022 17:36	-50.6
02-12-2022 17:37	-49.6
02-12-2022 17:38	-50.4
02-12-2022 17:39	-51.5
02-12-2022 17:40	-52.5
02-12-2022 17:41	-53.3
02-12-2022 17:42	-52.5
02-12-2022 17:43	-52.6
02-12-2022 17:44	-52.3
02-12-2022 17:45	-51.7
02-12-2022 17:46	-51.3
02-12-2022 17:47	-52.4
02-12-2022 17:48	-53.9
02-12-2022 17:49	-54.7
02-12-2022 17:50	-54.9
02-12-2022 17:51	-54.7
02-12-2022 17:52	-53.9
02-12-2022 17:53	-54
02-12-2022 17:54	-53.9
02-12-2022 17:55	-53.4
02-12-2022 17:56	-53.7
02-12-2022 17:57	-54.4
02-12-2022 17:58	-55.7
02-12-2022 17:59	-56.3
02-12-2022 18:00	-56.2
02-12-2022 18:01	-56
02-12-2022 18:02	-52.9
02-12-2022 18:03	-50.5
02-12-2022 18:04	-49.8
02-12-2022 18:05	-45.8
02-12-2022 18:06	-48.4

02-12-2022 18:07	-52.2
02-12-2022 18:08	-52.9
02-12-2022 18:09	-52.7
02-12-2022 18:10	-52.1
02-12-2022 18:11	-52
02-12-2022 18:12	-53.1
02-12-2022 18:13	-53.2
02-12-2022 18:14	-52.6
02-12-2022 18:15	-52.2
02-12-2022 18:16	-51.8
02-12-2022 18:17	-52.9
02-12-2022 18:18	-51.5
02-12-2022 18:19	-50.6

### Experimental readings of the heterogeneous mixture of Molecular Sieve 13x and activated alumina recorded by the dew point transmitter

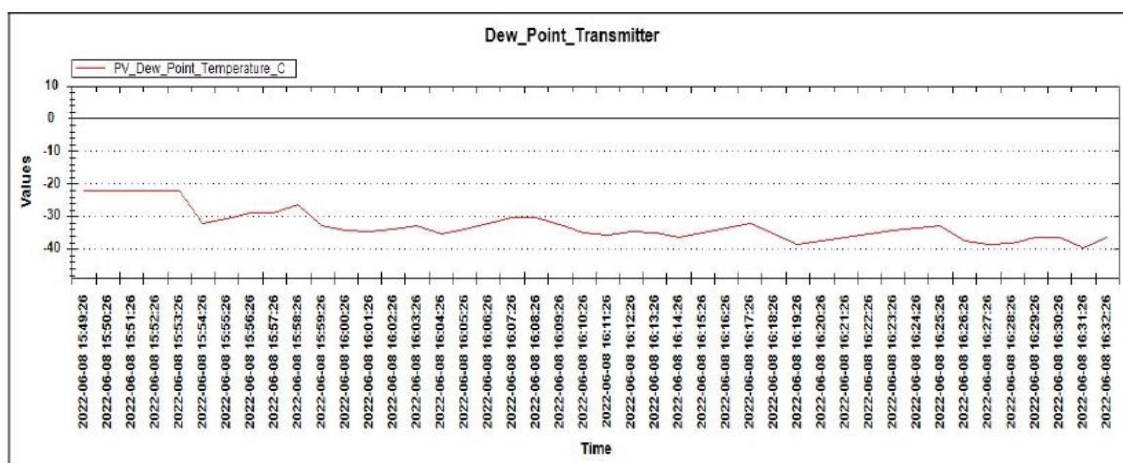


ChannelName	MIN	MAX	AVG
PV_Dew_Point_Temperature_C	-55	-18	-47.5

LogDateTime	PV_Dew_Point_Temperature_C
06-08-2022 16.58.03	-18
06-08-2022 16.59.59	-20
06-08-2022 17.01.30	-20
06-08-2022 17.03.30	-20
06-08-2022 17.05.30	-40
06-08-2022 17.07.30	-42
06-08-2022 17.09.30	-44
06-08-2022 17.11.30	-46
06-08-2022 17.13.30	-48

06-08-2022 17.15.30	-50
06-08-2022 17.17.30	-50
06-08-2022 17.19.30	-50
06-08-2022 17.21.30	-50
06-08-2022 17.25.30	-51
06-08-2022 17.27.30	-50
06-08-2022 17.29.30	-51
06-08-2022 17.31.30	-50
06-08-2022 17.33.30	-50
06-08-2022 17.35.30	-51
06-08-2022 17.37.30	-50
06-08-2022 17.39.30	-50
06-08-2022 17.41.30	-51
06-08-2022 17.43.30	-51
06-08-2022 17.45.30	-52
06-08-2022 17.47.30	-52
06-08-2022 17.49.30	-52
06-08-2022 17.51.30	-53
06-08-2022 17.53.30	-53
06-08-2022 17.55.30	-53
06-08-2022 17.57.30	-54
06-08-2022 17.59.30	-55
06-08-2022 18.01.30	-52
06-08-2022 18.03.30	-53
06-08-2022 18.05.30	-48
06-08-2022 18.07.30	-51
06-08-2022 18.09.30	-51
06-08-2022 18.11.30	-51
06-08-2022 18.13.30	-51

**Experimental readings of the heterogeneous mixture of silica gel and activated alumina recorded by the dew point transmitter**

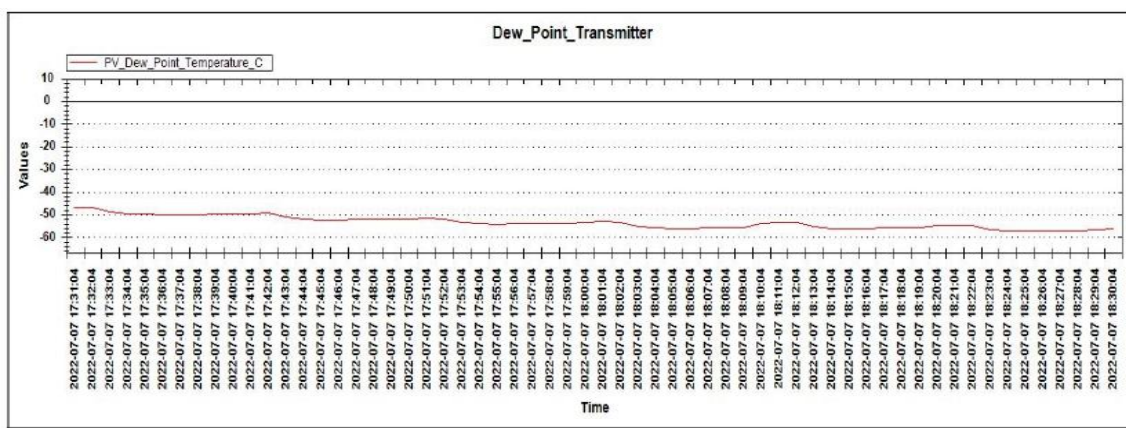


<b>ChannelName</b>	<b>MIN</b>	<b>MAX</b>	<b>AVG</b>
PV_Dew_Point_Temperature_C	-39.8	-22.1	-32.9

<b>LogDateTime</b>	<b>PV_Dew_Point_Temperature_C</b>
06-08-2022 15:49	-22.1
06-08-2022 15:50	-22.1
06-08-2022 15:51	-22.1
06-08-2022 15:52	-22.1
06-08-2022 15:53	-22.1
06-08-2022 15:54	-32.3
06-08-2022 15:55	-30.9
06-08-2022 15:56	-29.1
06-08-2022 15:57	-28.9
06-08-2022 15:58	-26.5
06-08-2022 15:59	-32.9
06-08-2022 16:00	-34.4
06-08-2022 16:01	-34.8
06-08-2022 16:02	-33.9
06-08-2022 16:03	-32.9
06-08-2022 16:04	-35.3
06-08-2022 16:05	-34
06-08-2022 16:06	-32.1
06-08-2022 16:07	-30.4
06-08-2022 16:08	-30.5
06-08-2022 16:09	-32.5
06-08-2022 16:10	-35.2
06-08-2022 16:11	-35.9
06-08-2022 16:12	-34.6
06-08-2022 16:13	-35.1
06-08-2022 16:14	-36.7
06-08-2022 16:15	-35.2
06-08-2022 16:16	-33.5
06-08-2022 16:17	-32.3
06-08-2022 16:18	-35.5
06-08-2022 16:19	-38.6
06-08-2022 16:20	-37.7
06-08-2022 16:21	-36.6
06-08-2022 16:22	-35.4
06-08-2022 16:23	-34.4
06-08-2022 16:24	-33.5
06-08-2022 16:25	-33

06-08-2022 16:26	-37.6
06-08-2022 16:27	-38.7
06-08-2022 16:28	-38.3
06-08-2022 16:29	-36.7
06-08-2022 16:30	-36.7
06-08-2022 16:31	-39.8
06-08-2022 16:32	-36.4

## Experimental readings of the heterogeneous mixture of silica gel and Molecular Sieve 13x recorded by the dew point transmitter



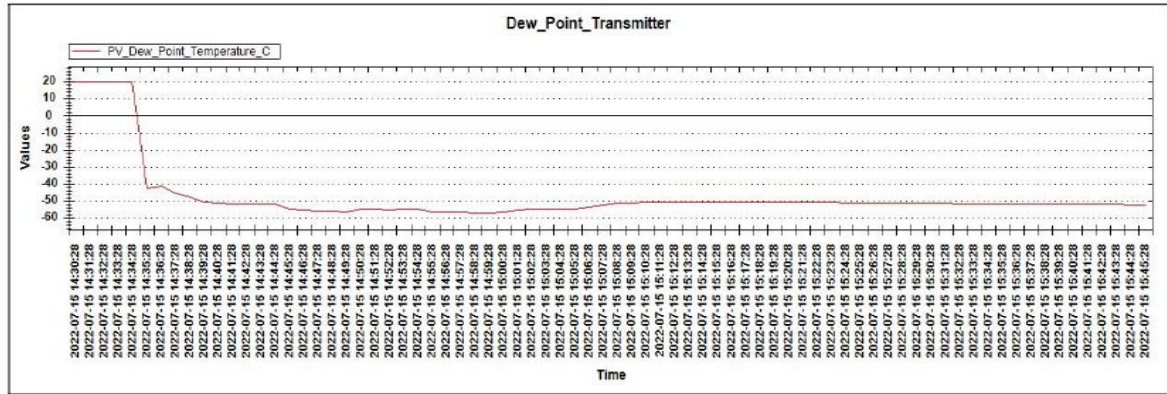
ChannelName	MIN	MAX	AVG
PV_Dew_Point_Temperature_C	-57.4	-47.1	-53.5

LogDateTime	PV_Dew_Point_Temperature_C
07-07-2022 17:31	-47.2
07-07-2022 17:32	-47.1
07-07-2022 17:33	-48.9
07-07-2022 17:34	-49.7
07-07-2022 17:35	-50
07-07-2022 17:36	-50.1
07-07-2022 17:37	-50.1
07-07-2022 17:38	-50.1
07-07-2022 17:39	-50
07-07-2022 17:40	-49.7
07-07-2022 17:41	-49.6
07-07-2022 17:42	-49.3
07-07-2022 17:43	-51.1
07-07-2022 17:44	-52



07-07-2022 17:45	-52.4
07-07-2022 17:46	-52.4
07-07-2022 17:47	-52.1
07-07-2022 17:48	-52.3
07-07-2022 17:49	-52.2
07-07-2022 17:50	-51.9
07-07-2022 17:51	-51.6
07-07-2022 17:52	-52.2
07-07-2022 17:53	-53.7
07-07-2022 17:54	-54.2
07-07-2022 17:55	-54.3
07-07-2022 17:56	-54.2
07-07-2022 17:57	-53.8
07-07-2022 17:58	-53.9
07-07-2022 17:59	-53.8
07-07-2022 18:00	-53.5
07-07-2022 18:01	-53.2
07-07-2022 18:02	-53.6
07-07-2022 18:03	-55.4
07-07-2022 18:04	-56
07-07-2022 18:05	-56.1
07-07-2022 18:06	-56.1
07-07-2022 18:07	-55.8
07-07-2022 18:08	-55.8
07-07-2022 18:09	-55.7
07-07-2022 18:10	-54.2
07-07-2022 18:11	-53.5
07-07-2022 18:12	-53.7
07-07-2022 18:13	-55.5
07-07-2022 18:14	-56.1
07-07-2022 18:15	-56.2
07-07-2022 18:16	-56.1
07-07-2022 18:17	-55.9
07-07-2022 18:18	-55.9
07-07-2022 18:19	-55.9
07-07-2022 18:20	-55
07-07-2022 18:21	-54.7
07-07-2022 18:22	-54.8
07-07-2022 18:23	-56.6
07-07-2022 18:24	-57.2
07-07-2022 18:25	-57.4
07-07-2022 18:26	-57.3
07-07-2022 18:27	-57.3
07-07-2022 18:28	-57.2
07-07-2022 18:29	-56.9

## Experimental readings of the heterogeneous mixture of Molecular Sieve 4A and Molecular Sieve 13x recorded by the dew point transmitter



ChannelName	MIN	MAX	AVG
PV_Dew_Point_Temperature_C	-57.3	19.8	-47.6

LogDateTime	PV_Dew_Point_Temperature_C
15-07-2022 14:30:28	19.8
15-07-2022 14:31:28	19.7
15-07-2022 14:32:28	19.7
15-07-2022 14:33:28	19.7
15-07-2022 14:34:28	19.7
15-07-2022 14:35:28	-42.9
15-07-2022 14:36:28	-41.3
15-07-2022 14:37:28	-45.7
15-07-2022 14:38:28	-47.6
15-07-2022 14:39:28	-50.8
15-07-2022 14:40:28	-51.1
15-07-2022 14:41:28	-51.7
15-07-2022 14:42:28	-51.8
15-07-2022 14:43:28	-51.7
15-07-2022 14:44:28	-52.1
15-07-2022 14:45:28	-54.6
15-07-2022 14:46:28	-55.6
15-07-2022 14:47:28	-56.1
15-07-2022 14:48:28	-56.3
15-07-2022 14:49:28	-56.4
15-07-2022 14:50:28	-55
15-07-2022 14:51:28	-55.1

15-07-2022 14:52:28	-55.2
15-07-2022 14:53:28	-54.8
15-07-2022 14:54:28	-55.1
15-07-2022 14:55:28	-56.5
15-07-2022 14:56:28	-56.8
15-07-2022 14:57:28	-56.9
15-07-2022 14:58:28	-57.3
15-07-2022 14:59:28	-57.3
15-07-2022 15:00:28	-56.4
15-07-2022 15:01:28	-55.2
15-07-2022 15:02:28	-55
15-07-2022 15:03:28	-54.6
15-07-2022 15:04:28	-54.6
15-07-2022 15:05:28	-54.9
15-07-2022 15:06:28	-53.7
15-07-2022 15:07:28	-52.5
15-07-2022 15:08:28	-51.6
15-07-2022 15:09:28	-51.1
15-07-2022 15:10:28	-50.8
15-07-2022 15:11:28	-50.8
15-07-2022 15:12:28	-50.9
15-07-2022 15:13:28	-50.9
15-07-2022 15:14:28	-50.9
15-07-2022 15:15:28	-51
15-07-2022 15:16:28	-50.9
15-07-2022 15:17:28	-50.9
15-07-2022 15:18:28	-50.9
15-07-2022 15:19:28	-50.8
15-07-2022 15:20:28	-50.8
15-07-2022 15:21:28	-50.9
15-07-2022 15:22:28	-51
15-07-2022 15:23:28	-51
15-07-2022 15:24:28	-51.2
15-07-2022 15:27:28	-51.5
15-07-2022 15:28:28	-51.6
15-07-2022 15:29:28	-51.6
15-07-2022 15:30:28	-51.5
15-07-2022 15:31:28	-51.6
15-07-2022 15:32:28	-51.9
15-07-2022 15:33:28	-51.9
15-07-2022 15:34:28	-52
15-07-2022 15:35:28	-52
15-07-2022 15:36:28	-51.9
15-07-2022 15:37:28	-52
15-07-2022 15:38:28	-52.1

15-07-2022 15:39:28	-52.1
15-07-2022 15:40:28	-52.1
15-07-2022 15:41:28	-52.1

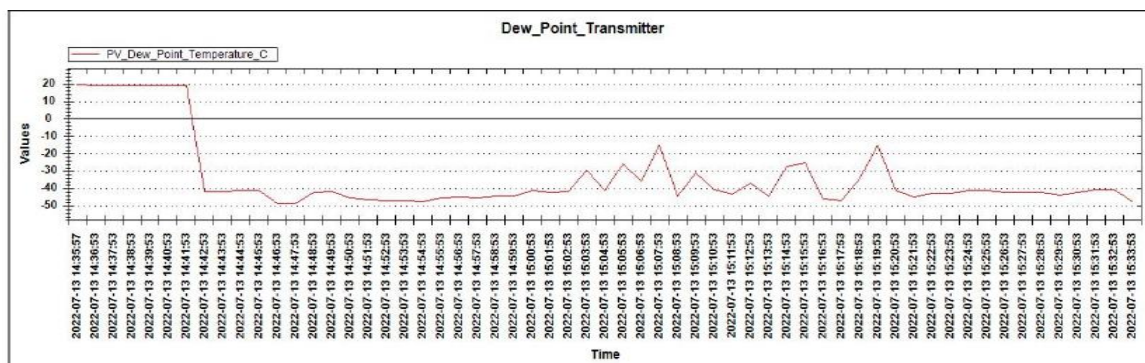
**Experimental readings of the heterogeneous mixture of Molecular Sieve 4A and silica gel recorded by the dew point transmitter**

ChannelName	MIN	MAX	AVG
PV_Dew_Point_Temperature_C	-45.6	19.7	-33.3

LogDateTime	PV_Dew_Point_Temperature_C
13-07-2022 12:37:08	19.7
13-07-2022 12:38:08	19.7
13-07-2022 12:39:08	-14.9
13-07-2022 12:40:08	-18.2
13-07-2022 12:41:08	-19.5
13-07-2022 12:42:08	-20.1
13-07-2022 12:43:08	-19.8
13-07-2022 12:44:08	-22.1
13-07-2022 12:45:08	-25.1
13-07-2022 12:46:08	-26.2
13-07-2022 12:47:08	-26.1
13-07-2022 12:48:08	-25.6
13-07-2022 12:49:08	-28.4
13-07-2022 12:50:08	-29.3
13-07-2022 12:51:08	-28.8
13-07-2022 12:52:08	-28.1
13-07-2022 12:53:08	-27.1
13-07-2022 12:54:08	-30.4
13-07-2022 12:55:08	-31
13-07-2022 12:56:08	-30.8
13-07-2022 12:57:08	-30.3
13-07-2022 12:58:08	-29.2
13-07-2022 12:59:08	-31.7
13-07-2022 13:00:08	-32.6
13-07-2022 13:01:08	-32.1
13-07-2022 13:02:08	-31.3
13-07-2022 13:03:08	-30.9
13-07-2022 13:04:08	-35.9
13-07-2022 13:05:08	-36.4

13-07-2022 13:06:08	-36
13-07-2022 13:07:08	-35.6
13-07-2022 13:08:08	-34.3
13-07-2022 13:09:08	-36.3
13-07-2022 13:10:08	-37.7
13-07-2022 13:11:08	-37.6
13-07-2022 13:12:08	-36.6
13-07-2022 13:13:08	-35.9
13-07-2022 13:14:08	-39
13-07-2022 13:15:08	-39.4
13-07-2022 13:16:08	-38.8
13-07-2022 13:17:08	-38
13-07-2022 13:18:08	-37.2
13-07-2022 13:19:08	-39
13-07-2022 13:20:08	-39.8
13-07-2022 13:21:08	-40.1
13-07-2022 13:22:08	-39
13-07-2022 13:23:08	-37.8
13-07-2022 13:24:08	-41.1
13-07-2022 13:25:08	-41.5
13-07-2022 13:26:08	-40.9
13-07-2022 13:27:08	-40
13-07-2022 13:28:08	-38.6
13-07-2022 13:29:08	-40.6
13-07-2022 13:30:08	-41.4
13-07-2022 13:31:08	-41.9
13-07-2022 13:32:08	-41.5
13-07-2022 13:33:08	-40.3
13-07-2022 13:34:08	-43.4
13-07-2022 13:35:08	-43.7
13-07-2022 13:36:08	-43.1
13-07-2022 13:37:08	-42.1
13-07-2022 13:38:08	-41.5
13-07-2022 13:39:08	-43.3
13-07-2022 13:40:08	-43
13-07-2022 13:41:08	-43.1
13-07-2022 13:42:08	-43.5
13-07-2022 13:43:08	-42.5
13-07-2022 13:44:08	-45.6

## Experimental readings of the heterogeneous mixture of activated alumina and Molecular Sieve 4A recorded by the dew point transmitter



ChannelName	MIN	MAX	AVG
PV_Dew_Point_Temperature_C	-48.7	19.7	-33.3

LogDateTime	PV_Dew_Point_Temperature_C
13-07-2022 14:35:57	19.7
13-07-2022 14:36:53	19.2
13-07-2022 14:37:53	19.2
13-07-2022 14:38:53	19.2
13-07-2022 14:39:53	19.2
13-07-2022 14:40:53	19.1
13-07-2022 14:41:53	19.2
13-07-2022 14:42:53	-41.9
13-07-2022 14:43:53	-41.7
13-07-2022 14:44:53	-41.4
13-07-2022 14:45:53	-41.4
13-07-2022 14:46:53	-48.4
13-07-2022 14:47:53	-48.7
13-07-2022 14:48:53	-42.4
13-07-2022 14:49:53	-41.9
13-07-2022 14:50:53	-45.2
13-07-2022 14:51:53	-46.4
13-07-2022 14:52:53	-47.2
13-07-2022 14:53:53	-47.2
13-07-2022 14:54:53	-47.6
13-07-2022 14:55:53	-45.3
13-07-2022 14:56:53	-44.9
13-07-2022 14:57:53	-45.5

13-07-2022 14:58:53	-44.4
13-07-2022 14:59:53	-44.4
13-07-2022 15:00:53	-41.1
13-07-2022 15:01:53	-42
13-07-2022 15:02:53	-41.6
13-07-2022 15:03:53	-29.6
13-07-2022 15:04:53	-41.4
13-07-2022 15:05:53	-25.7
13-07-2022 15:06:53	-36.1
13-07-2022 15:07:53	-15.5
13-07-2022 15:08:53	-44.5
13-07-2022 15:09:53	-30.9
13-07-2022 15:10:53	-40.8
13-07-2022 15:11:53	-43.2
13-07-2022 15:12:53	-37.2
13-07-2022 15:13:53	-44.1
13-07-2022 15:14:53	-27.4
13-07-2022 15:15:53	-25.1
13-07-2022 15:16:53	-46.2
13-07-2022 15:17:53	-47.1
13-07-2022 15:18:53	-34.4
13-07-2022 15:19:53	-15.4
13-07-2022 15:20:53	-41.2
13-07-2022 15:21:53	-45
13-07-2022 15:22:53	-42.8
13-07-2022 15:23:53	-42.8
13-07-2022 15:24:53	-41
13-07-2022 15:25:53	-41.3
13-07-2022 15:26:53	-42.1
13-07-2022 15:27:53	-42.1
13-07-2022 15:28:53	-42.2
13-07-2022 15:29:53	-43.6
13-07-2022 15:30:53	-42.5
13-07-2022 15:31:53	-40.9
13-07-2022 15:32:53	-40.7

**Experimental readings of testing on Molecular Sieve 4A used to train ANN**

<b>TIME</b>	<b>Process Air Out let Dew Point Temperatur e C</b>	<b>Process air Inlet Dew point temperature</b>	<b>Atmospheric relative humidity</b>	<b>Atmospheri c wet bulb temperature</b>	<b>Process Air Inlet Relative humidity</b>	<b>Process Air Inlet Wet Bulb Temperatur e</b>
14.56	7.4	7.7	30.86	18.8	28.56	18.51
15.38	6.7	7.7	30.86	18.8	28.56	18.51
16.34	-20.5	7.7	30.86	18.8	28.56	18.51
17.34	-20.5	7.7	30.86	18.8	28.56	18.51
18.34	-20.5	7.7	30.86	18.8	28.56	18.51
19.34	-20.5	7.7	30.86	18.8	28.56	18.51
20.34	-27.8	7.7	30.86	18.8	28.56	18.51
21.34	-40.6	7.7	30.86	18.8	28.56	18.51
22.34	-41.6	7.7	30.86	18.8	28.56	18.51
23.34	-43	7.7	30.86	18.8	28.56	18.51
24.34	-43	7.7	30.86	18.8	28.56	18.51
25.34	-44.1	7.7	30.86	18.8	28.56	18.51
26.34	-45.6	7.7	30.86	18.8	28.56	18.51
27.34	-47.4	7.7	30.86	18.8	28.56	18.51
28.34	-49.1	7.7	30.86	18.8	28.56	18.51
29.34	-50.4	7.7	30.86	18.8	28.56	18.51
30.34	-50.5	7.7	30.86	18.8	28.56	18.51
31.34	-50.3	7.7	30.86	18.8	28.56	18.51
32.34	-52.2	7.7	30.86	18.8	28.56	18.51
33.34	-53.6	7.7	30.86	18.8	28.56	18.51
34.34	-54.3	7.7	30.86	18.8	28.56	18.51
35.34	-53.9	7.7	30.86	18.8	28.56	18.51
36.34	-53.9	7.7	30.86	18.8	28.56	18.51
37.34	-53.7	7.7	30.86	18.8	28.56	18.51
38.34	-54.4	7.7	30.86	18.8	28.56	18.51
39.34	-55	7.7	30.86	18.8	28.56	18.51
40.34	-55.5	7.7	30.86	18.8	28.56	18.51
41.34	-54.9	7.7	30.86	18.8	28.56	18.51
42.34	-55.1	7.7	30.86	18.8	28.56	18.51
43.34	-55.1	7.7	30.86	18.8	28.56	18.51
44.34	-56.1	7.7	30.86	18.8	28.56	18.51
45.34	-54.5	7.7	30.86	18.8	28.56	18.51
46.34	-54.7	7.7	30.86	18.8	28.56	18.51
47.34	-55.5	7.7	30.86	18.8	28.56	18.51
48.34	-56.5	7.7	30.86	18.8	28.56	18.51
49.34	-57.2	7.7	30.86	18.8	28.56	18.51



50.34	-57.1	7.7	30.86	18.8	28.56	18.51
51.34	-57.6	7.7	30.86	18.8	28.56	18.51
52.34	-58.2	7.7	30.86	18.8	28.56	18.51
53.34	-59.2	7.7	30.86	18.8	28.56	18.51
54.34	-60.4	7.7	30.86	18.8	28.56	18.51
55.34	-60.6	7.7	30.86	18.8	28.56	18.51
56.34	-60.3	7.7	30.86	18.8	28.56	18.51
57.34	-60.3	7.7	30.86	18.8	28.56	18.51
58.34	-61	7.7	30.86	18.8	28.56	18.51
59.34	-60.2	7.7	30.86	18.8	28.56	18.51
60.34	-60.4	7.7	30.86	18.8	28.56	18.51
61.34	-59.6	7.7	30.86	18.8	28.56	18.51
62.34	-62.1	7.7	30.86	18.8	28.56	18.51
63.34	-63.4	7.7	30.86	18.8	28.56	18.51
64.34	-63.4	7.7	30.86	18.8	28.56	18.51
65.34	-63.4	7.7	30.86	18.8	28.56	18.51
66.34	-63.4	7.7	30.86	18.8	28.56	18.51
67.34	-63.4	7.7	30.86	18.8	28.56	18.51
68.34	-63.4	7.7	30.86	18.8	28.56	18.51
69.34	-63.4	7.7	30.86	18.8	28.56	18.51
70.34	-63.4	7.7	30.86	18.8	28.56	18.51
71.34	-63.4	7.7	30.86	18.8	28.56	18.51
72.34	-63.4	7.7	30.86	18.8	28.56	18.51
73.34	-63.4	7.7	30.86	18.8	28.56	18.51
74.34	-63.4	7.7	30.86	18.8	28.56	18.51
75.34	-63.4	7.7	30.86	18.8	28.56	18.51
76.34	-63.4	7.7	30.86	18.8	28.56	18.51
77.34	-63.4	7.7	30.86	18.8	28.56	18.51
78.34	-63.4	7.7	30.86	18.8	28.56	18.51
79.34	-63.4	7.7	30.86	18.8	28.56	18.51
80.34	-63.4	7.7	30.86	18.8	28.56	18.51
81.34	-63.4	7.7	30.86	18.8	28.56	18.51
82.34	-63.4	7.7	30.86	18.8	28.56	18.51
83.34	-63.4	7.7	30.86	18.8	28.56	18.51
84.34	-63.4	7.7	30.86	18.8	28.56	18.51
85.34	-63.4	7.7	30.86	18.8	28.56	18.51
86.34	-63.4	7.7	30.86	18.8	28.56	18.51
87.34	-63.4	7.7	30.86	18.8	28.56	18.51
88.34	-63.4	7.7	30.86	18.8	28.56	18.51
89.34	-63.4	7.7	30.86	18.8	28.56	18.51
90.34	-63.4	7.7	30.86	18.8	28.56	18.51
91.34	-63.4	7.7	30.86	18.8	28.56	18.51
92.34	-63.4	7.7	30.86	18.8	28.56	18.51
93.34	-63.4	7.7	30.86	18.8	28.56	18.51
94.34	-63.4	7.7	30.86	18.8	28.56	18.51

95.34	-63.4	7.7	30.86	18.8	28.56	18.51
96.34	-63.4	7.7	30.86	18.8	28.56	18.51
97.34	-63.4	7.7	30.86	18.8	28.56	18.51
98.34	-63.4	7.7	30.86	18.8	28.56	18.51
99.34	-63.4	7.7	30.86	18.8	28.56	18.51
100.34	-63.4	7.7	30.86	18.8	28.56	18.51
101.34	-63.4	7.7	30.86	18.8	28.56	18.51
102.34	-63.4	7.7	30.86	18.8	28.56	18.51
103.34	-63.4	7.7	30.86	18.8	28.56	18.51
104.34	-63.4	7.7	30.86	18.8	28.56	18.51
105.34	-63.4	7.7	30.86	18.8	28.56	18.51
106.34	-63.4	7.7	30.86	18.8	28.56	18.51
107.34	-63.4	7.7	30.86	18.8	28.56	18.51
108.34	-63.4	7.7	30.86	18.8	28.56	18.51
109.34	-63.4	7.7	30.86	18.8	28.56	18.51
110.34	-63.4	7.7	30.86	18.8	28.56	18.51
111.34	-63.4	7.7	30.86	18.8	28.56	18.51
112.34	-63.4	7.7	30.86	18.8	28.56	18.51
113.34	-63.4	7.7	30.86	18.8	28.56	18.51
114.34	-63.4	7.7	30.86	18.8	28.56	18.51
115.34	-63.4	7.7	30.86	18.8	28.56	18.51
116.34	-63.4	7.7	30.86	18.8	28.56	18.51
117.34	-63.4	7.7	30.86	18.8	28.56	18.51
118.34	-63.4	7.7	30.86	18.8	28.56	18.51
119.34	-63.4	7.7	30.86	18.8	28.56	18.51
120.34	-63.4	7.7	30.86	18.8	28.56	18.51
121.34	-63.4	7.7	30.86	18.8	28.56	18.51
122.34	-63.4	7.7	30.86	18.8	28.56	18.51
123.34	-63.4	7.7	30.86	18.8	28.56	18.51
124.34	-63.4	7.7	30.86	18.8	28.56	18.51
125.34	-63.4	7.7	30.86	18.8	28.56	18.51
126.34	-63.4	7.7	30.86	18.8	28.56	18.51
127.34	-63.4	7.7	30.86	18.8	28.56	18.51
128.34	-63.4	7.7	30.86	18.8	28.56	18.51
129.34	-63.4	7.7	30.86	18.8	28.56	18.51
130.34	-63.4	7.7	30.86	18.8	28.56	18.51
131.34	-63.4	7.7	30.86	18.8	28.56	18.51
132.34	-63.4	7.7	30.86	18.8	28.56	18.51
133.34	-63.4	7.7	30.86	18.8	28.56	18.51
134.34	-63.4	7.7	30.86	18.8	28.56	18.51
135.34	-63.4	7.7	30.86	18.8	28.56	18.51
136.34	-63.4	7.7	30.86	18.8	28.56	18.51
137.34	-63.4	7.7	30.86	18.8	28.56	18.51
138.34	-63.4	7.7	30.86	18.8	28.56	18.51
139.34	-63.4	7.7	30.86	18.8	28.56	18.51

140.34	-63.4	7.7	30.86	18.8	28.56	18.51
141.34	-63.4	7.7	30.86	18.8	28.56	18.51
142.34	-63.4	7.7	30.86	18.8	28.56	18.51
143.34	-63.4	7.7	30.86	18.8	28.56	18.51
144.34	-63.4	7.7	30.86	18.8	28.56	18.51
145.34	-63.4	7.7	30.86	18.8	28.56	18.51
146.34	-63.4	7.7	30.86	18.8	28.56	18.51
147.34	-63.4	7.7	30.86	18.8	28.56	18.51
148.34	-63.4	7.7	30.86	18.8	28.56	18.51
149.34	-63.4	7.7	30.86	18.8	28.56	18.51
150.34	-63.4	7.7	30.86	18.8	28.56	18.51
151.34	-63.4	7.7	30.86	18.8	28.56	18.51
152.34	-63.4	7.7	30.86	18.8	28.56	18.51
153.34	-63.4	7.7	30.86	18.8	28.56	18.51
154.34	-63.4	7.7	30.86	18.8	28.56	18.51
155.34	-63.4	7.7	30.86	18.8	28.56	18.51
156.34	-63.4	7.7	30.86	18.8	28.56	18.51
157.34	-63.4	7.7	30.86	18.8	28.56	18.51
158.34	-63.4	7.7	30.86	18.8	28.56	18.51
159.34	-63.4	7.7	30.86	18.8	28.56	18.51
160.34	-63.4	7.7	30.86	18.8	28.56	18.51
161.34	-63.4	7.7	30.86	18.8	28.56	18.51
162.34	-63.4	7.7	30.86	18.8	28.56	18.51
163.34	-63.4	7.7	30.86	18.8	28.56	18.51
164.34	-63.4	7.7	30.86	18.8	28.56	18.51
165.34	-63.4	7.7	30.86	18.8	28.56	18.51
166.34	-63.4	7.7	30.86	18.8	28.56	18.51
167.34	-63.4	7.7	30.86	18.8	28.56	18.51
168.34	-63.4	7.7	30.86	18.8	28.56	18.51
169.34	-63.4	7.7	30.86	18.8	28.56	18.51
170.34	-63.4	7.7	30.86	18.8	28.56	18.51
171.34	-63.4	7.7	30.86	18.8	28.56	18.51
172.34	-63.4	7.7	30.86	18.8	28.56	18.51
173.34	-63.4	7.7	30.86	18.8	28.56	18.51
174.34	-63.4	7.7	30.86	18.8	28.56	18.51
175.34	-63.4	7.7	30.86	18.8	28.56	18.51
176.34	-63.4	7.7	30.86	18.8	28.56	18.51
177.34	-63.4	7.7	30.86	18.8	28.56	18.51
178.34	-63.4	7.7	30.86	18.8	28.56	18.51
179.34	-63.4	7.7	30.86	18.8	28.56	18.51
180.34	-63.4	7.7	30.86	18.8	28.56	18.51
181.34	-63.4	7.7	30.86	18.8	28.56	18.51
182.34	-63.4	7.7	30.86	18.8	28.56	18.51
183.34	-63.4	7.7	30.86	18.8	28.56	18.51
184.34	-63.4	7.7	30.86	18.8	28.56	18.51

185.34	-63.4	7.7	30.86	18.8	28.56	18.51
186.34	-63.4	7.7	30.86	18.8	28.56	18.51
187.34	-63.4	7.7	30.86	18.8	28.56	18.51
188.34	-63.4	7.7	30.86	18.8	28.56	18.51
189.34	-63.4	7.7	30.86	18.8	28.56	18.51
190.34	-63.4	7.7	30.86	18.8	28.56	18.51
191.34	-63.4	7.7	30.86	18.8	28.56	18.51
192.34	-63.4	7.7	30.86	18.8	28.56	18.51
193.34	-63.4	7.7	30.86	18.8	28.56	18.51
194.34	-63.4	7.7	30.86	18.8	28.56	18.51
195.34	-63.4	7.7	30.86	18.8	28.56	18.51
196.34	-63.4	7.7	30.86	18.8	28.56	18.51
197.34	-63.4	7.7	30.86	18.8	28.56	18.51
198.34	-63.4	7.7	30.86	18.8	28.56	18.51
199.34	-63.4	7.7	30.86	18.8	28.56	18.51
200.34	-63.4	7.7	30.86	18.8	28.56	18.51
201.34	-63.4	7.7	30.86	18.8	28.56	18.51
202.34	-63.4	7.7	30.86	18.8	28.56	18.51
203.34	-63.4	7.7	30.86	18.8	28.56	18.51
204.34	-63.4	7.7	30.86	18.8	28.56	18.51
205.34	-63.4	7.7	30.86	18.8	28.56	18.51
206.34	-63.4	7.7	30.86	18.8	28.56	18.51
207.34	-63.4	7.7	30.86	18.8	28.56	18.51
208.34	-63.4	7.7	30.86	18.8	28.56	18.51
209.34	-63.4	7.7	30.86	18.8	28.56	18.51
210.34	-63.4	7.7	30.86	18.8	28.56	18.51
211.34	-63.4	7.7	30.86	18.8	28.56	18.51
212.34	-63.4	7.7	30.86	18.8	28.56	18.51
213.34	-63.4	7.7	30.86	18.8	28.56	18.51
214.34	-63.4	7.7	30.86	18.8	28.56	18.51
215.34	-63.4	7.7	30.86	18.8	28.56	18.51
216.34	-63.4	7.7	30.86	18.8	28.56	18.51
217.34	-63.4	7.7	30.86	18.8	28.56	18.51
218.34	-63.4	7.7	30.86	18.8	28.56	18.51
219.34	-63.4	7.7	30.86	18.8	28.56	18.51
220.34	-63.4	7.7	30.86	18.8	28.56	18.51
221.34	-63.4	7.7	30.86	18.8	28.56	18.51
222.34	-63.4	7.7	30.86	18.8	28.56	18.51
223.34	-63.4	7.7	30.86	18.8	28.56	18.51
224.34	-63.4	7.7	30.86	18.8	28.56	18.51
225.34	-63.4	7.7	30.86	18.8	28.56	18.51
226.34	-63.4	7.7	30.86	18.8	28.56	18.51
227.34	-63.4	7.7	30.86	18.8	28.56	18.51
228.34	-63.4	7.7	30.86	18.8	28.56	18.51
229.34	-63.4	7.7	30.86	18.8	28.56	18.51

230.34	-63.4	7.7	30.86	18.8	28.56	18.51
231.34	-63.4	7.7	30.86	18.8	28.56	18.51
232.34	-63.4	7.7	30.86	18.8	28.56	18.51
233.34	-63.4	7.7	30.86	18.8	28.56	18.51
234.34	-63.4	7.7	30.86	18.8	28.56	18.51
235.34	-63.4	7.7	30.86	18.8	28.56	18.51
236.34	-63.4	7.7	30.86	18.8	28.56	18.51
237.34	-63.4	7.7	30.86	18.8	28.56	18.51
238.34	-63.4	7.7	30.86	18.8	28.56	18.51
239.34	-63.4	7.7	30.86	18.8	28.56	18.51
240.34	-63.4	7.7	30.86	18.8	28.56	18.51
241.34	-63.4	7.7	30.86	18.8	28.56	18.51
242.34	-63.4	7.7	30.86	18.8	28.56	18.51
243.34	-63.4	7.7	30.86	18.8	28.56	18.51
244.34	-63.4	7.7	30.86	18.8	28.56	18.51
245.34	-63.4	7.7	30.86	18.8	28.56	18.51
246.34	-63.4	7.7	30.86	18.8	28.56	18.51
247.34	-63.4	7.7	30.86	18.8	28.56	18.51
248.34	-63.4	7.7	30.86	18.8	28.56	18.51
249.34	-63.4	7.7	30.86	18.8	28.56	18.51
250.34	-63.4	7.7	30.86	18.8	28.56	18.51
251.34	-63.4	7.7	30.86	18.8	28.56	18.51
252.34	-63.4	7.7	30.86	18.8	28.56	18.51
253.34	-63.4	7.7	30.86	18.8	28.56	18.51
254.34	-63.4	7.7	30.86	18.8	28.56	18.51
255.34	-63.4	7.7	30.86	18.8	28.56	18.51
256.34	-63.4	7.7	30.86	18.8	28.56	18.51
257.34	-63.4	7.7	30.86	18.8	28.56	18.51
258.34	-63.4	7.7	30.86	18.8	28.56	18.51
259.34	-63.4	7.7	30.86	18.8	28.56	18.51
260.34	-63.4	7.7	30.86	18.8	28.56	18.51
261.34	-63.4	7.7	30.86	18.8	28.56	18.51
262.34	-63.4	7.7	30.86	18.8	28.56	18.51
263.34	-63.4	7.7	30.86	18.8	28.56	18.51
264.34	-63.4	7.7	30.86	18.8	28.56	18.51
265.34	-63.4	7.7	30.86	18.8	28.56	18.51
266.34	-63.4	7.7	30.86	18.8	28.56	18.51
267.34	-63.4	7.7	30.86	18.8	28.56	18.51
268.34	-63.4	7.7	30.86	18.8	28.56	18.51
269.34	-63.4	7.7	30.86	18.8	28.56	18.51
270.34	-63.4	7.7	30.86	18.8	28.56	18.51
271.34	-63.4	7.7	30.86	18.8	28.56	18.51
272.34	-63.4	7.7	30.86	18.8	28.56	18.51
273.34	-63.4	7.7	30.86	18.8	28.56	18.51
274.34	-63.4	7.7	30.86	18.8	28.56	18.51

275.34	-63.4	7.7	30.86	18.8	28.56	18.51
276.34	-63.4	7.7	30.86	18.8	28.56	18.51
277.34	-63.4	7.7	30.86	18.8	28.56	18.51
278.34	-63.4	7.7	30.86	18.8	28.56	18.51
279.34	-63.4	7.7	30.86	18.8	28.56	18.51
280.34	-63.4	7.7	30.86	18.8	28.56	18.51
281.34	-63.4	7.7	30.86	18.8	28.56	18.51
282.34	-63.4	7.7	30.86	18.8	28.56	18.51
283.34	-63.4	7.7	30.86	18.8	28.56	18.51
284.34	-63.4	7.7	30.86	18.8	28.56	18.51
285.34	-63.4	7.7	30.86	18.8	28.56	18.51
286.34	-63.4	7.7	30.86	18.8	28.56	18.51
287.34	-63.4	7.7	30.86	18.8	28.56	18.51
288.34	-63.4	7.7	30.86	18.8	28.56	18.51
289.34	-63.4	7.7	30.86	18.8	28.56	18.51
290.34	-63.4	7.7	30.86	18.8	28.56	18.51
291.34	-63.4	7.7	30.86	18.8	28.56	18.51
292.34	-63.4	7.7	30.86	18.8	28.56	18.51
293.34	-63.4	7.7	30.86	18.8	28.56	18.51
294.34	-63.4	7.7	30.86	18.8	28.56	18.51
295.34	-63.4	7.7	30.86	18.8	28.56	18.51
296.34	-63.4	7.7	30.86	18.8	28.56	18.51
297.34	-63.4	7.7	30.86	18.8	28.56	18.51
298.34	-63.4	7.7	30.86	18.8	28.56	18.51
299.34	-63.4	7.7	30.86	18.8	28.56	18.51
300.34	-63.4	7.7	30.86	18.8	28.56	18.51
301.34	-63.4	7.7	30.86	18.8	28.56	18.51
302.34	-63.4	7.7	30.86	18.8	28.56	18.51
303.34	-63.4	7.7	30.86	18.8	28.56	18.51
304.34	-63.4	7.7	30.86	18.8	28.56	18.51
305.34	-63.4	7.7	30.86	18.8	28.56	18.51
306.34	-63.4	7.7	30.86	18.8	28.56	18.51
307.34	-63.4	7.7	30.86	18.8	28.56	18.51
308.34	-63.4	7.7	30.86	18.8	28.56	18.51
309.34	-63.4	7.7	30.86	18.8	28.56	18.51
310.34	-63.4	7.7	30.86	18.8	28.56	18.51
311.34	-63.4	7.7	30.86	18.8	28.56	18.51
312.34	-63.4	7.7	30.86	18.8	28.56	18.51
313.34	-63.4	7.7	30.86	18.8	28.56	18.51
314.34	-63.4	7.7	30.86	18.8	28.56	18.51
315.34	-63.4	7.7	30.86	18.8	28.56	18.51
316.34	-63.4	7.7	30.86	18.8	28.56	18.51
317.34	-63.4	7.7	30.86	18.8	28.56	18.51
318.34	-63.4	7.7	30.86	18.8	28.56	18.51
319.34	-63.4	7.7	30.86	18.8	28.56	18.51

320.34	-63.4	7.7	30.86	18.8	28.56	18.51
321.34	-63.4	7.7	30.86	18.8	28.56	18.51
322.34	-63.4	7.7	30.86	18.8	28.56	18.51
323.34	-63.4	7.7	30.86	18.8	28.56	18.51
324.34	-63.4	7.7	30.86	18.8	28.56	18.51
325.34	-63.4	7.7	30.86	18.8	28.56	18.51
326.34	-63.4	7.7	30.86	18.8	28.56	18.51
327.34	-63.4	7.7	30.86	18.8	28.56	18.51
328.34	-63.4	7.7	30.86	18.8	28.56	18.51
329.34	-63.4	7.7	30.86	18.8	28.56	18.51
330.34	-63.4	7.7	30.86	18.8	28.56	18.51
331.34	-63.4	7.7	30.86	18.8	28.56	18.51
332.34	-63.4	7.7	30.86	18.8	28.56	18.51
333.34	-63.4	7.7	30.86	18.8	28.56	18.51
334.34	-63.4	7.7	30.86	18.8	28.56	18.51
335.34	-63.4	7.7	30.86	18.8	28.56	18.51
336.34	-63.4	7.7	30.86	18.8	28.56	18.51
337.34	-63.4	7.7	30.86	18.8	28.56	18.51
338.34	-63.4	7.7	30.86	18.8	28.56	18.51
339.34	-63.4	7.7	30.86	18.8	28.56	18.51
340.34	-63.4	7.7	30.86	18.8	28.56	18.51
341.34	-63.4	7.7	30.86	18.8	28.56	18.51
342.34	-63.4	7.7	30.86	18.8	28.56	18.51
343.34	-63.4	7.7	30.86	18.8	28.56	18.51
344.34	-63.4	7.7	30.86	18.8	28.56	18.51
345.34	-63.4	7.7	30.86	18.8	28.56	18.51
346.34	-63.4	7.7	30.86	18.8	28.56	18.51
347.34	-63.4	7.7	30.86	18.8	28.56	18.51
348.34	-63.4	7.7	30.86	18.8	28.56	18.51
349.34	-63.4	7.7	30.86	18.8	28.56	18.51
350.34	-63.4	7.7	30.86	18.8	28.56	18.51
351.34	-63.4	7.7	30.86	18.8	28.56	18.51
352.34	-63.4	7.7	30.86	18.8	28.56	18.51
353.34	-63.4	7.7	30.86	18.8	28.56	18.51
354.34	-63.4	7.7	30.86	18.8	28.56	18.51
355.34	-63.4	7.7	30.86	18.8	28.56	18.51
356.34	-63.4	7.7	30.86	18.8	28.56	18.51
357.34	-63.4	7.7	30.86	18.8	28.56	18.51
358.34	-63.4	7.7	30.86	18.8	28.56	18.51
359.34	-63.4	7.7	30.86	18.8	28.56	18.51
360.34	-63.4	7.7	30.86	18.8	28.56	18.51
361.34	-63.4	7.7	30.86	18.8	28.56	18.51
362.34	-63.4	7.7	30.86	18.8	28.56	18.51
363.34	-63.4	7.7	30.86	18.8	28.56	18.51
364.34	-63.4	7.7	30.86	18.8	28.56	18.51

365.34	-63.4	7.7	30.86	18.8	28.56	18.51
366.34	-63.4	7.7	30.86	18.8	28.56	18.51
367.34	-63.4	7.7	30.86	18.8	28.56	18.51
368.34	-63.4	7.7	30.86	18.8	28.56	18.51
369.34	-63.4	7.7	30.86	18.8	28.56	18.51
370.34	-63.4	7.7	30.86	18.8	28.56	18.51
371.34	-63.4	7.7	30.86	18.8	28.56	18.51
372.34	-63.4	7.7	30.86	18.8	28.56	18.51
373.34	-63.4	7.7	30.86	18.8	28.56	18.51
374.34	-63.4	7.7	30.86	18.8	28.56	18.51
375.34	-63.4	7.7	30.86	18.8	28.56	18.51
376.34	-63.4	7.7	30.86	18.8	28.56	18.51
377.34	-63.4	7.7	30.86	18.8	28.56	18.51
378.34	-63.4	7.7	30.86	18.8	28.56	18.51
379.34	-63.4	7.7	30.86	18.8	28.56	18.51
380.34	-63.4	7.7	30.86	18.8	28.56	18.51
381.34	-63.4	7.7	30.86	18.8	28.56	18.51
382.34	-63.4	7.7	30.86	18.8	28.56	18.51
383.34	-63.4	7.7	30.86	18.8	28.56	18.51
384.34	-63.4	7.7	30.86	18.8	28.56	18.51
385.34	-63.4	7.7	30.86	18.8	28.56	18.51
386.34	-63.4	7.7	30.86	18.8	28.56	18.51
387.34	-63.4	7.7	30.86	18.8	28.56	18.51
388.34	-63.4	7.7	30.86	18.8	28.56	18.51
389.34	-63.4	7.7	30.86	18.8	28.56	18.51
390.34	-63.4	7.7	30.86	18.8	28.56	18.51
391.34	-63.4	7.7	30.86	18.8	28.56	18.51
392.34	-63.4	7.7	30.86	18.8	28.56	18.51
393.34	-63.4	7.7	30.86	18.8	28.56	18.51
394.34	-63.4	7.7	30.86	18.8	28.56	18.51
395.34	-63.4	7.7	30.86	18.8	28.56	18.51
396.34	-63.4	7.7	30.86	18.8	28.56	18.51
397.34	-63.4	7.7	30.86	18.8	28.56	18.51
398.34	-63.4	7.7	30.86	18.8	28.56	18.51
399.34	-63.4	7.7	30.86	18.8	28.56	18.51
400.34	-63.4	7.7	30.86	18.8	28.56	18.51
401.34	-63.4	7.7	30.86	18.8	28.56	18.51
402.34	-63.4	7.7	30.86	18.8	28.56	18.51
403.34	-63.4	7.7	30.86	18.8	28.56	18.51
404.34	-63.4	7.7	30.86	18.8	28.56	18.51
405.34	-63.4	7.7	30.86	18.8	28.56	18.51
406.34	-63.4	7.7	30.86	18.8	28.56	18.51
407.34	-63.4	7.7	30.86	18.8	28.56	18.51
408.34	-63.4	7.7	30.86	18.8	28.56	18.51
409.34	-63.4	7.7	30.86	18.8	28.56	18.51



410.34	-63.4	7.7	30.86	18.8	28.56	18.51
411.34	-63.4	7.7	30.86	18.8	28.56	18.51
412.34	-63.4	7.7	30.86	18.8	28.56	18.51
413.34	-63.4	7.7	30.86	18.8	28.56	18.51
414.34	-63.4	7.7	30.86	18.8	28.56	18.51
415.34	-63.4	7.7	30.86	18.8	28.56	18.51
416.34	-63.4	7.7	30.86	18.8	28.56	18.51
417.34	-63.4	7.7	30.86	18.8	28.56	18.51
418.34	-63.4	7.7	30.86	18.8	28.56	18.51
419.34	-63.4	7.7	30.86	18.8	28.56	18.51
420.34	-63.4	7.7	30.86	18.8	28.56	18.51
421.34	-63.4	7.7	30.86	18.8	28.56	18.51
422.34	-63.4	7.7	30.86	18.8	28.56	18.51
423.34	-63.4	7.7	30.86	18.8	28.56	18.51
424.34	-63.4	7.7	30.86	18.8	28.56	18.51
425.34	-63.4	7.7	30.86	18.8	28.56	18.51
426.34	-63.4	7.7	30.86	18.8	28.56	18.51
427.34	-63.4	7.7	30.86	18.8	28.56	18.51
428.34	-63.4	7.7	30.86	18.8	28.56	18.51
429.34	-63.4	7.7	30.86	18.8	28.56	18.51
430.34	-63.4	7.7	30.86	18.8	28.56	18.51
431.34	-63.4	7.7	30.86	18.8	28.56	18.51
432.34	-63.4	7.7	30.86	18.8	28.56	18.51
433.34	-63.4	7.7	30.86	18.8	28.56	18.51
434.34	-63.4	7.7	30.86	18.8	28.56	18.51
435.34	-63.4	7.7	30.86	18.8	28.56	18.51
436.34	-63.4	7.7	30.86	18.8	28.56	18.51
437.34	-63.4	7.7	30.86	18.8	28.56	18.51
438.34	-63.4	7.7	30.86	18.8	28.56	18.51
439.34	-63.4	7.7	30.86	18.8	28.56	18.51
440.34	-63.4	7.7	30.86	18.8	28.56	18.51
441.34	-63.4	7.7	30.86	18.8	28.56	18.51
442.34	-63.4	7.7	30.86	18.8	28.56	18.51
443.34	-63.4	7.7	30.86	18.8	28.56	18.51
444.34	-63.4	7.7	30.86	18.8	28.56	18.51
445.34	-63.4	7.7	30.86	18.8	28.56	18.51
446.34	-63.4	7.7	30.86	18.8	28.56	18.51
447.34	-63.4	7.7	30.86	18.8	28.56	18.51
448.34	-63.4	7.7	30.86	18.8	28.56	18.51
449.34	-63.4	7.7	30.86	18.8	28.56	18.51
450.34	-63.4	7.7	30.86	18.8	28.56	18.51
451.34	-63.4	7.7	30.86	18.8	28.56	18.51
452.34	-63.4	7.7	30.86	18.8	28.56	18.51
453.34	-63.4	7.7	30.86	18.8	28.56	18.51
454.34	-63.4	7.7	30.86	18.8	28.56	18.51

455.34	-63.4	7.7	30.86	18.8	28.56	18.51
456.34	-63.4	7.7	30.86	18.8	28.56	18.51
457.34	-63.4	7.7	30.86	18.8	28.56	18.51
458.34	-63.4	7.7	30.86	18.8	28.56	18.51
459.34	-63.4	7.7	30.86	18.8	28.56	18.51
460.34	-63.4	7.7	30.86	18.8	28.56	18.51
461.34	-63.4	7.7	30.86	18.8	28.56	18.51
462.34	-63.4	7.7	30.86	18.8	28.56	18.51
463.34	-63.4	7.7	30.86	18.8	28.56	18.51
464.34	-63.4	7.7	30.86	18.8	28.56	18.51
465.34	-63.4	7.7	30.86	18.8	28.56	18.51
466.34	-63.4	7.7	30.86	18.8	28.56	18.51
467.34	-63.4	7.7	30.86	18.8	28.56	18.51
468.34	-63.4	7.7	30.86	18.8	28.56	18.51
469.34	-63.4	7.7	30.86	18.8	28.56	18.51
470.34	-63.4	7.7	30.86	18.8	28.56	18.51
471.34	-63.4	7.7	30.86	18.8	28.56	18.51
472.34	-63.4	7.7	30.86	18.8	28.56	18.51
473.34	-63.4	7.7	30.86	18.8	28.56	18.51
474.34	-63.4	7.7	30.86	18.8	28.56	18.51
475.34	-63.4	7.7	30.86	18.8	28.56	18.51
476.34	-63.4	7.7	30.86	18.8	28.56	18.51
477.34	-63.4	7.7	30.86	18.8	28.56	18.51
478.34	-63.4	7.7	30.86	18.8	28.56	18.51
479.34	-63.4	7.7	30.86	18.8	28.56	18.51
480.34	-63.4	7.7	30.86	18.8	28.56	18.51
481.34	-63.4	7.7	30.86	18.8	28.56	18.51
482.34	-63.4	7.7	30.86	18.8	28.56	18.51
483.34	-63.4	7.7	30.86	18.8	28.56	18.51
484.34	-63.4	7.7	30.86	18.8	28.56	18.51
485.34	-63.4	7.7	30.86	18.8	28.56	18.51
486.34	-63.4	7.7	30.86	18.8	28.56	18.51
487.34	-63.4	7.7	30.86	18.8	28.56	18.51
488.34	-63.4	7.7	30.86	18.8	28.56	18.51
489.34	-63.4	7.7	30.86	18.8	28.56	18.51
490.34	-63.4	7.7	30.86	18.8	28.56	18.51
491.34	-63.4	7.7	30.86	18.8	28.56	18.51
492.34	-63.4	7.7	30.86	18.8	28.56	18.51
493.34	-63.4	7.7	30.86	18.8	28.56	18.51
494.34	-63.4	7.7	30.86	18.8	28.56	18.51
495.34	-63.4	7.7	30.86	18.8	28.56	18.51
496.34	-63.4	7.7	30.86	18.8	28.56	18.51
497.34	-63.4	7.7	30.86	18.8	28.56	18.51
498.34	-63.4	7.7	30.86	18.8	28.56	18.51
499.34	-63.4	7.7	30.86	18.8	28.56	18.51

500.34	-63.4	7.7	30.86	18.8	28.56	18.51
501.34	-63.4	7.7	30.86	18.8	28.56	18.51
502.34	-63.4	7.7	30.86	18.8	28.56	18.51
503.34	-63.4	7.7	30.86	18.8	28.56	18.51
504.34	-63.4	7.7	30.86	18.8	28.56	18.51
505.34	-63.4	7.7	30.86	18.8	28.56	18.51
506.34	-63.4	7.7	30.86	18.8	28.56	18.51
507.34	-63.4	7.7	30.86	18.8	28.56	18.51
508.34	-63.4	7.7	30.86	18.8	28.56	18.51
509.34	-63.4	7.7	30.86	18.8	28.56	18.51
510.34	-63.4	7.7	30.86	18.8	28.56	18.51
511.34	-63.4	7.7	30.86	18.8	28.56	18.51
512.34	-63.4	7.7	30.86	18.8	28.56	18.51
513.34	-63.4	7.7	30.86	18.8	28.56	18.51
514.34	-63.4	7.7	30.86	18.8	28.56	18.51
515.34	-63.4	7.7	30.86	18.8	28.56	18.51
516.34	-63.4	7.7	30.86	18.8	28.56	18.51
517.34	-63.4	7.7	30.86	18.8	28.56	18.51
518.34	-63.4	7.7	30.86	18.8	28.56	18.51
519.34	-63.4	7.7	30.86	18.8	28.56	18.51
520.34	-63.4	7.7	30.86	18.8	28.56	18.51
521.34	-63.4	7.7	30.86	18.8	28.56	18.51
522.34	-63.4	7.7	30.86	18.8	28.56	18.51
523.34	-63.4	7.7	30.86	18.8	28.56	18.51
524.34	-63.4	7.7	30.86	18.8	28.56	18.51
525.34	-63.4	7.7	30.86	18.8	28.56	18.51
526.34	-63.4	7.7	30.86	18.8	28.56	18.51
527.34	-63.4	7.7	30.86	18.8	28.56	18.51
528.34	-63.4	7.7	30.86	18.8	28.56	18.51
529.34	-63.4	7.7	30.86	18.8	28.56	18.51
530.34	-63.4	7.7	30.86	18.8	28.56	18.51
531.34	-63.4	7.7	30.86	18.8	28.56	18.51
532.34	-63.4	7.7	30.86	18.8	28.56	18.51
533.34	-63.4	7.7	30.86	18.8	28.56	18.51
534.34	-63.4	7.7	30.86	18.8	28.56	18.51
535.34	-63.4	7.7	30.86	18.8	28.56	18.51
536.34	-63.4	7.7	30.86	18.8	28.56	18.51
537.34	-63.4	7.7	30.86	18.8	28.56	18.51
538.34	-63.4	7.7	30.86	18.8	28.56	18.51
539.34	-63.4	7.7	30.86	18.8	28.56	18.51
540.34	-63.4	7.7	30.86	18.8	28.56	18.51
541.34	-63.4	7.7	30.86	18.8	28.56	18.51
542.34	-63.4	7.7	30.86	18.8	28.56	18.51
543.34	-63.4	7.7	30.86	18.8	28.56	18.51
544.34	-63.4	7.7	30.86	18.8	28.56	18.51

545.34	-63.4	7.7	30.86	18.8	28.56	18.51
546.34	-63.4	7.7	30.86	18.8	28.56	18.51
547.34	-63.4	7.7	30.86	18.8	28.56	18.51
548.34	-63.4	7.7	30.86	18.8	28.56	18.51
549.34	-63.4	7.7	30.86	18.8	28.56	18.51
550.34	-63.4	7.7	30.86	18.8	28.56	18.51
551.34	-63.4	7.7	30.86	18.8	28.56	18.51
552.34	-63.4	7.7	30.86	18.8	28.56	18.51
553.34	-63.4	7.7	30.86	18.8	28.56	18.51
554.34	-63.4	7.7	30.86	18.8	28.56	18.51
555.34	-63.4	7.7	30.86	18.8	28.56	18.51
556.34	-63.4	7.7	30.86	18.8	28.56	18.51
557.34	-63.4	7.7	30.86	18.8	28.56	18.51
558.34	-63.4	7.7	30.86	18.8	28.56	18.51
559.34	-63.4	7.7	30.86	18.8	28.56	18.51
560.34	-63.4	7.7	30.86	18.8	28.56	18.51
561.34	-63.4	7.7	30.86	18.8	28.56	18.51
562.34	-63.4	7.7	30.86	18.8	28.56	18.51

### Experimental readings of testing on silica gel used to train ANN

SL no.	Time	Inlet Dry Bulb Temp	Outlet Dew point Temperature	Inlet Relative humidity	Inlet wet bulb temperature	Outlet relative humidity	Moisture Removal	Effectiveness
1	4:58:03	31	-18.5	28.4	14.6	15.01	22.4952	47.147
2	04:58:59	31	-20.6	28.4	14.6	15.01	22.4952	47.14
3	04:59:59	31	-20.5	28.4	14.6	15.01	22.4952	47.14
4	05:00:34	31	-20.6	28.4	14.6	15.01	22.4952	47.14
5	05:01:30	31	-20.5	28.4	14.6	15.01	22.4952	47.14
6	05:02:30	31	-20.5	28.4	14.6	15.01	22.4952	47.14
7	05:03:30	31	-38.7	28.4	14.6	15.01	22.4952	47.14
8	05:04:30	31	-39.5	28.4	14.6	15.01	22.4952	47.14
9	05:05:30	31	-40.2	28.4	14.6	15.01	22.4952	47.14
10	05:06:30	31	-40.3	28.4	14.6	15.01	22.4952	47.14
11	05:07:30	31	-42.3	28.4	14.6	15.01	22.4952	47.14
12	5:08:30	31	-42.4	28.4	14.6	15.01	22.4952	47.14
13	05:09:30	31	-44.1	28.4	14.6	15.01	22.4952	47.14
14	05:10:30	31	-44.8	28.4	14.6	15.01	22.4952	47.14
15	05:11:30	31	-45.1	28.4	14.6	15.01	22.4952	47.14
16	05:12:30	31	-45	28.4	14.6	15.01	22.4952	47.14
17	05:13:30	31.50	-45.7	28.4	14.6	15.01	22.4952	47.14

18	05:14:30	31.50	-46.6	28.4	14.6	15.01	22.4952	47.14
19	05:15:30	31.50	-47.3	28.4	14.6	15.01	22.4952	47.14
20	05:16:30	31.50	-47.1	28.4	14.6	15.01	22.4952	47.14
21	05:17:30	31.50	-46.7	28.4	14.6	15.01	22.4952	47.14
22	05:18:30	31.50	-46.7	28.4	14.6	15.01	22.4952	47.14
23	05:19:30	31.50	-47.6	28.4	14.6	15.01	22.4952	47.14
24	05:20:30	31.50	-48.7	28.4	14.6	15.01	22.4952	47.14
25	05:21:30	31.50	-49.5	28.4	14.6	15.01	22.4952	47.14
26	05:22:30	31.50	-49.9	28.4	14.6	15.01	22.4952	47.14
27	05:23:30	31.50	-49.4	28.4	14.6	15.01	22.4952	47.14
28	05:24:30	31.50	-49.5	28.4	14.6	15.01	22.4952	47.14
29	05:25:30	31.50	-49	28.4	14.6	15.01	22.4952	47.14
30	05:26:30	31.50	-48.9	28.41	14.61	15.02	22.4952	47.131
31	05:27:30	31.50	-48.9	28.41	14.61	15.02	22.4952	47.131
32	05:28:30	31.50	-50.5	28.41	14.61	15.02	22.4952	47.131
33	05:29:30	31.50	-51.2	28.41	14.61	15.02	22.4952	47.131
34	05:30:30	31.50	-51.5	28.41	14.61	15.02	22.4952	47.131
35	05:31:30	31.50	-51.4	28.41	14.61	15.02	22.4952	47.131
36	05:32:30	31.50	-49.4	28.41	14.61	15.02	22.4952	47.131
37	05:33:30	31.50	-50.3	28.41	14.61	15.02	22.4952	47.131
38	05:34:30	31.50	-51.1	28.41	14.61	15.02	22.4952	47.131
39	05:35:30	31.50	-51.1	28.42	14.62	15.02	22.512	47.149
40	05:36:30	31.50	-50.6	28.42	14.62	15.01	22.5288	47.185
41	05:37:30	31.50	-49.6	28.42	14.62	15.02	22.512	47.149
42	05:38:30	31.50	-50.4	28.42	14.62	15.02	22.512	47.149
43	05:39:30	31.50	-51.5	28.42	14.62	15.02	22.512	47.149
44	05:40:30	31.50	-52.5	28.42	14.62	15.02	22.512	47.149
45	05:41:30	31.50	-53.3	28.43	14.63	15.02	22.5288	47.16
46	05:42:30	31.50	-52.5	28.43	14.63	15.02	22.5288	47.16
47	05:43:30	31.50	-52.6	28.43	14.63	15.02	22.5288	47.16
48	05:44:30	31.50	-52.3	28.43	14.63	15.02	22.5288	47.16
49	05:45:30	31.50	-51.7	28.43	14.63	15.02	22.5288	47.16
50	05:46:30	31.50	-51.3	28.43	14.63	15.02	22.5288	47.16
51	05:47:30	31.50	-52.4	28.43	14.63	15.02	22.5288	47.16
52	05:48:30	31.50	-53.9	28.43	14.63	15.02	22.5288	47.16
53	05:49:30	31.50	-54.7	28.43	14.63	15.03	22.512	47.13
54	05:50:30	31.50	-54.9	28.43	14.63	15.03	22.512	47.13
55	05:51:30	31.50	-54.7	28.43	14.63	15.03	22.512	47.13
56	05:52:30	31.50	-53.9	28.44	14.64	15.03	22.5288	47.15
57	05:53:30	31.50	-54	28.44	14.64	15.03	22.5288	47.15
58	05:54:30	31.50	-53.9	28.44	14.64	15.03	22.5288	47.15
59	05:55:30	31.50	-53.4	28.44	14.64	15.03	22.5288	47.15
60	05:56:30	31.50	-53.7	28.44	14.64	15.03	22.5288	47.15
61	05:57:30	31.50	-54.4	28.44	14.64	15.04	22.512	47.11
62	05:58:30	31.50	-55.7	28.44	14.64	15.04	22.512	47.114

63	05:59:30	31.50	-56.3	28.44	14.64	15.04	22.512	47.114
64	06:00:30	31.50	-56.2	28.44	14.64	15.04	22.512	47.114
65	06:01:30	31.50	-56	28.45	14.65	15.04	22.5288	47.135
66	06:02:30	31.50	-52.9	28.45	14.65	15.04	22.5288	47.135
67	06:03:30	31.50	-50.5	28.45	14.65	15.04	22.5288	47.135
68	06:04:30	31.50	-49.8	28.45	14.65	15.04	22.5288	47.135
69	06:05:30	31.50	-45.8	28.45	14.65	15.04	22.5288	47.135
70	06:06:30	31.50	-48.4	28.45	14.65	15.05	22.512	47.10
71	06:07:30	31.50	-52.2	28.45	14.65	15.05	22.512	47.10
72	06:08:30	31.50	-52.9	28.45	14.65	15.05	22.512	47.10
73	06:09:30	31.50	-52.7	28.45	14.65	15.05	22.512	47.10
74	06:10:30	31.50	-52.1	28.45	14.65	15.05	22.512	47.10
75	06:11:30	31.50	-52	28.45	14.65	15.05	22.512	47.10
76	06:12:30	31.50	-53.1	28.45	14.65	15.05	22.512	47.10
77	06:13:30	31.50	-53.2	28.46	14.66	15.05	22.5288	47.12
78	06:14:30	31.50	-52.6	28.46	14.66	15.05	22.5288	47.12
79	06:15:30	31.50	-52.2	28.46	14.66	15.05	22.5288	47.12
80	06:16:30	31.50	-51.8	28.46	14.66	15.06	22.512	47.08
81	06:17:30	31.50	-52.9	28.46	14.66	15.05	22.5288	47.12
82	06:18:30	31.50	-51.5	28.47	14.67	15.05	22.5456	47.14
83	06:19:30	31.50	-50.6	28.47	14.67	15.05	22.5456	47.14
84	06:20:30	31.50	-50.6	28.47	14.67	15.05	22.5456	47.14
85	06:21:30	31.50	-50.6	28.47	14.67	15.05	22.5456	47.14
86	06:22:30	31.50	-50.6	28.47	14.67	15.06	22.5288	47.10
87	06:23:30	31.50	-50.6	28.48	14.68	15.06	22.5456	47.12
88	06:24:30	31.50	-50.6	28.48	14.68	15.06	22.5456	47.12
89	06:25:30	31.50	-51.5	28.48	14.68	15.06	22.5456	47.12
90	06:26:30	32.00	-51.8	28.48	14.68	15.06	22.5456	47.12
91	06:27:30	32.00	-50.5	28.48	14.68	15.06	22.5456	47.12
92	06:28:30	32.00	-51.1	28.48	14.68	15.06	22.5456	47.12
93	06:29:30	32.00	-51.1	28.48	14.68	15.06	22.5456	47.12
94	06:30:30	32.00	-50.6	28.49	14.69	15.06	22.5624	47.14
95	06:31:30	32.00	-50.6	28.49	14.69	15.04	22.596	47.21
96	06:32:30	32.00	-52.2	28.49	14.69	15.06	22.5624	47.14
97	06:33:30	32.00	-51.8	28.49	14.69	15.06	22.5624	47.14
98	06:34:30	32.00	-52.9	28.49	14.69	15.07	22.5456	47.10
99	06:35:30	32.00	-51.5	28.49	14.69	15.07	22.5456	47.10
100	06:36:30	32.00	-53.1	28.49	14.69	15.07	22.5456	47.10
101	06:37:30	32.00	-53.2	28.49	14.69	15.07	22.5456	47.10
102	06:38:30	32.00	-53.2	28.49	14.69	15.07	22.5456	47.10
103	06:39:30	32.00	-53.2	28.49	14.69	15.06	22.5624	47.14
104	06:40:30	32.00	-53.2	28.5	14.7	15.08	22.5456	47.09
105	06:41:30	32.00	-53.2	28.5	14.7	15.08	22.5456	47.09
106	06:42:30	32.00	-53.2	28.5	14.7	15.08	22.5456	47.09
107	06:43:30	32.00	-53.2	28.5	14.7	15.08	22.5456	47.09

108	06:44:30	32.00	-53.2	28.5	14.7	15.08	22.5456	47.09
109	06:45:30	32.00	-53.2	28.5	14.7	15.08	22.5456	47.09
110	06:46:30	32.00	-53.2	28.51	14.71	15.08	22.5624	47.11
111	06:47:30	32.00	-53.2	28.51	14.71	15.08	22.5624	47.11
112	06:48:30	32.00	-53.2	28.51	14.71	15.08	22.5624	47.11
113	06:49:30	32.00	-53.2	28.51	14.71	15.08	22.5624	47.11
114	06:50:30	32.00	-53.2	28.51	14.71	15.08	22.5624	47.11
115	06:51:30	32.00	-53.2	28.51	14.71	15.08	22.5624	47.11
116	06:52:30	32.00	-53.2	28.51	14.71	15.09	22.5456	47.07
117	06:53:30	32.00	-53.2	28.52	14.72	15.09	22.5624	47.09
118	06:54:30	32.00	-53.2	28.52	14.72	15.09	22.5624	47.09
119	06:55:30	32.00	-53.2	28.52	14.72	15.09	22.5624	47.09
120	06:56:30	32.00	-52.2	28.52	14.72	15.07	22.596	47.16
121	06:57:30	32.00	-52.2	28.52	14.72	15.09	22.5624	47.09
122	06:58:30	32.00	-51.8	28.52	14.72	15.09	22.5624	47.09
123	06:59:30	32.00	-51.4	28.52	14.72	15.09	22.5624	47.09
124	07:00:30	32.00	-51	28.53	14.73	15.09	22.5792	47.11
125	07:01:30	32.00	-50.6	28.53	14.73	15.1	22.5624	47.07
126	07:02:30	32.00	-50.2	28.53	14.73	15.1	22.5624	47.07
127	07:03:30	32.00	-50.2	28.53	14.73	15.1	22.5624	47.07
128	07:04:30	32.00	-50.2	28.53	14.73	15.1	22.5624	47.07
129	07:05:30	32.00	-50.2	28.53	14.73	15.1	22.5624	47.07
130	07:06:30	32.00	-50.2	28.53	14.73	15.1	22.5624	47.07
131	07:07:30	32.00	-50.2	28.53	14.73	15.12	22.5288	47.00
132	07:08:30	32.00	-50.2	28.53	14.73	15.12	22.5288	47.00
133	07:09:30	32.00	-50.2	28.53	14.73	15.12	22.5288	47.00
134	07:10:30	32.00	-50.2	28.53	14.73	15.12	22.5288	47.00
135	07:11:30	32.00	-50.2	28.53	14.73	15.12	22.5288	47.00
136	07:12:30	32.00	-50.2	28.53	14.73	15.12	22.5288	47.00
137	07:13:30	32.00	-50.2	28.54	14.74	15.12	22.5456	47.02
138	07:14:30	32.00	-51.5	28.54	14.74	15.12	22.5456	47.02
139	07:15:30	32.00	-51.5	28.54	14.74	15.12	22.5456	47.02
140	07:16:30	32.00	-51.5	28.54	14.74	15.12	22.5456	47.02
141	07:17:30	32.00	-50.2	28.54	14.74	15.12	22.5456	47.02
142	07:18:30	32.00	-50.2	28.54	14.74	15.12	22.5456	47.02
143	07:19:30	32.00	-51.5	28.54	14.74	15.11	22.5624	47.06
144	07:20:30	32.00	-50.2	28.54	14.74	15.13	22.5288	46.99
145	07:21:30	32.00	-53.1	28.54	14.74	15.13	22.5288	46.99
146	07:22:30	32.00	-53.2	28.54	14.74	15.13	22.5288	46.99
147	07:23:30	32.00	-52.6	28.54	14.74	15.13	22.5288	46.99
148	07:24:30	32.00	-52.2	28.54	14.74	15.13	22.5288	46.99
149	07:25:30	32.00	-51.8	28.54	14.74	15.13	22.5288	46.99
150	07:26:30	32.00	-52.9	28.54	14.74	15.13	22.5288	46.99
151	07:27:30	32.00	-51.5	28.54	14.74	15.13	22.5288	46.99
152	07:28:30	32.00	-50.6	28.54	14.74	15.13	22.5288	46.99

153	07:29:30	32.05	-52.2	28.55	14.75	15.13	22.5456	47.01
154	07:30:30	32.05	-52.9	28.55	14.75	15.14	22.5288	46.97
155	07:31:30	32.05	-52.7	28.55	14.75	15.14	22.5288	46.97
156	07:32:30	32.05	-52.1	28.55	14.75	15.14	22.5288	46.97
157	07:33:30	32.05	-52	28.55	14.75	15.14	22.5288	46.97
158	07:34:30	32.05	-53.1	28.55	14.75	15.14	22.5288	46.97
159	07:35:30	32.05	-53.2	28.55	14.75	15.14	22.5288	46.97
160	07:36:30	32.05	-52.6	28.55	14.75	15.14	22.5288	46.97
161	07:37:30	32.05	-52.2	28.55	14.75	15.15	22.512	46.94
162	07:38:30	32.05	-51.8	28.55	14.75	15.15	22.512	46.94
163	07:39:30	32.05	-52.9	28.55	14.75	15.15	22.512	46.94
164	07:40:30	32.05	-51.5	28.55	14.75	15.15	22.512	46.94
165	07:41:30	32.05	-53.2	28.55	14.75	15.15	22.512	46.94
166	07:42:30	32.05	-52.6	28.55	14.75	15.15	22.512	46.94
167	07:43:30	32.05	-52.2	28.55	14.75	15.15	22.512	46.94
168	07:44:30	32.05	-51.8	28.55	14.75	15.15	22.512	46.94
169	07:45:30	32.05	-52.9	28.55	14.75	15.15	22.512	46.94
170	07:46:30	32.05	-51.5	28.55	14.75	15.16	22.4952	46.90
171	07:47:30	32.05	-50.6	28.56	14.76	15.16	22.512	46.92
172	07:48:30	32.05	-50.6	28.56	14.76	15.16	22.512	46.92
173	07:49:30	32.05	-50.6	28.56	14.76	15.16	22.512	46.92
174	07:50:30	32.05	-50.6	28.56	14.76	15.16	22.512	46.92
175	07:51:30	32.05	-50.6	28.56	14.76	15.17	22.4952	46.88
176	07:52:30	32.05	-50.6	28.56	14.76	15.17	22.4952	46.88
177	07:53:30	33.05	-51.5	28.56	14.76	15.17	22.4952	46.88
178	07:54:30	33.05	-51.8	28.56	14.76	15.17	22.4952	46.88
179	07:55:30	33.05	-50.6	28.56	14.76	15.17	22.4952	46.88
180	07:56:30	33.05	-50.6	28.56	14.76	15.17	22.4952	46.88
181	07:57:30	33.05	-50.6	28.56	14.76	15.17	22.4952	46.88
182	07:58:30	33.05	-50.6	28.56	14.76	15.18	22.4784	46.85
183	07:59:30	33.05	-50.6	28.56	14.76	15.18	22.4784	46.85
184	08:00:30	33.05	-51.5	28.56	14.76	15.18	22.4784	46.85



## ANNEXURE-E Uncertainty Analysis

It is incredibly challenging to measure physical quantities accurately. When measuring any physical quantity, there are always uncertainties due to technical, physical, and human shortcomings. Klein's Method is used to calculate uncertainty analysis and can be represented as.

$$w_r = \left[ \left( \frac{\partial R}{\partial x_1} w_1 \right)^2 + \left( \frac{\partial R}{\partial x_2} w_2 \right)^2 + \dots + \left( \frac{\partial R}{\partial x_n} w_n \right)^2 \right]^{\frac{1}{2}} \quad (D.1)$$

Here, R is a predefined function of the independent variables  $x_1, x_2, \dots, x_n$ , and  $w_1, w_2, \dots, w_n$  are the corresponding variables' uncertainty.

To determine the performance of the desiccant in the heatless air dryer, the following calculation of moisture removal rate and dehumidifier effectiveness are performed.

$$X = m_a (Z_1 - Z_2) \quad (5)$$

Where,

$m_a$  = the mass flow rate of the compressed air at the inlet of the dehumidification tower.

$Z_1$  = the compressed air humidity ratios at the input.

$Z_2$  = the compressed air humidity ratios at the output.

The dehumidification tower's effectiveness  $\varepsilon_{DW}$  is calculated as the ratio of the change in real air humidity ratio to the highest feasible change in humidity ratio.

$$\varepsilon_{DW} = \frac{(Z_1 - Z_2)}{(Z_1 - Z_{2\text{ ideal}})} \quad (6)$$

Where,

The ideal humidity ratio of the air stream at the desiccant dehumidifier's exit is  $Z_{2\text{ ideal}}$ . The value of  $Z_{2\text{ ideal}}$  is set to zero by presuming that the air is totally dehumidified at this stage. (Jani et al., 2016c)

**Step-1 Uncertainty in measurement devices.**

**TABLE B.1 Uncertainty in measurement devices**

Sr. No.	Device Name	Parameter	Nomenclature	Unit	Uncertainty
1	Hygrometer	Humidity Ratio	Z	g/kg of dry air	$\pm 2\%$
2	Dew point Temperature Transmitter	Temperature	T	$^{\circ}\text{C}$	$\pm 0.5^{\circ}\text{C}$

**Values of fixed properties**

**TABLE B.2 Values of fixed properties**

Sr. No.	Name of Property	Nomenclature	Unit	Value
1	Air flow rate	$m_a$	m <sup>3</sup> /hr	16.99
2	Compressed air humidity ratios at the input	$Z_1$	g/kg of dry air	28.4
3	Compressed air humidity ratios at the output	$Z_2$	g/kg of dry air	15
4	Moisture Removal Rate	X	kg/hr	0.0225

**Step-2 Calculation of uncertainty in measurement devices.**

$$w_X = \left[ \left( \frac{\partial X}{\partial m_a} w_{m_a} \right)^2 + \left( \frac{\partial X}{\partial Z_1} w_{Z_1} \right)^2 + \left( \frac{\partial X}{\partial Z_2} w_{Z_2} \right)^2 \right]^{\frac{1}{2}}$$

$$\frac{\partial X}{\partial m_a} = (Z_1 - Z_2) = 13.4$$

$$\frac{\partial X}{\partial Z_1} = m_a = 0.00168$$

$$\frac{\partial X}{\partial Z_2} = m_a = 0.00168$$

By putting values in equation 1, uncertainty in  $w_X$  is 0.07182 kg/hr. Thus, uncertainties in moisture removal rate measurement can be given by following relation.

$$\frac{\partial X}{X} * 100 = \pm 7.18\%$$

Hence it can be said the uncertainty in results of moisture removal rate is  $\pm 7.18\%$

## **ANNEXURE-F List of Publications**

1. A.J. D'souza, P.K.Brahmbhatt (2022) "Experimental investigation on use of Molecular Sieve 4A as desiccant in heatless air dryer." International Journal of Mechanical Engineering, ISSN: 0974-5823, Special Issue-I, Vol. 7 , pp. 625-632, Feb, 2022 .
2. A.J. D'souza, P.K.Brahmbhatt, R.K. Shukla (2022) "A Review on the Recent Developments on Solid Desiccant-Based Technology in HVAC Applications" Asian Journal of Organic & Medicinal Chemistry, ISSN Online: 2456-8937, Vol. 7 No. 2 pp. 334-342 (April - June, Special Issue – I 2022)
3. D'souza, A.J., Brahmbhatt, P.K. (2023). Experimental Investigation on Use of Activated Alumina and Molecular Sieve 13× In Heatless Desiccant Air Dryer. In: Banerjee, J., Shah, R.D., Agarwal, R.K., Mitra, S. (eds) Recent Advances in Fluid Dynamics. Lecture Notes in Mechanical Engineering. Springer, Singapore. [https://doi.org/10.1007/978-981-19-3379-0\\_9](https://doi.org/10.1007/978-981-19-3379-0_9)
4. A.J. D'souza, P.K.Brahmbhatt, R.K. Shukla (2022) "Experimental investigation on use of Silica gel as desiccant in heatless air dryer." presented a paper in Third international conference on " Sustainable Energy Solutions for a Better Tomorrow (SESBT 2022)" organized in virtual mode by School of Mechanical Engineering , Vellore Institute of Technology (VIT Chennai) in collaboration with ESRIG, University of Groningen, Netherlands on 24th July 2022. (Paper will be published in Scopus Indexed Materials Today Proceeding)